3-11-2011

Retrospective Geospatial Modeling of PM10 Exposures from Open Burning at Joint Base Balad, Iraq

John P. Rinker

RETROSPECTIVE GEOSPATIAL MODELING OF PM10 EXPOSURES FROM OPEN BURNING AT JOINT BASE BALAD, IRAQ

THESIS

John P. Rinker, MSgt, USAF

AFIT/GIH/ENV/11-M03

DEPARTMENT OF THE AIR FORCE
AIR UNIVERSITY

AIR FORCE INSTITUTE OF TECHNOLOGY

Wright-Patterson Air Force Base, Ohio

The views expressed in this thesis are those of the author and do not reflect the official policy or position of the United States Air Force, Department of Defense, or the United States Government.

AFIT/GIH/ENV/11-M03

RETROSPECTIVE GEOSPATIAL MODELING OF PM10 EXPOSURES FROM OPEN BURNING AT JOINT BASE BALAD, IRAQ

THESIS

Presented to the Faculty

Department of Systems and Engineering Management

Graduate School of Engineering and Management

Air Force Institute of Technology

Air University

Air Education and Training Command

In Partial Fulfillment of the Requirements for the

Degree of Master of Science in Industrial Hygiene

John P. Rinker, BS

MSgt, USAF

March 2011

AFIT/GIH/ENV/11-M03

RETROSPECTIVE GEOSPATIAL MODELING OF PM10 EXPOSURES FROM OPEN BURNING AT JOINT BASE BALAD, IRAQ

THESIS

John P. Rinker, BS
MSgt, USAF

Approved:

//signed//	10 March 2011
Lieutenant Colonel Dirk P. Yamamoto (Chairman)	Date
//signed//	10 March 2011
Lieutenant Colonel William E. Sitzabee (Member)	Date
//signed//	10 March 2011
Lieutenant Colonel Jeremy M. Slagley (Member)	Date

Abstract

Predicting, determining, and linking theater-related source-specific exposures to health effects has proven difficult, from Agent Orange to Gulf War Syndrome to today's burn pit concerns. The purpose of this research is to delineate retrospective exposure zones using spatially interpolated particulate air sampling point data from Joint Base Balad, create burn pit exposure isopleths from dispersion model outputs, and merge into a combined exposure model in GIS.

In this study, interpolated monitoring results provided by the U.S. Army Public Health Command and dispersion modeling results were combined to compare modeled exposures across the installation area. Also, burn pit contribution to total PM10 was modeled, with percent contributions to monitoring sites ranging between less than 5% and greater than 60%. From the dispersion map, it was determined that although more mass is lost during flaming combustion, there is potential for much greater exposure to smoldering combustion when neutrally buoyant plumes are present.

The combined dispersion and interpolation map showed an intersection of elevated concentrations within a 1 kilometer buffer of the burn pit. Buildings located within this modeled high exposure area were identified by geoprocessing within the ArcMap GIS software. Also, the east side of the base receives greater burn pit-specific PM10, compared to the west side of base. The west side of base showed high ambient PM10 from monitoring results, but it could not be determined whether this was due to spatial or temporal effects. PM10 monitoring result geometric means ranged from 73 to 976 $\mu g/m^3$, with higher variability in the summer months than the winter months, and

higher variability in 2008 than 2007. High temporal variability highlights the need for temporally representative sampling across the geographical area throughout the year. Small sample sizes, especially on the west side of base, reduce confidence in the spatial interpolation model.

It was shown that source-specific individual exposures can be estimated with dispersion model isopleth maps and knowledge of individual time-activity patterns. The dispersion model, the exposure model, and the source-specific contribution determination can all be refined with improved estimates of emission rates.

Acknowledgments

First, I would like to thank God for this incredible opportunity to pursue the excellence of an AFIT education, and for the fortitude to complete the program.

I owe a tremendous debt of gratitude to my academic advisors, Lt Col Jeremy Slagley and Lt Col Dirk Yamamoto, for mentorship, guidance, and steadfast commitment to our learning. Thank you for expecting the highest achievement, and for believing in us. Some of the challenges seemed impossible, but meeting those challenges provided momentum and confidence that carried me through. Also, to Lt Col Sitzabee, whose mentorship and expertise made me a true SAP (Spatially Aware Professional).

Thanks also to my classmates, who made the academic challenges not only bearable, but fun. I look forward to working with you all at our next assignment and throughout our Air Force careers.

I would like to thank my parents for teaching me the value of education, for always having the highest of standards of achievement, and for their love, support, and encouragement, and also the incredible support of my in-laws. I also thank my awesome kids for making my job easy, and for always giving me something to smile about.

Finally, I would like to thank my wife, for her patience through the difficult quarters, for her optimism, for her faith, and for her love. Whenever I was convinced that I would not make it through this, with a few words, a smile, and a prayer, she would convince me otherwise. I have always believed, and still believe, that there is absolutely nothing in the world that we can't achieve together.

John P. Rinker

Table of Contents

Page

Abstract 1
Acknowledgments 3
Table of Contents 4
List of Figures 6
List of Tables 9
I. Introduction 10
Background 10
Problem Statement 15
Research Objectives 18
Research Focus 19
Assumptions 20
Implications 21
II. Literature Review 23
Open Burning Emissions 23
Overview of Exposure Models 36
Proximity Models 38
Spatial Interpolation Models 39
Land Use Regression (LUR) Models 45
Atmospheric Dispersion Models 47
Hybrid/Integrated Exposure Models 53
Model Integration and Linking Exposure to Disease in GIS 55
Ambient Exposure Modeling Studies 60
Climatological Issues 65
III. Methodology 67
Data Sources 69
Exploratory Data Analysis 71
Dispersion Modeling 74
Processing in ArcMap 82
Assumptions 82
IV. Results and Analysis 86
Exploratory Data Analysis 89
Spatial Analysis 96
Dispersion Modeling Results and Analysis 106
Exposure Modeling With Exposure Maps 130

Page

Limitations and Uncertainty 133

V. Conclusions 137
Suggested Methodology Improvements 141

Strengths and Limitations 142

Recommendations for Future Research 144

Appendix A: Balad Particulate Monitoring Results, 2003-2010 (USAPHC, 2010).. 154
Appendix B: Joint Base Balad Sampling Locations with Coordinates..... 165
Appendix C: Meteorological Surface Data File Used in Annual SCIPUFF Plumes. 166
Appendix D: One-way Analysis and Variability Charts..... 172
Appendix E: SASEM Output File..... 174
Appendix F. GIS Data Sources and Procedure Log 179

List of Figures

Page

Figure 1: EPA Estimates of Household Waste Composition (source: Lemieux, 1998) ... 29

Figure 2: EPA Estimates of Household Waste Composition (source: Lemieux, 1998) ... 35

Figure 3: Comparison of Interpolators (Courtesy: Esri, Inc.) ... 41

Figure 4: Thiessen polygon created around point to be interpolated ... 42

Figure 5: Combined Spatial Interpolation and Dispersion Model Mapping Process ... 67

Figure 6: Pasquill-Gifford Stability Classes (Source: EPA, 2011) ... 79

Figure 7: Number of Joint Base Balad PM10 Sampling Sites Per Month, 2003-2009 ... 89

Figure 8: PM10 Frequency Distribution at Balad Sites (N≥3), 2007-2008 (USAPHC, 2010) ... 91

Figure 9: Average Monthly Dust Storm Frequency,Joint Base Balad (14WS, 2010) ... 92

Figure 10: Annual Wind Rose, Based on KQTO Balad 2003-2009 Wind Frequency Data (14WS, 2010) ... 94

Figure 11: Monthly Wind Roses, KQTO, Balad, 2003-2009 Wind Frequency Data (14WS, 2010) ... 95

Figure 12: Joint Base Balad Elevation Map ... 97

Figure 13: Joint Base Balad PM10 Sampling Site Map with Numbers of Samples, 2007-2008 ... 98

Figure 14: Inverse Distance Weighting Interpolation: Continuous Concentration Surface of PM10, Joint Base Balad, 2007-2008 ... 100

Figure 15: Inverse Distance Weighting Interpolation: Isoplethed Concentration Surface of PM10, Joint Base Balad, 2007-2008..... 101

Page

Figure 16: Overlaying Continuous Exposure Surface Layer in Google Earth 103

Figure 17: Joint Base Balad PM10 Sampling Sites, 2007-2008, N≥3..... 104

Figure 18: Joint Base Balad PM10 Sampling Sites, 2007-2008, N≥3..... 106

Figure 19: Annual PM10 Surface Dosage From Joint Base Balad Burn Pit 108

Figure 20: Annual PM10 Surface Dosage From Joint Base Balad Burn Pit 109

Figure 21: SCIPUFF Dispersion Modeling Export Grid for Loose-Coupling in GIS.... 110

Figure 22: Dispersion Modeled Flaming PM10 Concentration..... 112

Figure 23: Dispersion Modeled Smoldering PM10 Concentration 113

Figure 24: Dispersion Modeled Flaming + Smoldering PM10 Concentration..... 114

Figure 25: Dispersion Modeled Smoldering PM10 Concentration 116

Figure 26: Balad PM10 Sampling Sites By Year, 2007-2008, With PM10 IDW Interpolation..... 119

Figure 27: Inverse Distance Weighting Interpolation, Ambient PM10, Balad, 2007..... 120

Figure 28: Inverse Distance Weighting Interpolation, Ambient PM10, Balad, 2008..... 121

Figure 29: Month Within Year Variability Chart, Balad PM10, 2007-2008..... 122

Figure 30: Identification of Buildings Within 1 km of Burn Pit Source 124

Figure 31: Attribute Table for 1 km Buffer-Buildings Intersection Layer 125

Figure 32: ArcMap Layers in Google Earth 126

Figure 33: Identification of Off-Base Receptor Areas in Google Earth (Light Blue).... 127

Figure 34: Dispersion Modeled Burn Pit-Specific Total PM10 Concentration vs. Inverse Distance from Sampling Sites to Burn Pit 129

Figure 35: Dispersion Modeled Smoldering + Flaming PM10 132

Page

Figure 36: Oneway Analysis, Balad – PM10 (µg/m^3) by Month, 2007-2008 172

Figure 37: Balad PM10 Variability Charts, January 2007-November 2008 173

List of Tables

Page

Table 1: Emission Factors for Particulates Released During Open Burning..... 33

Table 2: PC-SCIPUFF Assumed Boundary Layer Depth Based on Stability Class 80

Table 3: Descriptive Statistics Summary, Balad Georeferenced PM10 Samples, 2007-2008..... 90

Table 4: Geometric Means for Joint Base Balad Sampling Sites (n≥3), 2007-2008..... 96

Table 5: Distance From Burn Pit to Balad PM10 Sampling Sites (n≥3), 2007-2008..... 105

Table 6: Balad PM10 Sample Frequencies Per Site Per Month, 2007-2008..... 117

Table 7: Balad PM10 Sample Frequencies Per Site Per Year, 2007-2008..... 118

Table 8: Dispersion Modeled Burn Pit-Contributed PM10 Concentration and Percentage of Monitored Concentration at Balad Sampling Sites 127

Table 9: Sampling Sites 165

RETROSPECTIVE GEOSPATIAL MODELING OF PM10 EXPOSURES FROM OPEN BURNING AT JOINT BASE BALAD, IRAQ

I. Introduction

Background

Open burning of solid waste can release a host of toxins into the air. Researchers have not only sampled smoke plumes from various open burns, they have also developed methods to describe emission factors of some of the greatest toxins of concern, such as dioxins (Akagi S. K., et al., 2010; Estrellan & Iino, 2009; Gullett, Lemieux, Lutes, Winterrowd, & Winters, 2001; Lemieux, Lutes, & Santoianni, 2004; Gullett, Wyrzykowska, Grandesso, Touati, Tabor, & Ochoa, 2010). Burn pit smoke is considered one of three primary air pollutant types in CENTCOM locations (Engelbrecht J. P., McDonald, Gillies, Jayanty, Casuccio, & Gertler, 2009).

Recent epidemiological studies indicate higher rates of respiratory symptoms (Smith, Wong, Smith, Boyko, Gackstetter, & Ryan, 2009), and new-onset asthma (Szema, Peters, Weissinger, Gagliano, & Chen, 2010), though DoD studies do not show higher outcomes with burn pit exposure (Armed Forces Health Surveillance Center; Naval Health Research Center; US Army Public Health Command, 2010). The DoD studies consider assignment location within five miles of a burn pit as "exposure," and do not consider the exposure pathway.

A 2008 health risk screening report from the United States Army Center for Health Promotion and Preventive Medicine (USACHPPM) (now the US Army Public Health Command) and the Air Force Institute for Operational Health (AFIOH) (now the

US Air Force School of Aerospace Medicine) includes Defense Health Board comments indicating strong interest in multivariate correlations between exposures and health effects, and relationships between personnel location and exposure (Vietas, Taylor, Rush, & Deck, 2008).

The National Academies of Science Institute of Medicine (IOM) has formed a committee to investigate long term health effects of burn pit emissions exposure. Their project scope, as posted on the project website states (The National Academies, 2010):

> The committee will explore the background on the use of burn pits in the military. Areas of interest to the committee might include but are not limited to investigating:
>
> 1. Where burn pits are located, what is typically burned, and what are the by-products of burning;
> 2. The frequency of use of burn pits and average burn times; and
> 3. Whether the materials being burned at Balad are unique or similar to burn pits located elsewhere in Iraq and Afghanistan.

Although the highly publicized "burn pit" at Balad has ceased to operate, open burning has not been universally discontinued. According to personnel overseeing health risk exposure assessments in the area, as operations increase in Afghanistan and increasing amounts of personnel move into Bagram, dormitories may move increasingly closer to the air curtain incinerators currently in use, in which solid waste is burned. While there are current MILCON projects to install permanent incinerators at large bases, the volume of waste may require continued use of the air curtain incinerators as well as open burning.

CENTCOM does not routinely track the total number of burn pits and locations at any given time, and the exact number of pits varies with troop levels and the number of bases. According to GAO, there were 67 burn pits in Iraq in November 2009; in April

2010, there were 52, and in August 2010, there were only 22. This reduction is attributed to the troop reduction in Iraq, as well as the increase of incinerator use. Between 2005 and 2010, the number of operational incinerators in Iraq increased from 2 to 39. Also, air curtain incinerators, also known as air curtain destructors or "burn boxes," are used in some locations (Government Accountability Office, 2010).

In 2009, Congress signed into law Section 317, "Prohibition on Disposing of Waste In Open-Air Burn Pits," of the 2009 National Defense Authorization Act, H.R. 2647. The legislation prohibits the use of open-air burn pits during contingency operations, unless the Secretary of Defense determines that there is no feasible alternative disposal method. The statement of infeasibility must be provided to Congress within 30 days of the determination, and for each 180-day period following the initial determination, the Secretary must provide justification for continuing operation of open-air pits.

Per the 2009 legislation, the Secretary was also required to submit a report on the use of open-air pits, including situations in which pits may be used; detailed descriptions of wastes authorized for burning; a plan for development of alternatives to open burning; health and compliance standards for both military and contractor operations, and an assessment of whether those standards are being met; a description of the environmental, health, and operational impacts of plastic burning; and an assessment of medical surveillance programs used to identify and track exposures, including recommendations for improvement of those programs.

Not included in the legislation, but included in the original bill, titled "Military Personnel War Zone Toxic Exposure Prevention Act," (H.R. 2419), are the following

requirements: deployment locations and dates of exposed members, the approximate distance of the living and working quarters of members from a hazardous disposal site, the types of materials disposed of at the site, the length of time the member was exposed to such site, any symptoms experienced by members while deployed, and any symptoms that may have been a result of waste site exposure.

The initial submission and final requirements are significant for several reasons. First, distances of living and working quarters from disposal sites are not currently tracked, and would require significant resources and effort to document in current systems. Though this provision did not make it into the final authorization, it was reviewed and recommended by 23 co-sponsors in Congress. It is conceivable that during a hearing, the question may arise of whether distance from a source or location in an increased exposure zone is a risk factor for symptoms. Second, records of materials disposed of at sites are generally poor or nonexistent, as exposed by the GAO (Government Accountability Office, 2010). Third, the current system does not track exposures to burn pit emissions. Ambient sampling is performed to characterize "worst-case" exposures from all contaminants at any given site, without consideration to location-based source contribution variations, generally with only one to a few sites chosen based on subjective "worst-case" location determinations, generally near the living and working areas of the bulk of the base population.

In response to the National Defense Authorization Act of 2009, the DoD released "Directive-type Memorandum (DTM) 09-032 – Use of Open-air Burn Pits in Contingency Operations" (Department of Defense, 2010). Minimum requirements of this directive include:

1) A solid waste management plan for the contingency operation; burn pits are not to be used unless included in the plan, and the plan must address disposal of "covered" wastes, including hazardous and medical waste.

2) The plan ensures burn pits are: a) located to prevent exposures to personnel in living, working, and dining areas; b) operated safely and securely for those disposing of waste; c) located in safe areas with respect to wildlife attraction, aircraft flight, and aircraft controller visibility; d) inspected regularly; e) monitored for effective operations by qualified engineering personnel and for unacceptable exposures by qualified occupational and environmental health personnel, f) properly closed with documented location information; g) not used for "covered" waste.

3) Plastics are prohibited, except insignificant amounts.

4) Specific medical and engineering guidance that "maximize protection of human health and safety" are to be issued when alternative disposal methods are not feasible.

Despite the recent regulatory requirements on control and evaluation of burn pits, the Government Accounting Office (Government Accountability Office, 2010) found that compliance with key regulatory elements has been poor. Burn pit operators continued to burn prohibited items, such as plastic, for several reported reasons, including operational constraints, resource limitations, and contracts conflicting with regulatory guidance. GAO also determined that DoD has not conducted cost-benefit analyses of alternative waste disposal methods, such as source reduction. Additionally, the report notes that waste streams have not been analyzed, making waste stream toxicity reduction and waste minimization difficult. Finally, the report states:

> "U.S. Forces in Afghanistan and Iraq do not sample or monitor burn pit emissions as provided by a key CENTCOM regulation, and the health impacts of burn pit exposure on individuals are not well understood, partly because the military does not collect required data on emissions or exposures from burn pits…DOD and VA have commissioned studies to enhance their understanding of burn pit emissions, but the lack of data on emissions specific to burn pits and related exposures limit efforts to characterize potential health impacts on service personnel, contractors, and host-country nationals."

The GAO and the Defense Health Board both recommend determination of burn pit contribution of total exposure (Government Accountability Office, 2010). As previously mentioned, GAO recommends direct burn pit emissions testing, in accordance with DoD directives. The Defense Health Board recommends characterization of particulate size distribution from air in proximity to burn pits, and comparison with distribution of background air. The GAO and the DHB recommend better inventories of major sources of ambient air pollution, including materials burned in pits. DoD, in responses to both GAO and DHB, maintains that it is less concerned with source-specific emissions and exposures than it is with total "worst-case" personal exposures. GAO, however, makes the compelling argument that "in the absence of data and information on burn pit exposures and individuals' burn pit exposure, the potential health impacts of burn pit emissions on individuals are not well understood."

Problem Statement

Determining the burn pit contribution to overall ambient air pollution exposure, as recommended by GAO and DHB, is a challenging endeavor. Higher levels of particulate concentration are expected in close proximity and downwind from a burn pit, than at farther upwind locations. An air sampling grid would show the distance decay if confounding sources were not present. Unfortunately, ambient particulate levels from

regional dust events can exceed 1,000 µg/m^3, and dust events in Baghdad occur on over 50 percent of summer days (Draxler, Gillette, S., & Heller, 2001; Wilkerson, 1991). Also, activities such as agriculture, industry, traffic, and installation operations contribute to overall levels of pollution at the local scale, further confounding efforts to determine source-specific concentration across a geographic area.

Atmospheric dispersion models can be used to overcome these limitations when emissions, meteorology, and topography are known. Though emissions from the open burning of theater military waste have not been determined, emission factors from municipal and industrial waste burning can be used as a starting point to determine rough estimates. Point or area source contributions can be defined over a geographic area, and exposure zones delineated based on modeled concentration isopleths. Alternatively, an assumed continuous large release of particulate can be applied to model relative exposure zones over a geographical area based on, for example, the interquartile range of concentration.

Though extensive air sampling was accomplished between 2003 and 2010, the usual strategy was to characterize total exposure to expected pollutants with samplers placed in densely populated areas, using the entire installation as an exposure group, and conservatively assigning these "worst-case" exposures to all personnel. The sampling strategy was not designed to determine burn pit contributions of particulate matter to the total concentration of particulate matter, nor to differentiate exposure groups by geographical location. This strategy, while conservative in assigning "worst-case" levels to less-exposed populations, makes epidemiological and health effects studies difficult; if everyone has equal exposures, there are no comparison cohorts. Additionally, "when

there is a significant amount of variation in particulate concentrations across an urban area, the use of central sites or a sites may result in exposure misclassification that induces error in long-term cohort epidemiological study designs" (Wilson & Zawar-Reza, 2006).

Qualitative differences may exist in local and regional components of particulates, and so the two should not be treated in a simple additive fashion when modeling. Also, gravimetric particulate analyses represent the blind sum of all sources. There may be important compositional differences between source types; for example, particulate suspended from a desert floor may be different from combustion-emitted particulate. If combustion-emitted particulate is more important in a health-effects study, then the concentrations from that source must be accounted. (Briggs D. , 2005). The importance of determining source-specific particulate exposures, rather than gross summation of particulate, is further supported by research showing significant proportions of organic pollutants bound to particles emitted by open burning (Barakat, 2003).

The degree of spatial heterogeneity in particulate matter concentration across the base is undetermined. If the concentration/exposure surface is homogeneous across the base, then applying a single ambient air concentration result to all personnel is valid if there are not significant compositional differences in particulate that vary over space and time. If, however, there is a significant degree of variability across the base geography, then personnel in different receptor areas, or exposure zones, may have different exposures corresponding to different levels of risk.

Using monitoring results and performing spatial interpolation techniques in a geographical information system (GIS), a map can be created that reveals the

concentration surface over space, which aids in visualizing possible "hot spots" and weaknesses in the sampling grid. Also, individual or exposure group assessments can be enhanced by determining time spent per monitored or modeled exposure zone, and population and activity information can be viewed with concentration zones overlaid in GIS, allowing visual correlation between hot spots and populations or sources. Finally, differences in exposure over time, such as seasonal or diurnal variations, or increases in concentration due to troop buildup and higher activity levels, can be visualized on different temporal scales across an area.

Research Objectives

The objective of this research is to delineate retrospective exposure zones using spatially interpolated particulate air sampling point data from Joint Base Balad, create burn pit exposure isopleths from dispersion model outputs, and merge into a combined exposure model in GIS.

1. Determine spatial and temporal patterns with monitored particulate data
2. Model burn pit ambient exposure zones with a dispersion model
3. Estimate relative burn pit contribution to overall exposure, and determine whether modeled dispersion concentration differences predict monitored concentration differences
4. Identify sampling needs to improve spatial modeling
5. Create a method to model relative source-specific ambient exposures for individuals or similar environmental exposure groups.

These objectives support the following USAF Bioenvironmental Engineering Capabilities (Department of the Air Force, 2009):

1. Execute Surgeon General (SG) related vulnerability assessment
2. Conduct predictive exposure assessments - "use data, intelligence products, and modeling information…as a baseline for predicting potential OEH (Occupational and Environmental Health) exposures…"
3. Execute Occupational & Environmental Health Site Assessment (OEHSA)
4. Identify OEH hazards
5. Analyze OEH hazards
6. Control OEH hazards
7. Associate exposure with affected personnel - "tie completed or potentially completed exposure pathways to individuals using spatial and temporal reference marks."
8. Assist with health risk management

Research Focus

This research will focus on PM10 exposures at Joint Base Balad, Iraq, for the monitoring period between 2007 and 2008. Additionally, the period of May-June 2009 was examined, for several reasons. Though incinerators were in operation during the May-June 2009 period, open burning continued on a smaller scale, and a high degree of variability is apparent between sites on the same sampling days. Also, three sites were simultaneously covered for the majority of sampling days in this period. Finally, this period represents the greatest number of samples taken for the dry summer months in which wind is predominantly from the northwest direction, and at greater speeds than during other parts of the year. As the receptor areas are primarily south to southeast of the burn pit, and buoyant plume rise would be expected to be limited by higher wind velocities, the summer months may represent the worst case time frame for burn pit exposures.

PM10 was chosen because it was the most frequently sampled ambient pollutant at Balad, and for this research, sample size was too small for other pollutants. Atmospheric dispersion can be accomplished for all years, but since there is great uncertainty in waste composition and emission factors, and dispersion modeling at a fine resolution is computationally intense and requires experience and finesse in working with meteorological and dispersion software, this task is deemed more appropriate after emission factors have been determined experimentally.

The extent of the spatial interpolation modeling in this research is the installation boundary. The dispersion models can be applied to determine relative exposures to receptor areas off base. The interpolation models are inappropriate for determining off-base population exposure, since the monitoring network was confined to a somewhat small area on base.

The exposure models in this research apply only to personnel deployed during the modeled time frames. In addition, the total exposures for their entire deployment depends on other factors, including ambient exposures in the remainder of their deployment, and their occupational, transit, indoor, and recreational exposures.

Assumptions

1. Published data for municipal waste were used to determine emissions factors for the atmospheric dispersion model. These data may not reflect emissions for military-specific waste burning. Emission factors for military-specific waste have not been determined.

2. Burn characteristics and waste composition are unknown. Department of Defense reports indicate that the burn pit operated on a 24/7 basis (US Army Public Health Command (Provisional), 2010). A continuous burn, with continuous emissions from both flaming and smoldering phases of combustion, was assumed for this research.
3. The amount of waste burned was unknown, but a DoD report estimated 200 tons per day burned. 200 tons per day was used as the assumed mass burned. Contributions from incinerators or other disposal methods were not modeled in this research.
4. The atmospheric model assumption assumes that physical or chemical transformation does not occur between emission and transportation to receptor areas.
5. The methods for determination of sampling site grid coordinates did not accompany the georeferenced monitored ambient air pollution dataset. Standard or measurement error was also not included with the set. It is assumed that the measured pollution concentrations and grid coordinate estimations provided were reasonably accurate, though the National Academies of Science noted that methods for particle collection in the United States may be unsuitable for use in atmospheres with excessive particle concentrations, such as those found in the Middle East (National Research Council, 2010).

Implications

There are several implications for this research. First, it lays groundwork for linking exposures and health outcomes. Ambient exposure is equal to the sum of the concentrations of the occupied zones multiplied by time spent in those zones, divided by total time. Determination of differential exposures to specific sources is possible with

this methodology, if personnel time-activity patterns are also tracked, and health outcomes can be linked to differential exposures.

Also, a determination of the heterogeneity of the concentration surface and modeled exposure isopleths from interpolated monitored data will determine whether the process of averaging of samples from multiple sites and applying the result to all base personnel is valid. If some areas are modeled as higher than others in specific receptor zones, then individuals working or living in these areas can be treated as separate exposure groups for exposure to total ambient PM10 (burn pit contributed + regional ambient + other locally contributed sources).

If the dispersion models reveal significant differences across the base spatial domain, then populations working or living within higher modeled isopleth areas may be at greater risk from burn pit contributed pollutants than populations working or living within low modeled concentration isopleth areas.

The reproducibility of this research will provide a method to model concentrations across a geographical space and allow georeferenced population health data, such as acute respiratory symptoms or long-term respiratory illness, to be overlaid. This would require a method to georeference and store individual activity locations, such as work and living areas, for either all individuals or for those who become ill. Incidence rates within high-exposure isopleth zones could then be compared with rates in lower-exposure isopleth zones to determine relative risks for specific periods. Maps with health data overlaid on adjustable pollutant exposure zone isopleth layers that can be turned on, off, or combined, may allow quick visualization of disease clustering within exposure zones, and provide valuable information to complete epidemiological studies.

II. Literature Review

The literature review comprehensively appraises the current state of knowledge regarding open burning emissions and exposure modeling, and provides examples of experimental applications of dispersion and geospatial exposure models. Also, the literature review details concepts upon which research methods and conclusions are founded. The fields of atmospheric dispersion modeling and geospatial modeling are rapidly growing, and as technology allows greater refinement and faster processing of information, new methods for exposure assessment modeling are created on a seemingly continual basis.

Open Burning Emissions

Open burning has been defined as "the burning of any matter in such a manner that products of combustion resulting from the burning are emitted directly into the ambient or surrounding outside air without passing through an adequate stack, duct or chimney" (Estrellan & Iino, 2009). Lemieux more simply defines open burning as "the unenclosed combustion of materials in an ambient environment" (Lemieux, Lutes, & Santoianni, 2004). According to the Intergovernmental Panel on Climate Change (IPCC), open burning is "the combustion of unwanted combustible materials such as paper, wood, plastics, textiles, rubber, waste oils and other debris in nature (open-air) or in open dumps, where smoke and other emissions are released directly into the air without passing through a chimney or stack." IPCC also specifically includes incineration devices that do not work properly, adding that "open burning can also include incineration devices that do not control the combustion air to maintain an

adequate temperature and do not provide sufficient residence time for complete combustion." Thus, "burn boxes," also known as "air curtain incinerators" or "air curtain destructors" with inoperable air flow devices that are not used according to manufacturer specifications may be considered "open burning" under the IPCC definition.

Several process parameters affect open burning emissions. For example, open burning occurs with less than ideal combustion conditions, including lower temperatures, poor mixing of fuel and air, and gas-phase residence times that are insufficient for complete combustion. Waste pile configuration, waste composition, variations in combustion conditions, bulk density, moisture content, and ignition techniques are among the determinants of emission quantities and composition (Gullett, Wyrzykowska, Grandesso, Touati, Tabor, & Ochoa, 2010; Gullett & Raghunathan, Observations on the Effects of Process Parameters on Dioxin/Furan Yield in Municipal Waste and Coal Systems, 1997; Lemieux, Lutes, & Santoianni, 2004; Carroll, Miller, & Thompson, 1977). Higher moisture content, lower burn temperatures, longer periods of smoldering, poor air-fuel mixing, and headfire ignition techniques result in higher particulate emissions, and higher wind speeds result in poorer plume rise and higher ground concentrations. Also, though smoldering phase burning emits greater amounts of toxicants, a study on cereal burning emissions determined that most of the mass that is burned occurs during the flaming phase (de Zarate, Ezcurra, Lacaux, & Dinh, 2000). Of total fire-exposed carbon, 88% was converted to carbon dioxide during the flaming phase, compared with 74% during the smoldering phase. Additionally, only 3% of the total particulate produced was soluble, primarily in the forms of K^+ and Cl^-. Mass percentages burned was found to be 90% during the flaming phase plus 10% during the

smoldering phase. Therefore, most of the toxicants produced during open burning may be the result of low-temperature burning of a small fraction of the initial mass burned.

The current literature shows open burning emissions to contain soot, particulate matter, carbon monoxide, methane, volatile organic carbons (VOCs), semi-volatile organic carbons (SVOCs), polycyclic aromatic hydrocarbons (PAHs), carbonyls, and chlorobenzenes. Also, depending on the source material, metals, including lead and mercury, may be present. At lower-temperature smoldering phases, different chemical pathways lead to increased formation of polychlorinated dibenzo-*p*-dioxins (PCDD), polychlorinated dibenzofurans (PCDF), polybrominated dibenzo-*p*-dioxins (PBDD), polybrominated dibenzo-*p*-furans (PBDF) and polybrominated diphenyl ethers (PBDE) (Gullett, Wyrzykowska, Grandesso, Touati, Tabor, & Ochoa, 2010) (Lemieux, Lutes, & Santoianni, 2004). Polybrominated compound emissions have been found when materials treated with flame retardants are burned (Gullett, Wyrzykowska, Grandesso, Touati, Tabor, & Ochoa, 2010).

Several studies have discussed emissions from open burning of wastes in categories, including agricultural, municipal, household, and industrial wastes, as well as wood combustion (Estrellan & Iino, 2009; Gullett & Raghunathan, Observations on the Effects of Process Parameters on Dioxin/Furan Yield in Municipal Waste and Coal Systems, 1997; Gullett, Lemieux, Lutes, Winterrowd, & Winters, 2001; Gullett, Wyrzykowska, Grandesso, Touati, Tabor, & Ochoa, 2010; Lemieux, Lutes, & Santoianni, 2004). Other research has focused on emissions from burning specific materials, such as scrap tires (DeMarini, Lemieux, Ryan, Brooks, & Williams, 1994), wood treated with chromated copper arsenate (Wasson, et al., 2005), plastics (Simoneit, Medeiros, & Didyk,

2005), electronics (Gullett & Linak, 2007), and complex munitions (Wilcox, Entezam, Molenaar, & Shreeve, 1996). Documentation on emissions from the open burning of typical military theater waste was not found. Military theater waste, which would be expected to consist of significant amounts of unserviceable military equipment and large numbers of plastic bottles where recycling is not practiced, may differ significantly in composition from municipal and industrial wastes for which emissions factors have been published. T

Two comprehensive reviews summarize emissions from open burning; one compiles toxic emissions in general (Estrellan & Iino, 2009), and the other compiles toxic organic emissions (Lemieux, Lutes, & Santoianni, 2004). Also, the Environmental Protection Agency (EPA) has dedicated a section of its *Compilation of Air Pollutant Emission Factors* to emissions from open burning (Environmental Protection Agency, 2011).

Biomass burning, including firewood burning, wildfires, and agricultural field burning, has been shown to release significant amounts of several pollutants. Rice and wheat straw burning releases significant amounts of both fine and coarse fraction particulate matter, polycyclic aromatic hydrocarbons (PAH), PCDD/F, and other pollutants, with experimentally determined emission factors tabulated by Estrellan (2009). Several studies found regional-scale seasonal differences in particulate matter levels and composition, corresponding to agricultural burning versus non-agricultural burning periods (Ryu, Kwon, Kim, Kim, & Chun, 2007; Cheng, Horng, Sua, Lin, Lin, & Chou, 2009). Results from Fourier transform infrared spectrometer from spectra taken at several heights above 24 smoldering fires indicated dominant products of “carbon

dioxide, carbon monoxide, methane, ethene, ethyne, propene, formaldehyde, 2-hydroxyethanol, methanol, phenol, acetic acid, formic acid, ammonia, hydrogen cyanide, and carbonyl sulfide" (Susott, Ward, Reardon, & Griffith, 1997). Also, 2-hydroxyethanal was found to be a significant smoke component and hydrogen cyanide (HCN) was found to be the dominant emission from smoldering organic soil.

Wood burning is an important source of ambient PAH and PCDD/F. Increased PCDD/F emissions have been found in preserved versus unpreserved woods. Emissions of genotoxic and total PAH under fast and slow burning conditions were tabulated, showing generally higher PAH emissions during slow burning (Estrellan & Iino, 2009).

The U.S. Government Accountability Office found significant amounts of anthropogenic material burned in theater burn pits, including prohibited materials (Government Accountability Office, 2010). Though emissions from burning of military-specific waste have not been documented, some studies have provided information on emissions from burning of domestic and industrial waste, and from landfill fires.

Domestic waste consists of household waste and may be highly variable over time and across geographic areas. The EPA prepared estimations of waste composition for a typical households (Figure 1), including non-recyclers and avid recyclers, and carried out burn experiments based on estimated percentage compositions (Lemieux P. M., 1998). Plastic was estimated to consist of 7.6 percent of total waste for a non-recycler and 15.5 percent of total waste for an avid recycler. Waste composition estimates for Balad burn pits were recently determined, based on feedback from military preventive medicine assets (Army Institute of Public Health, 2010). Waste composition, as a percentage by characterization type of the total waste stream, was determined as follows:

Large Forward Operating Bases

Plastics: 5-6%

Wood: 6-7%

Miscellaneous Non-Combustible: 3-4%

Metal: 1-2%

Combustible Materials: 81-84%

Small Forward Operating Bases

Plastics: 3-4%

Wood: 1-2%

Miscellaneous Non-Combustible: 1-2%

Metal: 1-2%

Combustible Materials: 90-94%

The report stated that these were generalized percentages, and did not specify whether the percentages represent volume or mass.

Experimental burns and documentation of emission factors based on theater military waste composition would be extremely valuable to environmental health professionals.

Table 1. Composition of household wasted prepared by EPA.

	Non-Recycler (%)	Avid Recycler (%)
PAPER		
Newspaper, books and office paper	32.8	3.3
Magazines and junk mail	11.1	—
Corrugated cardboard and kraft paper	7.6	—
Paperboard, milk cartons, and drink boxes	10.3	61.9
PLASTIC RESIN[a]		
PET #1 (bottle bill)	0.6	—
HDPE: #2, LDPE #4, and PP #5	6.6	10.4
PVC: #3	0.2	4.5
PS: #6	0.1	0.3
MIXED #7	0.1	0.3
FOOD WASTE	5.7	—
TEXTILE/LEATHER	3.7	—
WOOD (treated/untreated)	1.1	3.7
GLASS/CERAMICS		
Bottles/jars (bottle bill)	9.7	—
Ceramics (broken plates and cups)	0.4	6.9
METAL - FERROUS		
Iron - cans	7.3	4.0
NON-FERROUS		
Aluminum - cans (bottle bill), foil, other	1.7	1.0
Other non-iron (wire, copper pipe, batteries)	1.1	3.7
TOTAL WEIGHT GENERATED PER HOUSEHOLD FOR DISPOSAL IN BURN BARRELS (kg/day)	4.9	1.5

[a]PET=POLYETHYLENE TEREPHTHALATE; HDPE=high-density polyethylene; LDPE=low density polyethylene; PP=polypropylene; PVC=polyvinyl chloride; and PS=polystyrene

Table 2. Comparison between open burning of household waste and controlled combustion of municipal waste in a MWC; emissions are in μg/kg waste burned.

	Avid Recycler	Non-Recycler	MWC
PCDDs	46.7	38.25	0.0016
PCDFs	222.9	6.05	0.0019
CBs	1,007,450	424,150	1.16
PAHs	23,974.7	66,035.65	16.58
VOCs	2,052,500	4,277,500	1.17

Figure 1: EPA Estimates of Household Waste Composition (source: Lemieux, 1998)

Chlorinated plastics and copper wire burning in domestic wastes have been shown to result in increased amounts of PCDD/F and precursors. Flue gas and ash testing also showed increases in PCDD/F when chlorinated plastics were burned (Nakao, Aozasa, Ohta, & Miyata, 2006). In another study, mixed household waste, including plastics, paper, cartons, and cardboard waste, as well as yard waste, was burned in open piles, an oil barrel, and galvanized drums (Wevers, De Fre, & Desmedt, 2004). Poor air flow conditions in galvanized drums and oil barrels resulted in increased PCDD/F emissions compared to open pile burning. Significant quantities of endocrine-disrupting

compounds, including dioctyl phthalate, bisphenol A, and oxygenated PAHs were found in air samples from burning non-recyclable plastic, shoes, and food packaging (Sidhu, Gullett, Striebich, Klosterman, Contreras, & DeVito, 2005). Emission factors for PBDEs and PCDD/Fs from open burning in two residential waste dump sites in Mexico were determined in a field experiment by direct plume measurement with boom-mounted high-volume samplers (Gullett, Wyrzykowska, Grandesso, Touati, Tabor, & Ochoa, 2010). Burn combustion conditions were determined by determining CO/CO_2 percentage, with a higher ratio indicating poorer combustion. Again, smoldering combustion conditions resulted in increased PBDE and PCDD/F.

In EPA experiments, household waste burned in barrels released consistent amounts of VOC, SVOC, and particulates, but repeated trials resulted in magnitudes of difference in PCDD/F emissions (Lemieux P. M., 1998; Lemieux P. , Lutes, Abbott, & Aldous, 2000). According to these experiments, emission factors for PM_{10} were 19000 mg/kg burned for a non-recycler, and 5800 mg/kg burned for an avid recycler. Mass burned does not equal the mass of the original pile, but the mass that is lost in combustion. According to the EPA study, the fraction of waste loss from burning was 66.7% for a recycler and 49.1% for a non-recycler. Figure 2 is the full list of air contaminant emission factors from the experiments. Measurable emissions include benzene, styrene, naphthalene, phenol, chlorinated benzenes, aldehydes, PCDD/F, PCB, hydrochloric acid (HCl) and hydrogen cyanide (HCN). Ash residuals include PCDD/F, PCB, chromium, copper, lead, and zinc. Note that although maximum bed temperatures are higher for non-recyclers, due to higher material heat release, emissions are also higher for non-recyclers.

A study in Greece, where waste is composed of approximately 20% plastic, found high concentrations of PAH in open-burned emitted particulate, as well as presence of persistent free radicals (Valavanidis, Iliopoulos, Gotsis, & Fiotakis, 2008). Mutagenicity of particulates emitted from the open burning of plastics was determined by laboratory burning of polyvinyl chloride (PVC), polyethylene (PE), polystyrene (PS), and polyethyleneterephthalate (PET) materials and particulate treatment on *S. typhimurium* plate assays (Lee, Wang, & Shih, 1995). PVC was found to have the greatest mutagenicity, followed by PET, PS, and PE. Mutagenicity was associated with levels of nitropyrenes and dinitropyrenes extracted from the particulate. Ninety extractable organic compounds from plastic burning smoke were listed and quantified, with new PE containing the greatest particulate extract and residue (Simoneit, Medeiros, & Didyk, 2005). Compounds were found in the range of 5.4 to 17.5 milligrams per gram of particulate matter emitted. Elemental carbon (black carbon) emissions ranged between 7 and 68 milligrams per gram of particulate. Lee identified specific tracers emitted from plastic combustion, and named 1, 3, 5-triphenylbenzene as the the most useful chemical that can be used as a tracer for determination of plastic burning in domestic waste. (Lee, 1995).

The EPA declares that incomplete combustion in landfill fires may result in significant airborne levels of dioxins and other pollutants. (Environmental Protection Agency, 2008) Additionally, these fires contain carbon monoxide, particulate matter, and hazardous gases, and significantly high concentrations of landfill gases. EPA lists variables in landfill fire emissions as: burning material composition, surrounding waste

composition, burn temperature, and presence of oxygen. EPA adds that direct testing of emissions is the sole reliable method for estimating landfill fire emissions.

Lemieux (2004) found little data on emissions from landfills, but speculates that landfill fires, may be a major source of PCDD/F in the U.S. There were not enough data available in his research to determine emission factors, but plume concentration data were available. Still, comparisons of relative emissions of backyard barrel burning of household waste to published concentration data from landfill fires, total PCB was higher than individual PAHs in landfill fires, but individual PAHs were found in lower concentrations than from open burning in barrels, by an order of magnitude. Therefore, the authors conclude that extrapolation of emission factors from barrel burning may not be appropriate for fires from landfills and dumps, due to different combustion conditions. The Balad burn pit was reported to have burned 200 tons per day, which is probably closer to a landfill fire or dump fire condition than backyard burning in barrels. Some smaller trash burning operations at forward operating bases may fall somewhere in between. In the absence of emissions testing and determination of emission factors, municipal waste burning estimates may be a "best guess" until those studies are complete.

Electronic waste burning is a special concern and only one of four bases visited by GAO was found to comply with the prohibition of disposing of electronic waste and coated electrical wires in burn pits (Government Accountability Office, 2010). Burning electronic waste resulted in lead concentrations 20 times higher than allowed for secondary lead smelters and 200 times the U.S. regulatory limit for municipal incinerators. Fly ash analysis also revealed significant amounts of other metals and

halogens. Emission factors for particulate matter reached 17 grams per kilogram of initial disposed mass, and bottom ash was found to exceed EPA landfill limits for lead. PCDD/F emissions were 100 times higher than those found in backyard burning of household waste in burn barrels, and PBDD/F concentrations were 100 times higher than those found in burning of other polychlorinated materials.

Since the pollutant modeled in this paper is PM_{10}, an emission factor that can be used for a generation rate in atmospheric dispersion models must be selected from the literature. Table 1 is a list of emission factors for particulates from various sources and materials that may be relevant to burn pits. These values must be used cautiously, as there is large variability in emissions due to factors previously mentioned. There are numerous determinants of relative amounts of fuel consumption by smoldering and flaming combustion, resulting in significant variability in emissions, including airborne pollutant emissions, including fuel configuration, fire growth patterns, moisture content, and wind velocity. (Akagi S. , et al., 2010).

Table 1: Emission Factors for Particulates Released During Open Burning

Material Burned	Emission Factor (mg/kg burned)			Source
	PM10	PM2.5	TPM	
Household Waste, U.S. (non-recycler)	19000	17.4	not determined	Lemieux, 1998
Household Waste, U.S. (avid recycler)	5800	5.3	not determined	Lemieux, 1998
Circuit Board	not determined	not determined	15600	Gullett, 2008
Insulated Wire	not determined	not determined	17500	Gullett, 2008
Municipal Refuse	not determined	not determined	8000	EPA, 2011
Automobile Components	not determined	not determined	50000	EPA, 2011
Field Crops, unspecified	not determined	not determined	11000	EPA, 2011

Forest Residues, Unspecified	not determined	not determined	8000	EPA, 2011
Forest Residues, Hemlock, Douglas Fir, Cedar	not determined	not determined	4000	EPA, 2011
Forest Residues, Ponderosa Pine	not determined	not determined	12000	EPA, 2011
Leaf Burning (depends on species)	not determined	not determined	5000-46000	EPA, 2011
Garbage Burning	not determined	9800	not determined	Akagi, 2010

If emission factors are used to determine total exposure, then all sources must be considered at all scales, including microenvironmental, neighborhood, local, urban, regional, and global sources. Any pollution-generating source or activity that may affect exposures, whether nearby or hundreds of miles away, must be considered. Similarly, if trying to determine the contribution of a single source from monitoring, confounding pollutants at different scales must be accounted. Emission factors have been published for some military-specific sources, such as 10-100 kW U.S. military diesel generators (Zhu, et al., 2009) and unpaved road dust emissions from a variety of military vehicles (Gillies, Etyemezian, Kuhns, Nikolic, & Gillette, 2005).

Parameter	Average, per mass lost		
	Recycler	Non-Recycler	Ratio
WASTE COMPOSITION			
total daily waste (kg)	1.5	4.9	0.31
PVC in waste (kg)	0.07	0.01	7.00
paper waste (kg)	0.98	3.02	0.32
all plastics (kg)	0.23	0.36	0.64
food (kg)	0	0.28	0.00
textiles, leather (kg)	0	0.18	0.00
wood (kg)	0.06	0.05	1.20
glass/ceramics (kg)	0.1	0.5	0.20
metals (kg)	0.14	0.49	0.29
COMBUSTION RESULTS			
max. bed temp (°C)	370	740	0.50
fractoin burned (%)	66.7	49.1	1.36
unburned residue (kg)	0.50	2.49	0.20
AIR CONTAMINANT EMISSIONS		(mg/kg burned)	
benzene	725	1240	0.58
acetone	190	940	0.20
styrene	310	740	0.42
total TICs[a]	4000	14400	0.28
naphthalene[b]	40	48	0.83
phenol	85	140	0.61
dichlorobenzenes	320	160	2.00
trichlorobenzenes	400	110	3.64
tetrachlorobenzenes	140	74	1.89
pentachlorobenzene	100	53	1.89
hexachlorobenzene	48	22	2.18
acenaphthylene	3.4	11	0.31
naphthalene[c]	5.2	18	0.29
phenanthrene	3.3	7.3	0.45
aldehydes & ketones	140	2800	0.05
total PCDD	0.047	0.038	1.24
total PCDF	0.22	0.0061	36
total PCB	0.97	2.86	0.34
PM10	5800	19000	0.31
PM2.5	5.3	17.4	0.30
HCl	2400	284	8.47
HCN	200	468	0.43
RESIDUALS IN ASH	µm (or ng) per kg ash		
PCDD, ng/kg	14851	1556	9.54
PCDF, ng/kg	34040	5800	5.87
PCB, µg/kg	220	122	1.80
Cr	300	92	3.26
Cu	4910	343	14
Pb	164	32	5.13
Zn	11500	721	16

Figure 2: EPA Estimates of Household Waste Composition (source: Lemieux, 1998)

Overview of Exposure Models

Models may be used for predictive or retrospective determination of exposures. Exposure models may be classified as mechanistic or empirical, and as deterministic or stochastic (World Health Organization, 2005). Mechanistic models deal with agent transportation and transformation. Mechanistic models can be considered mathematical constructions based upon physical and chemical agent properties, as well as transport dynamics both in the environment and within the organism. In contrast, empirical models are based on direct environmental measurements, for example, a multiple linear regression model of exposure based on multiple determinants, created from sampling data and known quantities of chemicals used.

In deterministic models, "a given set of input variables produces a fixed output." (World Health Organization, 2005). Stochastic models are probabilistic, and consider randomness and uncertainty in space and time. Mechanistic and empirical models may be either stochastic or deterministic, and hybrid models can be created between types.

Military environmental health professionals are often concerned with exposures at the regional, urban, local, and human scales. Linking wartime-related exposures with health effects has been a challenging endeavor. Population locations and exposures at specific locations and time frames must be documented to create this linkage, and exposures from confounding sources at different scales complicate the task. For example, determination of burn pit-specific exposures can be extremely difficult when the emission rates result in pollutant concentrations one or two orders below the concentration levels from regional, urban, and other local sources, such as dust storms,

traffic, and generators, and the sampling method used was a centrally located ambient air monitor.

Using a centrally located monitor, or a few monitors placed in "worst case" locations, may appear to be determining personal exposure by assigning ambient monitoring results to all individuals. In reality, this, too, is modeling, by extrapolating one point concentration value or an averaged monitored value to represent concentration across an entire area. In risk analysis, interpolation is inherent, whether explicit or implicit, since risk analysts currently must interpolate and extrapolate from limited sets of environmental data to geographical areas or populations. (Hargrove, Levine, Miller, Coleman, Pack, & Durfee, 1996).

Assigning one risk level determined by a single monitor or a sparse network to the entire population is probably not valid, as numerous studies have shown that in areas where there is a high density of sources, such as intra-urban or urban areas, there is significant spatial variability in pollutant concentrations (Briggs D. , 2005; Hoek, et al., 2008; Jerrett, et al., 2005; Ott, Kumar, & Peters, 2008). Urban source-specific concentrations are often highly variable even at scales less than 1 km, with concentrations rapidly leveling off within short distances, rendering point monitoring locations more appropriately classified as independent than as representative of a larger area (Wilson & Zawar-Reza, 2006; Stein, Isakov, Godowitch, & Draxler, 2007; Ott, Kumar, & Peters, 2008; Jerrett, et al., 2005). Zhou and Levy (2007) found that the "spatial extent" of mobile source impact for elemental carbon and particulate matter is on the order of 100-400 meters; for nitrogen dioxide, 200-500 meters; and for ultrafine particulate, 100-300 meters. Ambient environmental health effects have been shown to vary at highly local

scales; increased infant wheezing was found (adjusted odds ratio 2.50, 95% C.I. 1.15-5.42), in residences within 100 meters of stop-and-go bus traffic (Ryan P. , et al., 2005). In light of this research, modeling to link exposures to health effects must be done at a resolution that captures short-range differences in exposures, and the entire populous of a source-rich area should not be considered a homogeneous exposure group. Modeling at a fine scale will need to account for all significant sources, and several types of models described below may need to be combined. Though this research will combine two types of models – dispersion and interpolation, these models can be preserved as GIS layers, refined, and combined with other models as they are created.

Several methods to model intra-urban or local-scale air pollution exposures have been evaluated in the literature (Jerrett, et al., 2005; Zou, Wilson, Zhan, & Zeng, 2009). These methods include: a) proximity models, b) statistical interpolation, c) land use regression, d) air dispersion models, and f) hybrid models (Jerrett, et al., 2005).

Proximity Models

Proximity models simply use distance from a source as a proxy for exposure. For example, buffers of 1 kilometer radius may be extended from a burn pit, and populations within each successive buffer approaching the burn pit is assumed to have increasing exposure. To date, DoD epidemiological studies regarding burn pits have used simplified proximity models to determine exposure – only one buffer is used, so that if an individual is stationed within five miles from a burn pit, he or she is considered to have been "exposed" to burn pit emissions. This approach can be considered a binary proximity model, in which a person or population is assumed to be exposed if within the buffer, and not exposed if outside the buffer. This type of model has been described as "crude" and

is recommended for a base case only (Jerrett, et al., 2005). A critical review of 157 studies over 29 years that utilized proximity, dispersion, hybrid, human inhalation, and biomarker exposure assessment methods concluded that the proximity method is a questionable technique, since the assumption that increased proximity equals increased exposure may not be true (Zou, Wilson, Zhan, & Zeng, 2009).

Spatial Interpolation Models

Interpolation models use geostatistical techniques, generally performed with a Geographical Information System (GIS), and use existing (past) monitoring data to interpolate unsampled points in the area of concern, resulting in a continuous modeled exposure grid. Spatial interpolation methods may be deterministic (e.g., inverse distance weighting, natural neighbor), or stochastic (e.g., kriging, co-kriging). All spatial interpolation methods are based on the assumption that values (or concentrations) that are near a given point are more similar to that point and to each other than they are similar to distant points, a concept commonly known as spatial autocorrelation. Spatial interpolation has been called "the GIS version of intelligent guesswork" (Longley, Goodchild, Maguire, & Rhind, 2011). A comparison table between common interpolation methods summarizes these methods (Table 3).

Commonly used interpolation methods for air pollution modeling include kriging, inverse-distance weighting, and natural neighbor modeling. Wong describes these spatial interpolation methods as "weighted average" methods, and offers the same basic interpolating relationship for each (Equation 1), where z represents the contaminant concentration at an unsampled point $x_{0,}$ given a set of sampled locations x_i with values z_i, with neighboring value weights λ_i (Wong, 2004).

$$z(x_0) = \sum_{i=1}^{n} \lambda_i \cdot z(x_i) \quad (1)$$

Also,

$$\sum_{i=1}^{n} \lambda_i = 1 \quad (2)$$

The interpolation process requires three distinct steps: define the "search area," or "neighborhood," that surrounds the point to be interpolated; locate the existing observations within this search area; and weight each observed point according to the interpolation methodology used.

Nearest neighbor interpolation is a simple deterministic method: the concentration value nearest the point to be interpolated is assigned a weight of 1 (Wong, et al., 2004). For example, to determine rainfall amount at a given point, assign the amount from the nearest rainfall gauge (Longley, Goodchild, Maguire, & Rhind, 2011). ArcGIS uses a "natural neighbor" interpolation method, which applies weights to the nearest subset of neighboring samples based on proportionate areas, and has also been called "area-stealing" interpolation (Esri, Inc., 2010). An interpolation point's natural neighbors are monitoring or sampling points that lay within Thiessen polygons that neighbor the interpolation point. Thiessen polygons are built around a sampling point and all inclusive points within that polygon are closer to the associated sampling point than they are to any other sampling point in a network. For example, in Figure 4, a point to be interpolated (green) is nested in a new Thiessen polygon (orange) that is created within its neighboring polygons. The weights given by the neighboring points are determined

from the proportional area “borrowed” from each neighboring polygon, or percentage overlap.

It has been suggested that although the natural neighbor method via Thiessen triangulation does not provide estimates of error, the method produces reasonable estimates and may be more appropriate in cases where the monitoring network is sparse and error may be large (Jerrett, et al., 2005). In such cases, this may be a good method for rough estimates.

Method	Type	Output Surfaces	Speed	Exact Interpolator	Flexibility	Advantages	Disadvantages	Assumptions*
Inverse Distance Weighted	Deterministic	Prediction	Fast	Yes	Little flexibility; few parameter decisions	Few decisions	No assessment of prediction errors; bull's-eyes around data locations	None
Global Polynomial	Deterministic	Prediction	Fast	No	Little flexibility; few parameter decisions	Few decisions	No assessment of prediction errors; may be too smooth; edge points have large influence	None
Local polynomial	Deterministic	Prediction	Fairly fast	No	Some flexibility; more parameter decisions	Flexible	No assessment of prediction errors; may be hard to choose a good local neighborhood	None
Radial Basis Functions	Deterministic	Prediction	Fairly fast	Yes	Flexible; more parameter decisions	Flexible	No assessment of prediction errors; may be too automatic	None
Kriging	Stochastic	Prediction; Standard Error; Probability; Quantile	Fairly fast	Yes--without measurement error; No--with measurement error	Very flexible; assess spatial autocorrelation; obtain prediction standard errors; many decisions	Flexible with modeling tools; prediction standard errors	Many decisions on transformations, trends, models, parameters, and neighborhoods	Stationarity; some methods require a normal data distribution
Cokriging	Stochastic	Prediction; Standard Error; Probability; Quantile	Fairly fast	Yes--without measurement error; No--with measurement error	Very flexible; use info in multiple data sets; assess spatial crosscorrelation; very many decisions	Flexible with modeling tools; prediction standard errors	Many decisions on transformations, trends, models, parameters, and neighborhoods	Stationarity; some methods require a normal data distribution

* We assume that all methods are predicting a smooth surface from noisy data.

Figure 3: Comparison of Interpolators (Courtesy: Esri, Inc.)

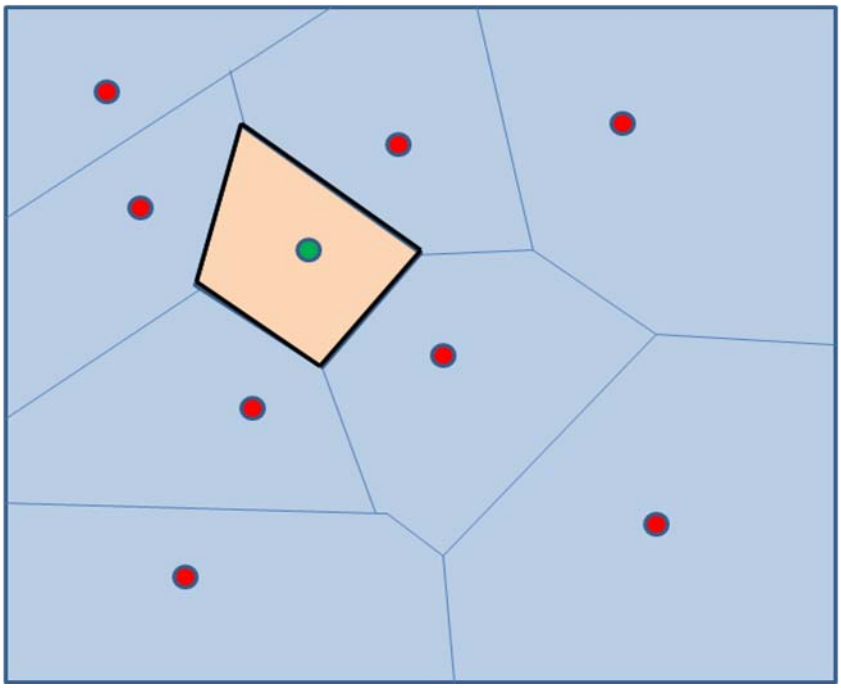

Figure 4: Thiessen polygon created around point to be interpolated

Inverse distance weighting (IDW), another deterministic interpolation method, uses monitoring points surrounding an interpolation point within a defined search area, with the nearest points weighted the most heavily. The influence of neighboring points is diminished as a function of increasing distance. Equation 3 represents the IDW model in its simplest form, where z represents the contaminant concentration at an unsampled point $x_{0,}$ given a set of sampled locations x_i with values z_i, with neighboring value weights λ_i; d_{ij} represents the distance of observations to the interpolation point, raised to the power α for distance decay, and k_j is an adjustor to ensure that the sum of weights equals 1 (Equation 3).

$$z(x_0) = k_j \sum_{i=1}^{n} \frac{1}{d_{ij}^{\alpha}} \cdot z(x_i) \qquad (3)$$

$$k_j = \sum_{i=1}^{n} \frac{1}{d_{ij}^{\alpha}} \quad (4)$$

Estimation or measurement of the distance decay is important when interpolating using IDW. This can be problematic when there are multiple sources for the same pollutant, and the distance decay differs between sources. For example, an elevated column, or stack, may release particulates at a height such that ground concentrations decrease at a much slower rate than a ground-level source in complex terrain.

Kriging has been a very common method in air pollution interpolation, as it incorporates randomness and statistical probability in the interpolation, and provides estimates of error, where deterministic methods such as inverse distance weighting and Thiessen polygons do not. Kriging, like IDW, assigns weights to measured points, but unlike IDW, weights are not solely based on distance, but also on calculated variation between observed sampling points as a function of distance (Environmental Protection Agency, 2004). Though all interpolation methods depend on spatial autocorrelation for validity, in the case of kriging, a fitted semi-variogram (quantification of spatial variation) is required. Like any statistical model, there are assumptions that must be true for kriging to be valid (Environmental Protection Agency, 2004). Spatial variation must be homogeneous throughout the area of concern, depending only on distance between sampling points. This is often not the case at urban, intra-urban, community, and neighborhood scales, where variation in source activity effects concentrations over short distances (Ryan & LeMasters, 2007; Hoek, et al., 2008). For simple kriging, there must be a known constant mean and an absence of an underlying trend. Ordinary kriging assumes an unknown constant mean based on monitored data. Universal kriging assumes a surface trend, and should only be used when decay relationship, or trend, is known.

Because of these requirements, spatial exploratory data analysis should be performed prior to kriging.

A disadvantage of geospatial modeling is the necessity of a robust sampling grid (Jerrett, et al., 2005). Interpolation methods rely on spatial autocorrelation, and determination of autocorrelation depends on an adequate number of sample points. If there are too few sampling sites in the network, spatial autocorrelation can be very difficult to determine, and resulting exposure surfaces are unreliable. Moran's I, for example, a commonly used technique to determine spatial autocorrelation, is recommended only when there are thirty or more (preferably evenly spaced) sampling sites in a grid, per the Law of Large Numbers. This can be difficult in theater, where cost and resource availability can limit efforts, but high-cost sampling methods have been supplemented with passive methods (Ott, Kumar, & Peters, 2008), and lower-cost surrogates that correlate with pollutants of concern may also be used.

A comparison of four spatial interpolation methods (spatial averaging, nearest neighbor, inverse distance weighting, and kriging) was performed on estimations of ozone and PM10 (Wong, Yuan, & Perlin, 2004). Areas with low monitor density showed little difference between methods, whereas areas with high monitor density revealed significant differences in exposure estimates. Areas with high monitor density, such as the southern California Air Basin, are likely targeted for more robust coverage due to high population densities and greater densities of point and area sources. These conditions may be expected to result in higher spatial variability between sampling points and when this variability occurs between points, and the neighboring point weighting between interpolation methods differs, the differences will show in the modeled surfaces.

Land Use Regression (LUR) Models

Land use regression models are generally used to predict urban or intra-urban exposures based on land use and traffic density. Land Use Regression is used in prediction of pollution surfaces, with topography, traffic, and site-specific geographic variables as independent variables. For example, predictors of exposure may be location within a buffered distance from a road with known traffic activity, size of a census block, population density, and elevation. Buffers are generally created based on distance decay of pollutants of interest. Geographical information systems (GIS) are commonly employed in the application of LUR models, since creation of buffers, intersections, and identifying features such as residences, within buffer zones or intersections is a basic spatial analysis function in GIS.

A review of 12 land use regression models used in six studies revealed four major classes of variables used: road type, traffic count, elevation, and land cover (Ryan & LeMasters, 2007). Of the four primary variable classes, traffic count was the most important. Another review which included 25 LUR studies added population density and climate as significant predictors (Hoek, et al., 2008). If LUR was applied to theater bases, other variables may be more important, such as number of generators or numbers of types of vehicles, road type, and waste disposal practices. R^2 model values for explanation of exposure estimate variability ranged from 0.54 to 0.81 for the regression models. In those studies, the number of sampling sites needed to create the LUR model was not as important as exposure variability between sites; there was a weak inverse correlation between number of sampling sites and explained variability.

In other words, increasing the number of sampling sites decreased the R^2. The authors explained that this effect may indicate that total number of sampling sites may be less important than capturing land characteristic variations when evaluating a monitoring network, and sampling site location may be more important than the number of sampling locations. This may also be expected in the case of burn pits and traffic patterns in theater.

There are several advantages of land use regression models. They may outperform other models in capturing small scale variability in intra-urban environments and much of the literature in which LUR is used is on the intra-urban scale in North America and Europe. LUR has outperformed or equaled both dispersion models and geostatistical interpolation models in urban environments, successfully predicting NO_2, NO_x, and $PM_{2.5}$ annual means (Hoek, et al., 2008). Both Ryan (2007) and Hoek (2008) assert that LUR outperforms spatial interpolation at urban and intra-urban scales, because at small urban scales, spatial variability is highly affected by local determinants, such as point sources and local roads, and is not modeled well by the gradually varying concentration surface that is modeled with interpolators. This is especially problematic when the sampling network is too sparse to capture that variability in interpolation methods.

The requirement for monitoring data to associate concentration with a land use characteristic is a disadvantage of LUR. Well-placed sampling sites may require fewer samples than are required for a well-interpolated model (Ryan et al, 2007), but Hoek (2008) recommends 40-80 sites. Temporal variability can also be a problem when validating a model. In the case of military operations, established bases may resemble

intra-urban areas in that there is high activity and population density at a small scale, but the LUR model would have to be built from the ground up, by inventorying suspected determinants, then monitoring to determine buffer radii. Even then, climatological factors may confound results, especially when there are temporal climatological phenomena such as frequent dust storms during a particular season, or increased seasonal agricultural biomass burning that effects pollutant levels on a regional scale. Hoek considers atmospheric dispersion models as superior in determining source contributions to total concentration, since LUR calibration depends on monitoring sites that are subject to contributions from all sources (Hoek, 2008).

Atmospheric Dispersion Models

Air dispersion models can be used for short-term or long-term exposure estimations at short or long-range scales. These can be used to predict exposures or to retrospectively estimate past exposures. Dispersion models are useful to estimate relative concentrations from a specific source, especially when other pollutants confound monitoring results. If source contributions to total exposures are important to quantify, receptor-based exposure assessments such as personal monitoring, ambient monitoring, interpolation, and land use regression may be poor choices, especially in urban environments, since they do not discriminate well when multiple confounding sources are present. Dispersion models have been called "superior" when quantification of source-specific contribution to a total concentration is required (Hoek, et al., 2008).

Dispersion models are also relatively inexpensive to run, requiring only software and hardware to create output; however, they require source emission information, which can be costly to obtain. Source emission information, meteorological data, and

topographical information are typical input requirements for these models. Though mechanistic and deterministic in nature, dispersion models, especially in the case of complex emission scenarios such as burn pits, rely on input collected by empirical and stochastic methods. Thus, error in emissions estimation, topography determination, and meteorological inputs will reflect as error in model output. A sensitivity analysis of two EPA-used dispersion models, ISCST3 and AERMOD, found a difference in modeled benzene concentrations in Houston differed by approximately 35% on average. Uncertainties in benzene emissions, however, were estimated to result in uncertainty factors of 2.8 for ISCST3 and 2.6 for AERMOD. These results indicate that uncertainty associated with emissions dominate emission model result uncertainties (Touma, Isakov, & Ching, 2006).

Not all models are appropriate for all applications – plume rise, meteorological changes, and other variables are handled well by some models but not others. Some models perform well at the local scale, but poorly at regional scales, and others excel at regional scale modeling, but are poor at local scales. For example, Computational Fluid Dynamics dispersion models are very useful when dealing with complex terrain, such as metropolitan neighborhoods with large buildings, where complicated flow and turbulence scenarios can be expected. At larger scales, however, the computational effort required to run these models may outweigh the benefit derived. Also, dispersion models require varying depth of expertise in meteorological processes.

The U.S. EPA maintains a website dedicated to documentation and guidance on air quality models, complete with computer code, processors, and input information (Environmental Protection Agency, 2010). These models, however, are evaluated by the

EPA for adequacy in determining regulatory compliance with National Ambient Air Quality Standards (NAAQS). There are other models available and the selection of an appropriate model depends on objectives and conditions of use. EPA-"Preferred/Recommended" models for determination of compliance include the AERMOD Modeling System, a steady-state dispersion model based upon turbulence structure of the planetary boundary layer and scaling concepts, which models surface and elevated sources, and can model in both simple and complex terrain environmentsand the CALPUFF Modeling System, which is a non-steady state Lagrangian puff model simulating time- and space- dependent variations in meteorological conditions on atmospheric pollutant transport. (Environmental Protection Agency, 2010). AERMOD is recommended for short-range dispersion where steady-state Gaussian plume assumptions are appropriate, with a range up to 50 kilometers (Code of Federal Regulations, Title 40, Part 51, 2005). For regulatory modeling, CALPUFF is recommended for long-range use with a range of 50 to several hundred kilometers (Code of Federal Regulations, Title 40, Part 51, 2005), though it is also designed for use at scales at tens of meters. Both models require both surface and upper-air meteorological data, preferably on a fine scale for an airbase-sized installation. A search for archived data, both open-source as well as on DoD weather systems (14 WS (US Air Force 14th Weather Squadron), 2010) that are ready to be processed through the meteorological pre-processors for each system turned up empty and preparation of surface, upper-air, and terrain files for meteorological processing requires training and expertise.

There are other notable dispersion models that have been used for exposure assessment, listed by the EPA as "Alternative Models" (Environmental Protection

Agency, 2010). The Atmospheric Dispersion Modeling System (ADMS-3), is an advanced model for determining continuously emitted concentrations from point, line, area, and volume sources, or discrete emissions from point sources. It handles complex terrain, plume rise, and a range of averaging times. The current version offered by the software vendor is ADMS-4, and is available as commercial off-the-shelf software for a price.

ISC3, which was replaced by AERMOD as the EPA model of choice, is a steady-state Gaussian plume model designed to determine compliance from industrial complex sources. It handles point, line, area, and volume sources, and also models plume rise. Both short-term and long-term versions are available. SCREEN3 is a worst-case screening version of ISC3. Code for both models is available on the "Alternative Models" website.

The Open Burning Open Detonation Model (OBODM) was created specifically for modeling of open detonation and open burning of military equipment, and handles plume rise and dispersion for both instantaneous and "quasi-continuous" sources. Modeling with OBODM is restricted to daytime hours.

The Second-Order Closure Integrated PUFF Model (SCIPUFF), which is the dispersion model used in the Defense Threat Reduction Agency software Hazard Prediction Assessment Capability (HPAC), is a validated Lagrangian puff model that uses a collection of Gaussian puffs and predicts three-dimensional time-dependent concentrations. SCIPUFF can use surface observation files, upper air observations, and gridded three-dimensional meteorological data. It is appropriate for both short-range and long-range applications. SCIPUFF is flexible in options for meteorological input, which

makes it more useful when retrospectively modeling dispersion with limited availability of meteorological information; a plume can be created with a single "fixed" wind with constant speed and direction. A public domain version of PC-SCIPUFF Version 1.2 is available at http://www.sage-mgt.net/services/modeling-and-simulation/pc-scipuff-download.

The EPA website dedicated to atmospheric models is not all-inclusive. There are other dispersion models commercially available and many are downloadable as freeware. Some been validated more extensively than others and each has its own advantages and limitations. The National Oceanic and Atmospheric Administration (NOAA) Air Resources Laboratory PC-Windows based HYSPLIT (Hybrid Single Particle Lagrangian Integrated Trajectory) model is commonly used to calculate back-trajectories in source analyses and also has a dispersion model. There is also a web version for forecast and archive analyses. HYSPLIT offers several advantages, including that it contains integrated meteorology and expertise in manipulating weather files is not required. It is also free and tutorials, documentation, and training are readily available. HYSPLIT dispersion isopleths are readily exportable into Google Earth and ArcGIS formats. A disadvantage is that meteorology files are large (global meteorological data sets are approximately 600 MB each, and cover one week) and take time to download via file transfer protocol server. Also, although fine resolution meteorology is available for North America, global archive meteorology from NOAA servers is at a low resolution. The Global Data Assimilation System (GDAS) has a 1-degree resolution, and while most dispersion models are limited by hourly observation data, GDAS is run only four times

per day, at 00, 06, 12, and 18 UTC (National Oceanic and Atmospheric Association, 2010).

The CAMEO/ALOHA dispersion model is a popular Gaussian plume model commonly used for short-term emergency response applications and is also used for predictive emergency modeling in vulnerability assessments. It is bundled with the MARPLOT mapping software, which does not contain global maps. Also, ALOHA does not model particulate dispersion (Environmental Protection Agency; National Oceanic and Atmospheric Association, 2007).

At the local scale, when modeling dispersion from a single source, steady-state Gaussian plume models are the usual choice and the plume centerline is assumed as a straight line that is aligned with wind direction as reported by a meteorological station (Touma, Isakov, & Ching, 2006). Non-steady state puff models are preferred when complex wind fields are expected, such as in complex terrain scenarios, or for urban areas with paved areas between rows of tall buildings, in highly uneven terrain, on coastlines, or in forested areas, , as they are suited to allow different wind speeds and directions across the area to be modeled. "Complex terrain" is defined by the EPA as "terrain exceeding the height of the stack being modeled" (Code of Federal Regulations, Title 40, Part 51, 2005). A ground-level release, or a below-ground level release, such as a burn pit release, then, is considered a release in "complex terrain" unless there are no terrain features higher in elevation than source-level. Buoyant plume rise considerations, however, can result in lift of a plume to levels higher than the level of release.

Air dispersion models can be used alone or combined into hybrid dispersion models. "Hand-off" between optimal portions of dispersion model types has been used

successfully. Combinations of methods can be used to strengthen predictive accuracy of exposure models. Hybrid models have been used successfully in epidemiological studies linking exposure to disease, including combinations of air dispersion models and ambient or personal monitoring; regional grid and local plume dispersion models; and regional, urban, and local model combinations (Zou, Wilson, Zhan, & Zeng, 2009).

Dispersion of dioxin from burning oil from the BP Deepwater Horizon spill in the Gulf of Mexico was modeled with a combination of AERMOD, to model short-range dispersion, and HYSPLIT, to model long-range dispersion and deposition (Schaum, et al., 2010). In another study, a hybrid modeling approach was used to model ambient benzene concentrations, resolving contributions from regional and urban scales to urban locations in Houston (Stein, Isakov, Godowitch, & Draxler, 2007). In this study, a combination of the Community Multi-Scale Air Quality Model (CMAQ) was used to determine background concentrations, and HYSPLIT and AERMOD were used to determine spatially resolved concentrations from local sources. Meteorological fields created by the high-resolution (1km x 1km) Mesoscale Model 5 (MM5) were used to optimize model resolution. The predicted high-resolution urban concentrations from the hybrid model outperformed modeling by CMAQ alone when compared to monitoring results at six locations.

Hybrid/Integrated Exposure Models

An integrated exposure monitoring system was suggested by Clench-Aas (1999). This system provides identification of most exposed populations, the number of people exposed to concentrations exceeding guidelines, subgroup population exposures, predictions of abatement effects, establishment of risk assessment and management

programs, and epidemiological studies of short and long-term effects. The dynamic exposure assessment model (DINEX) included dispersion calculations, adjustment with monitored measurements to account for local or regional effects, exposure modeling considering time-activity information, information storage in a database, and analysis and display in GIS, all in one software package, named "AirQUIS." This system was to include both manual and automatic data entry, on-line monitoring availability, a monitoring database for both meteorology and monitored results, consumption and emission inventories, dispersion models, a population exposure effects module, statistics modules, and import/export functionality. All of these elements were to be integrated into maps.

Jerrett emphasized the limitations of personal monitoring alone, citing the high cost, low numbers of observations, high sample biases, and the need for people to wear samplers and keep a record of activities and locations. Instead, he suggested that hybrid approaches should include both personal monitoring and another type of modeling, such as land use regression, dispersion modeling, or interpolation (Jerrett, 2005). Zou reviewed 157 studies on exposure modeling, including four classifications of hybrid models: personal monitoring and regional monitoring; dispersion modeling and regional or personal monitoring; local plume and regional grid modeling; and local, urban, and regional models (Zou, 2009). Zou states that the main advantage of hybrid models is greater accuracy in exposure estimation, by integration of regional and personal monitoring data. Zou also suggests using regional monitored background concentrations and combining results with local models. This would be highly beneficial in burn pit exposure modeling, since regional ambient concentrations of particulate are very high

and temporally variable, and may mask the relatively minor particulate contributions from burn pits.

The EPA has embarked on a research program to integrate regional and local scale air quality modeling to determine human exposure (EPA, 2010). According to their white paper on the program, the EPA's Atmospheric Modeling and Analysis Division (AMAD) is progressing on a project in which data from regional and local-scale modeling and monitoring campaigns are blended to provide concentrations that are specific to desired spatial and temporal scales in support of health studies and exposure assessments.The advantages of data blending are listed as follows:

> 1) produces accurate, spatially resolved estimates of the daily air pollution field at receptors of interest within a metropolitan area;
> 2) harnesses the strengths and compensates for the weaknesses of each data source; accounts for bias in the numerical models;
> 3) accounts for spatial and temporal dependence; and
> 4) avoids the limitations of other statistical methods.

Model Integration and Linking Exposure to Disease in GIS

GIS provides extremely useful information when modeling spatial information, such as environmental exposures and disease patterns across an area. Graphical display of models across a map of interest allows immediate and direct visual association of concentrations and land features, including population locations, and may also indicate source information. GIS can also help visualize process dynamics, and can help predict exposures by examining exposure trends over time.

The EPA recognizes the ability to combine geographical data layers as a key strength of GIS, where various combinations of information can be displayed on a map quickly and easily (Environmental Protection Agency, 2004). EPA also touts the

flexibility that GIS allows in working with broad classes of layers, and the ability to view combinations of spatial information "in abrupt fashion." For example, quarterly changes due to seasonal wind differences in a pollutant plume emanating from a source can be combined with work or residence locations of people who make emergency visits to hospitals due to acute respiratory effects.

In this way, overlaying maps of population locations and exposure can help identify populations at different levels of risk. Exposure mapping in GIS can be accomplished by several means, including interpolation, dispersion model isoplething, land use regression mapping, simple proximity modeling, or, as Hargrove (1996) proposes, by displaying monitoring result charts directly at monitor points on a map. Combinations of these methods can be displayed alone as layers or together in a GIS. Jarup states that disease mapping can be performed in GIS by using cluster analysis tools (such as those included in ArcGIS), to display baseline health data, and to reveal spatiotemporal disease patterns (Jarup, 2004). Linking exposure and health effects, however, depends on the accuracy of the exposure assessment in addition to the elapsed time between health effects and exposures. As latency times increase, exposure is more difficult to associate with disease. Jarup concludes that dispersion models, validated with monitored data, and displayed in GIS, are superior to proximity models, and that maps are more powerful than tables in communicating geographical risk differences.

In a 15-study review, the following steps in the exposure assessment process, which are also required for environmental epidemiological studies, were aided by the use of GIS: (Nuckols, Ward, & Jarup, 2004):

a) defining the study population,
b) identifying source and potential routes of exposure,

c) estimating environmental levels of target contaminants, and
d) estimating personal exposures.

Epidemiological studies are only enhanced, however, when the data used to produce the exposure assessments are accurate and valid. Nuckols states that "garbage in, garbage out" remains true in GIS modeling, and that "mapped garbage is still garbage." In a case possibly resembling burn pit scenarios, an epidemiological study involving landfill sites was performed, using data that was not useful in exposure assessments. Landfill waste characterization was not performed and volumes of disposed trash were not recorded. Types of waste disposed were assumed to be in accordance with landfill operator license types (hazardous/special versus non-hazardous). Monitoring data for specific emitted chemicals were not collected, and extent of contamination was unknown. The determination of "exposed" was based solely on published information from previous studies (a simple 2 kilometer proximity buffer), and a common relative risk was assigned to all landfill sites, regardless of other conditions. Nuckols deemed that a lack of validation of exposure metrics used in the study, namely, a lack of validation of source information and spatial concentration information, led to misclassification of exposures.

Nuckols presents a contrasting lung cancer epidemiological study in which adequate source emission and monitoring data were available to calibrate and validate predicted concentrations of NO_2 in Stockholm (Bellander, Jonson, Gustavsson, Pershagen, & Järup, 2001). Study participant locations were also validated using geographical service companies. The authors were able to predict lung cancer risk for the period 1955-1990 due to traffic-caused exposure to NO_2 with a 95% confidence limit.

In another paper exposing the potential of GIS exposure modeling to enable environmental epidemiology, a step-by-step process to reconstruct past exposures was

presented, based on a review of exposure reconstruction literature (Beyea and Hatch, 1999):

1. Determine which pollutants are to be modeled
2. Review pollutant usage history; review nature of environmental releases
3. Determine time frame and population
4. Quantify source release rates over time
5. Determine major exposure pathways to the study population
6. Choose a transport model for each pathway
7. Determine whether additional modeling is needed
8. Convert concentration to dose or integrated exposures
9. Ensure convenience in applicability of results to epidemiological analyses

The first step implies knowledge about emissions from a process. If a process has unknown emissions, then modeling cannot continue. The second step, "review pollutant usage history," involves determining historical chemical or substance usage, and modeling dispersion of releases for the defined time range. For burn pit exposures, this would entail reviewing logs of burn start times and materials burned. Unfortunately, these do not exist. In step three, "determine time frame and population," the study time range is to be defined; for burn pits, this would include those periods for which the pits are in operation. The population to be modeled will generally be the base populous, though there may be circumstances, such as congressional or executive interest, in which off-base populations may also be modeled. For open burning, the fourth step, "quantify pollutant release rates," is not possible without some knowledge of emission factors. A literature review will provide some detail on emission factors for specific categories and

types of waste, but there are no published emission factors for the open burning of military waste with recycling versus non-recycling. The fifth step involves determination of pathways and exposure media, such as air, soil, water, and food, and routes of entry, such as inhalation, contact, absorption, and ingestion. In the sixth step, transformations during transport are considered. This is especially important in the case of reacting or aggregating pollutants. In step seven, information from the previous steps is examined to determine whether additional modeling components that are not readily available are required. Step eight is a conversion of concentration units to dose, so that a dose comparison can be made between exposed populations, and health effects related to dose can be determined. Step nine entails clear presentation of model results, error, and validation.

GIS applications can aid this process in several ways, according to Beyea and Hatch (1999). They can provide estimates of variability and magnitude of exposure across populations, and are especially helpful when multiple sources are present. Geographic modeling can also assist in creating questionnaires. For example, one may wish to inquire about proximity and time spent near a visible feature. Also, GIS can aid in the sampling strategy by revealing areas that may be expected to be high or low in variability based on features and land use. Additionally, GIS may help in modeling multiple sources that are sufficiently close to each other to merge their impacts. Past exposure maps can be compared to present ones, revealing differences in exposure estimates over time and pointing to possible source differences. Population migration can also be tracked in GIS; for example, a layer of buildings for a deployed location in

2004 may be considerably different than a layer of buildings for that same location in 2008, especially with significant troop buildup.

Integrated, dynamic modeling has been encouraged, in which the modeling of temporal patterns is accomplished with dispersion models, source attribution to total exposures, and population dynamics combined in GIS, so that exposure can be estimated real-time, as people move through varying environments of differing concentrations (Briggs D. , 2005). Hargrove suggested that dynamics can be easily visualized in a spreadsheet format, with images of GIS-interpolated exposure surfaces, meteorological patterns, dispersion model plumes, population movements, or some combination of these, displayed in rows and columns over time, instead of numbers (Hargrove, 1996). Briggs and Crabbe emphasize that matching pollutant patterns with time-activity patterns are crucial to accurately determining environmental exposures (Briggs, 2005; Crabbe, 2000). If most of the pollutant contributing to monitor results occurs during times when people are away from that area (e.g., at work or in school) and residential locations are used as a proxy for exposure, then exposure will be misclassified. Capturing the dynamics of both study populations and pollutants are necessary to determine risks, and to link exposures to health effects. Capture of movement patterns can be simple, by geocoding work and living locations of individuals, and recording times spent in each by use of questionnaires (Crabbe, 2000), or by tracking individuals considered to be "representative" of the exposure groups with portable GPS devices (Nuckols, 2004).

Ambient Exposure Modeling Studies

There are numerous studies in which dispersion models or interpolation models were used alone or within GIS to assess or predict exposures, or to perform

spatiotemporal epidemiology. Several recent studies combine dispersion models with other models in GIS. A few relevant papers were reviewed to obtain insight in exposure assessment methodologies in GIS and to determine the optimal ways to visualize and model burn pit exposures in GIS.

The AERMOD dispersion model and ArcGIS were used to study air pollution and asthma in the Bronx, New York City (Maantay, Tu, & Maroko, 2009). Five pollutants (PM_{10}, $PM_{2.5}$, NO_x, CO, and SO_2), were modeled in AERMOD from stationary sources. Terrain information, such as building locations and heights, elevation, population data, and source data were processed in GIS, and imported into AERMOD. Since AERMOD dispersion isopleth files contained only a few concentration isopleth values and discarded gridded point data, the isopleth files were discarded in favor of gridded concentration values. The process of running a separate model outside of a GIS, then importing gridded values for modeling within GIS, is called "loose-coupling." Kriging interpolation was performed in GIS on 9000 gridded AERMOD-generated values to create a continuous exposure surface and a "plume buffer" was created with the highest concentrations modeled by AERMOD. Asthma rates inside the plume buffer were compared to asthma rates in a simple proximity buffer. Higher asthma hospitalization rates were associated with residence within the plume buffer.

Having discussed model limitations previously, two limitations are evident in this study. First, residence within the plume buffer is a proxy for exposure assumes that people living in the area are in contact with the pollutants. This may not be the case, if peak pollutant levels occur when much of the population is at work or in school. Also, though a high-resolution state-of-the-art dispersion model was used, reducing the output

to a single buffer creates a simple binary proximity model – a refined binary proximity model that does not assume isotropy, but a binary model nonetheless.

It should be noted that several other commonly used dispersion models are similar to AERMOD, in that their isopleth outputs only include a few concentration values along which isopleth lines run, which is not an optimal format for interpolation in GIS. HYSPLIT and SCIPUFF work in the same way. SCIPUFF, however, provides a simple method for exporting ASCII files with gridded and geocoded concentration data, and are easily imported into ArcGIS. HYSPLIT provides isopleths that can be imported directly into ArcGIS or Google Earth, but concentration at a single point of interest is simply assigned the isopleth value for the isopleth that it falls within, rather than the actual modeled concentration.

Another study modeled particulate dispersion of open burning of piled beetle-infested pine trees in the Prince George, British Columbia airshed (Ainslie & Jackson, 2008). The CALPUFF dispersion model was used to determine safe burn areas, and although the dispersion was not imported into GIS, land features and land use characteristics were imported from GIS into CALPUFF. An iterative process was used, in which the city center was located, and radial distances from the city center were located. Dispersion models were run at each point location using three years of historical meteorological mean conditions. Modeled pollutant concentrations that may lead to overall particulate exceeding regulatory limits to downwind populations, and safe areas for burning were determined.

Limitations of this study are related to the lack of loose-coupling the dispersion output into GIS. First, demographic information from GIS can help identify populations

that are at higher risk; for instance, locations where elderly people may be clustered, as well as high-density population areas. The second point, related to the first, is that in GIS, with demographic information and epidemiological information, a prediction of numbers of increased numbers of people with health effects can be made. Compliance with air quality standards is important, but protection of health is the desired result of standards in the first place.

An assessment of The Air Pollution Model (TAPM), an intra-urban Integrated Meteorological-Emission (IME) model, was performed by comparing modeled and monitored PM_{10} results from a dense monitoring network in Christchurch, New Zealand, to model exposures for use in epidemiological cohort studies (Wilson & Zawar-Reza, 2006). TAPM is an off-the-shelf, Windows-based mesoscale dispersion modeling software package that contains a Lagrangian particle model for point sources, and a dust module that handles PM_{30}, PM_{20}, PM_{10}, and $PM_{2.5}$. Isopleth plots were constructed by importing results into ESRI ArcMap 9.0, and using the spline interpolation in the spatial analyst extension, creating a continuous surface so that model points could be compared with monitoring points. The model performed well, with the mean observed (monitored) concentration equal to 42.9 $\mu g/m^3$ and the mean modeled concentration equal to 43.4 $\mu g/m^3$, with good agreement at individual sites.

The TAPM study showed that a high-resolution dispersion model using accurate source emission and terrain information can provide accurate predictions of pollutant concentrations, but there is a time and computing cost; computer runtime was 5 days for each simulation on a 1.6 GHz processor. Without accurate emission information, the benefit may not be worth the cost.

A geostatistical software package to create an arsenic and copper soil concentration surface by kriging monitored results from 83 sampling sites in proximity to an incinerator source (Williams & Ogston, 2002). It was found that to adequately create an interpolated surface of the entire risk area, a prohibitively large and expensive sampling grid network would have been required. Since wind direction frequency predicted a strongly southeastern trend, creating a narrow concentration plume and a highly diluted proximity buffer, a sampling strategy based on dispersion and meteorology-predicted pollutant was recommended.

Plume dilution from World Trade Center collapse-generated particulate was modeled with CALPUFF, and computational fluid dynamics models were run with the Colorado State University RAMS-HYPACT meteorological-dispersion package (Huber, 2004). Since emissions were unknown, the models were not able to estimate pollutant levels. Instead, a large release was modeled to determine where the plume traveled through time, to determine populations at relatively greater risk for epidemiological study. A wind rose centered at Ground Zero was combined with the CALPUFF dilution map to assist in visualization of plume dilution and determination of areas at higher risk. To provide ambient input for the EPA's Statistical Human Exposure and Dose System (SHEDS), model simulations were combined with results from the existing $PM_{2.5}$ monitoring network. A World Trade Center-specific geodatabase was recommended to support further exposure assessment and epidemiological efforts.

In another example of a retrospective study where emission quantities were unknown, a diffusion equation based on local mean meteorological frequencies was used to create quartile isopleths around an asbestos plant in Hashima, Japan (Kumagai,

Kurumatani, Tsuda, Yorifuji, & Suzuki, 2010). Since concentrations could not be determined without emission information, "relative asbestos concentrations" were estimated (in units of m^{-3}). Increased risk of lung cancer mortality was associated with residence within the highest relative concentration isopleth, after controlling for smoking, domestic exposure, and occupational exposure.

In a final example, resource constraints and unknown emissions from a refinery prevented direct environmental monitoring and local-scale dispersion modeling of airborne pollutants. Instead, a simple meteorologically estimated exposure (MEE) calculation was performed to determine individual dose to school children in a defined school district area, to emissions from a petrochemical refinery, in order to determine increased risk of asthma symptoms (White, teWaterNaude, van der Walt, Ravenscroft, Roberts, & Ehrlich, 2009). The MEE was determined with an equation based on wind direction, wind velocity, and the annual proportion of each velocity. GIS was used to map residence locations, overlay the annual wind rose, and determine straight line distance from the point source to each residence. The MEE was highly predictive of increased risk for asthma symptoms, with an odds ratio of 8.92 for frequent waking with wheezing (95% C.I. 4.79-16.63). Distance from the source alone was not associated with any video questionnaire responses in the epidemiological study, but MEE was significantly associated with six asthma-related symptoms.

Climatological Issues

According to the National Center for Medical Intelligence Iraqi summers (May-October) are dry, hot, and cloudless, with temperatures that can routinely reach a daily high of 44°C (111°F) and an extreme evening low of 6°C (43°F) (NCMI, 2006),. Winter

temperatures (November-April) range from 2°C (36°F) to 31°C (88°F). The wettest and most humid season period is from December to February. Between December and April, heavy rains have resulted in flooding of low-lying areas (14 WS (US Air Force 14th Weather Squadron), 2010).

Prevailing winds throughout the country are generally from the northwest, with a second prevailing wind from the southeast. In June through September, wind directions occur more frequently from the west and northwest, and higher wind speeds are more frequent, than in other months. The months of December through May see significantly greater frequencies of southeastern winds.

Monitored PM10 exceeded 1,000 micrograms per cubic meter and approached 10,000 micrograms per cubic meter on days in which major dust storms blanketed the region (Vietas, 2008). In some areas, visibility was reported as reduced due to dust for more than 50 percent of days (Kutiel, 2003). In addition to safety problems from reduced visibility, dust storms contribute to respiratory illness, reduced soil fertility, crop damage, inefficiency of solar devices, and equipment damage (Kutiel, 2003). The problem appears to be worsening, with the 2009 storm called "the worst in recent memory" (Mohammed, 2009), and caused 300 hospital visits to *one hospital* in Baghdad. Dust storms are likely to be a significant confounder in attempts to model source-specific particulate.

III. Methodology

The general procedure in creating the exposure model is depicted in Figure 5:

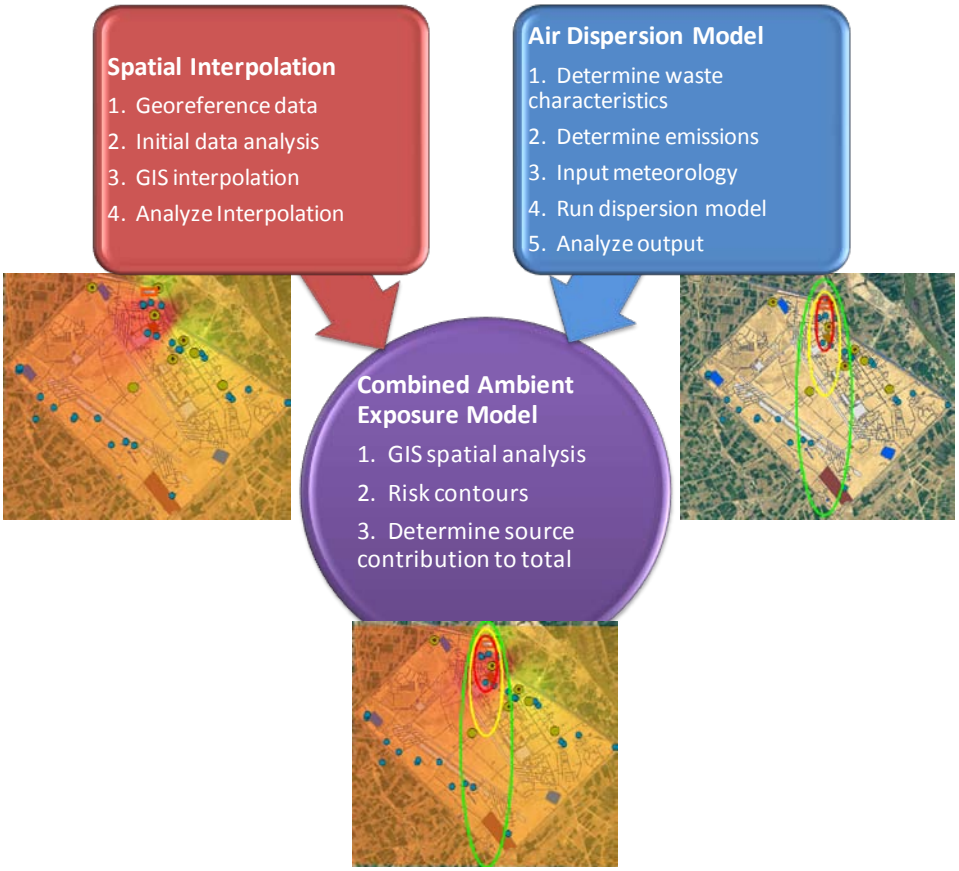

Figure 5: Combined Spatial Interpolation and Dispersion Model Mapping Process

1. Collect, georeference, and perform initial analysis on monitoring data
2. Perform spatial analysis and create interpolated exposure maps with monitoring data
3. Determine or estimate emission rates

4. Model plume rise and dispersion; estimate specific source contribution

5. Overlay drawn dispersion modeled isopleths over interpolated exposure maps

6. Determine high risk intersections between monitored and modeled data

The U.S. Army Public Health Command (Provisional) provided georeferenced particulate monitoring data used in this research. The datasets provided ranged from 2003 to 2010. Exploratory data analysis of monitoring data was accomplished with Microsoft Excel 2007, JMP 8 statistical software and Esri ArcGIS Desktop 10 Geographical Information System software (*ArcGIS 10*, 2010).

Geographical information was obtained from Air Combat Command (ACC) A7ZG Installation Geospatial Information and Services GeoBase, available on the Air Force Portal (U.S. Air Force, 2010). ArcGIS Desktop Version 10 with Spatial Analyst and Geostatistical Analyst extensions were used to create the spatially interpolated exposure surfaces based on mean concentration values from the monitoring data.

The atmospheric dispersion models used were Second-order Closure Integrated Puff Model (SCIPUFF) for grid plotting. The dispersion model table outputs with concentrations at assigned grid points were spatially interpolated in ArcGIS using the radial basis function tool in the Spatial Analyst extension. Plume height due to buoyant rise of heated air was determined with the Simple Approach Smoke Estimation Model (SASEM 4.0) program.

Receptor areas were determined with satellite imagery of the base. Layers created in ArcGIS were exported into Google Earth-compatible files with the Layer to KML Conversion Tool in ArcGIS, and imported into Google Earth, which has superior satellite imagery compared with Bing Maps images native to ArcGIS, or GeoBase images on the

Air Force Portal. Dispersion model isopleths of increasing concentrations were overlaid on the spatially interpolated model from monitoring data. Sampling sites were labeled. These layers – sampling sites, receptor zones, interpolated concentration isopleths from monitoring, and atmospheric dispersion model isopleths, were combined into one map to allow instant comparison of modeled burn pit-specific concentrations (atmospheric dispersion), and monitoring results (spatial interpolation of monitored data). Also, inclusion of sampling sites and receptor zones on the map allows visualization of sampling grid shortcomings.

Hourly weather observations from the Balad Air Base weather station (KQTO) for use in the HPAC model were obtained from the 14th Weather Service website (14 WS (US Air Force 14th Weather Squadron), 2010).

Data Sources

Existing Monitoring Data

Initially, the USACHPPM/AFIOH screening report on burn pit exposures was reviewed. While particulate matter results exceeding the 1-year Air-Military Exposure Guidelines were listed, a comprehensive listing was not included (Vietas, Taylor, Rush, & Deck, 2008). Ambient air monitoring results and reports from Balad were then queried in the Defense Occupational & Environmental Health Surveillance Portal (DOEHS) Document Library, and 56 documents were returned and downloaded. Site locations were not georeferenced, and in most cases, the specific sampling locations were not listed on sampling result spreadsheets; rather, most were labeled simply as “Balad” or “Anaconda.”

An official list of georeferenced sample locations with PM_{10} and $PM_{2.5}$ results from 2003 to 2010 (Appendix A) was provided by the U.S. Army Public Health Command (Provisional) by request. These were 24-hour samples taken in theater at ambient monitoring sites, with particulate high-volume air samplers. Specifics on the sampling methods used are in the screening reports (US Army Public Health Command (Provisional), 2010; Vietas, Taylor, Rush, & Deck, 2008). Not all samples on this list were georeferenced. Since geographical coordinates on sample locations are required for spatial data analysis in this research, only the georeferenced subset was used for data analysis.

Geographical Information

Sampling locations with coordinates were provided by U.S. Army Public Health Command (Provisional), by request. Thirty sites were included from around the base and the geographical coordinates of all georeferenced sampling sites between 2003 and 2010 are shown in Appendix B. These may not represent the entire set of ambient air sampling sites at Balad; some sites may not have been documented with coordinates.

Maps, shapefiles (*.shp), and database files (*.dbf) for Joint Base Balad were downloaded from the Air Combat Command (ACC) A7ZG Installation Geospatial Information and Services GeoBase, available on the Air Force Portal (U.S. Air Force, 2010). Installation area, buildings, water body locations, roads, and flightline were layers used in maps. The geographic coordinate system for the downloaded maps was World Geographic System (WGS) 1984 and the datum was WGS 1984. The projected

coordinate system was WGS 1984 UTM 38 N (Transverse Mercator projection), with false easting of 500000.

Dispersion Modeling Software

The screening model, Simple Approach Smoke Estimation Model (SASEM), version 4.0, and documentation, were downloaded from the Arizona Department of Environmental Quality website, http://www.azdeq.gov/environ/air/smoke/fires.html. The EPA Alternative Model PC-SCIPUFF dispersion modeling program, Version 1.2 and its documentation, were downloaded from Sage Management (2010).

Meteorology

Site-specific METAR data for the weather station located on Joint Base Balad was obtained from the Air Force Weather Agency 14th Weather Squadron's website database (registration required), for the period of interest (14 WS (US Air Force 14th Weather Squadron), 2010). Wind roses and meteorological averages from 2003 to 2009 were also downloaded from the same database.

Exploratory Data Analysis

Microsoft Excel 2007 and the JMP, Version 8.0 statistical software package were used for exploratory data analysis. Excel was used to determine the number of samples taken at each site, per month, and per year, to determine random sampling over the spatiotemporal domain. Variability charts were created with JMP, to visualize variability within and between days, months, and years. Arithmetic means and standard deviations (SD), as well as geometric means and standard deviations (GM and GSD),

were calculated in Excel. The frequency distribution of concentration was produced in JMP, and outliers were identified with the histograms.

Sample locations were imported into ArcMap, using number of samples as an elevation attribute to help visualize numbers of samples taken at each site across the spatial domain.

The Moran's I tool was attempted, but there were fewer sampling points available than recommended by the method (i.e., 30), and spatial autocorrelation could not be determined using this tool. ArcMap was also used to analyze elevation to allow visualization of possible low-lying areas, and to determine whether terrain was relatively flat or uneven. This information was necessary, because meteorology and dispersion is affected by terrain, and choice of dispersion model, as well as choices within a dispersion model, depend on terrain flatness or irregularity. An elevation isopleth map of Joint Base Balad was created with ArcMap.

Spatial Analysis

ESRI ArcMap 10 with Spatial Analyst extension was used to interpolate continuous concentration surfaces using monitoring data, for the purpose of creating monitored exposure isopleths and visualizing spatial heterogeneity in concentration. There are several software packages available for spatial modeling, including two packages that are free: the Spatial Analysis and Decision Assistance model, funded by the EPA and the Nuclear Regulatory Commission, and developed by the University of Tennessee (University of Tennessee, 2007), and GeoDa, a spatial statistical package developed by Arizona State University (Arizona State University). ArcMap 10 was

selected for several reasons, including user training and familiarity, ease of importing shapefiles and geocoded data from several formats without extensive processing, ease in working with several layers simultaneously, and the ability to produce maps with numerous options in graphical display of modeled data.

Spreadsheets were created with individual sampling sites as features, georeferenced with decimal degree coordinates for (x, y) locations. A map of sampling sites was created in ArcMap, and straight-line distance was determined with the ArcMap distance tool for sites with n>3 from 2007-2008. Sites were also tagged in Google Earth imagery to reveal sample locations in relation to possible population locations by visual association with high-resolution satellite imagery.

PM10 air sampling results tabulated with sites that had been sampled at least three times ($n \geq 3$) for the 2007-2008 monitoring period. Geometric mean (GM) was used as the elevation value for spatial interpolation. The georeferenced data were imported from the spreadsheets directly into ArcMap. The Inverse Distance Weighting tool from the ArcMap Spatial Analyst extension was used to interpolate continuous concentration surfaces. The inverse distance weighting method was chosen because it is fast, and does not make assumptions about the data. Since extremely high temporal variation was expected to have skewed site results, and there was low confidence in the site geometric means due to high variability and low within-site sample sizes, interpolators that would ordinarily be more useful in providing error and predicting concentrations, such as kriging, were not used. As previously mentioned, the predictive value of kriging depends on fitting a semivariogram, and using ArcGIS to observe geometric means for this data set indicated a lack of a pattern in semivariance as a function of distance. This is also

apparent when looking at the maps. The guard tower, which is the closest point to the burn pit, is consistently lower in concentration, while points farther away are higher in concentration. Concentration isopleths were created at designated concentration intervals to indicate areas of higher modeled concentration from the monitored interpolation.

Dispersion Modeling

Plume rise was calculated with SASEM Version 4.0 software, based on average monthly wind speed, piled hardwood fuel, and 10 burning piles, each consisting of 300 cubic meters of fuel, assuming ten simultaneously burning heaps of hardwood measuring 10 square meters in area and three meters in height. There is uncertainty in these estimates, as there are no records of burn patterns or quantities except for approximate daily total amounts burned. Waste composition and burn patterns are likely to have varied significantly, and plume rise likely fluctuated along with fire dynamics. It is difficult to determine an "average" plume height, SASEM was used to obtain a range from which a conservative height could be selected for modeling. SASEM was selected for calculation of plume rise, due to its simplicity, speed, production of desired concentration, distance, and plume rise parameters, and its incorporation of Briggs' plume rise equations. SASEM bases heat release rate on the type of fuel burned and material configuration.; For example, a broadcast (spread) area of grasses produces a different plume than a piled area of hardwood (Riebau, Fox, Sestak, Dailey, & Archer, 1988). There is additional uncertainty in the SASEM modeling for these purposes, as emission factors and heat release rates are determined based on hardwood burning. A literature search revealed no results for heat release of military waste burning or other

mixed wastes that resemble military waste composition, although a U.S. Department of Agriculture study of heat release rates of wood-plastic composites showed increasing heat release rates with increasing mass concentrations of plastics (Stark, White, & Clemons, 1997). Higher burn temperatures would correspond to higher plume rise and lower concentrations. However, to be conservative, plume rise was calculated based on burning hardwood only. In addition to calculating plume rise, SASEM also provides concentration estimates. These, however, were not used, since the particulate emission rate for municipal waste is higher than the emission rate for burning wood only.

The public domain version of SCIPUFF (PC-SCIPUFF, Version 1.2), was used to model dispersion of particulate matter emitted from the burn pit. SCIPUFF, a Lagrangian transport and diffusion model, was recommended for dispersion modeling by Mr. Jeff Kirkpatrick of the U.S. Army Public Health Command, who collaborated with the NOAA in creating models for estimation of PM10 from dust storms in Iraq (Draxler, Gillette, S., & Heller, 2001). According to its technical documentation (Sykes, Parker, Henn, Cerasoli, & Santos, 1998), SCIPUFF simulates the release of Gaussian puffs, and tracks them to provides a three-dimensional concentration field that is time-dependent. It accurately models wind shear, and uses puff splitting when single point meteorology is unrepresentative. SCIPUFF can be used in situations when complex flow is expected, such as urban terrain environments.

SCIPUFF is appropriate for both short-range (<50km) and long-range applications. It is able to model both steady-state and non-steady state particulate emissions, and can model continuous plumes or instantaneous puffs. The mathematical

models used in SCIPUFF are found in its documentation, and are available at the Sage Management website: http://www.sage-mgt.net/services/modeling-and-simulation/pc-scipuff-download.

SCIPUFF requires completion and internal auditing of the following input parameter sections: Release, Time, Weather, Material, Domain, Audit, and Options. Specific parameter inputs for dispersion modeling entered into SCIPUFF for this paper are as follows:

1. Material

The material chosen to be released was a user-created particulate, PM10, which was defined as particulate broken into ten size bins, ranging from 0.10 microns to 10 microns, with unit density (1000 kg/m^3). Size bin boundaries were automatically generated in SCIPUFF by choosing the logarithmic distribution option.

2. Release

Release location coordinates were 33.9660 N Latitude, 44.3660 E Longitude, which is the location of the southwest corner of the burn pit. The release heights used were 100 meters, for a conservative flaming phase height, and 10 meters, for neutrally buoyant smoldering phase emissions. A smoldering 10 meter release was not modeled for the May-June 2009 daily modeling. Mass median diameter used was 1.00 micron. The actual particle size distribution has not been determined for burn pit emissions, since direct plume sampling has not been accomplished. Even if plume sampling was accomplished, large size distribution variability is likely, due to the variety of burning conditions and types of waste burned. Future sampling of burn pit plumes may provide a particle size distribution, which can help refine the dispersion modeling.

The duration used was the averaging time. For daily average concentrations, 24 hours was entered, and for average concentration, 303 hours was used, based on the special meteorological input file prepared, as described in the "Weather" section below. Generation rates were based on 200 tons per day burned for the 2007-2008 time period, and 200 tons per day burned for the 2009 sampling period, with the emission rate of 19000 mg/kg, as reported by Lemieux (1998). The generation rate calculations are as follows:

$$19000\frac{mg}{kg} \times 907\frac{kg}{ton} \times 200\frac{tons}{day} \times \frac{1day}{24hours} \times \frac{1kg}{10^6 mg} = 144\ kg/hour \qquad (5)$$

Assuming that 0.75 of the initial 200 tons per day burns in the flaming phase and 0.25 burns in the smoldering phase, the flaming phase steady-state release rate is 144 kg/hr x 0.75=108 kg/hr, which is modeled with a release height of 100 meters, and the remaining smoldering phase release rate is 36 kg/hr, modeled with a release height of 10 meters.

$$19000\frac{mg}{kg} \times 907\frac{kg}{ton} \times 10\frac{tons}{day} \times \frac{1day}{24hours} \times \frac{1kg}{10^6 mg} = 7.2\ kg/hour \qquad (6)$$

Again, these generation rates are based on household waste burning and emission factors for open burning of military waste in burn pits have not been determined. Also, the dispersion is modeled as a constantly emitting source with generation rates described above, though this was probably not the case for actual burning. In reality, particle size distribution, plume rise, particle composition, and emissions would vary over time.

3. Time

For the annual modeling, start and stop time corresponded to the meteorological surface file range, a 303-hour run beginning on 1 Jan 2012, for successive 24-hour days, stopping at day 12.6.

4. Domain

The horizontal domain was selected to cover the entire Joint Base Balad installation area. Minimum and maximum latitude values were 33.87 N and 34.00 N; minimum and maximum longitude values were 44.25 E and 44.49 E, with default resolution, and default vertical domain (2500 meters).

5. Weather

For the annual 2007-2008 period, a special meteorological file based on meteorological means and wind rose frequency data for Balad from 2003 to 2009 was created. The surface meteorological file used in SCIPUFF modeling is in Appendix C. Temperature was held constant at the annual average of 298.15 Kelvin. Wind speed and direction frequency data were obtained from wind rose data, with frequency per year converted to number of hours per 303 hours. The conversion to hours was made since SCIPUFF uses hourly input. The reason for shrinking the averaging time from 365 days per year to 303 hours was computer-related. Attempts were made to run the model over a longer period, but the software crashed each time after several hours of work, and the processor overheated once, shutting down the laptop on which the software was installed.

Number of hours at each wind direction was rounded up to the nearest integer, so if a wind direction was represented less than 0.5 hours of 303 hours, it was not used in the model. Frequencies of wind speed at each direction were then determined, and added to the meteorology file. For example, assume a wind direction of 320 degrees for 1/15 of a

year, or approximately 20 days per year. This equates to 303/15 hours, or 20 hours. Further, assume that wind speed for 10 days was 1.5 meters per second, and for the remaining days, 3.5 meters per second. Then 10 hours were modeled with a wind direction of 320 degrees at 1.5 meters per second and the remaining 10 hours at 320 degrees and 3.5 meters per second.

METAR observation data from the KQTO weather station at Balad, obtained from 14 WS, can be used to create a surface file in the format that SCIPUFF requires, for more refined modeling. Pasquill-Gifford stability conditions can be determined based the table in Figure 6 (Environmental Protection Agency, 2011).

Table 6-1. Key to stability categories

Surface wind	Insolation			Night	
Speed (at 10 m) (m/s)		Moderate	Slight	≥ 4/8 low cloud cover*	≤ 3/8 cloud cover
< 2	A	A-B	B	-	-
2-3	A-B	B	C	E	F
3-5	B	B-C	C	D	E
5-6	C	C-D	D	D	D
> 6	C	D	D	D	D

* Thinly overcast

Note: Neutral Class D should be assumed for overcast conditions during day or night.

Figure 6: Pasquill-Gifford Stability Classes (Source: Environmental Protection Agency, 2011)

Numerical "stability index" values are required on SCIPUFF surface meteorology files, corresponding to 1 for class A, and 6 for class F. The blanks in the "Night" columns in Figure 6 are designated "7" in the SCIPUFF surface file.

Pasquill-Gifford stability categories are used to determine mixing height in SCIPUFF, when "Observations" are selected as the "Boundary Layer Type" option. Actual boundary layer mixing heights could be determined with archived upper air profile data, but these data were not available. PC-SCIPUFF uses assumed boundary layer mixing heights based on stability class, as shown in Table 2. A quicker, but less accurate option would be to select "Simple Diurnal" for Boundary Layer Type, which assigns a night-time inversion height of 50 meters and a daytime inversion height of 1000 meters.

Table 2: PC-SCIPUFF Assumed Boundary Layer Depth Based on Stability Class

Stability Index	Pasquill-Gifford Stability Class	Boundary Layer Height(m)
1	A	1000
2	B	1000
3	C	1000
4	D	1000
5	E	125
6	F	65
7	G	25

When "Calculated" is selected as the Boundary Layer Type option, mixing height is determined with Bowen Ratio (the ratio of sensible to latent heat flux), Albedo (the fraction of incident light reflected by the surface), and Cloud Cover. For "desert shrubland," the Bowen Ratio ranges from 3 to 6, depending on the season. For desert

shrubland, albedo ranges from 0.28 to 0.45, depending on the season. SCIPUFF determines boundary layer height from input values with an evolution equation that models convective and mechanical entrainment into stable overlying air. Albedo and Bowen Ratio typical values are provided as tables in the SCIPUFF Help file. The "Calculated" selection could have been useful for the annual model, but unfortunately, could not be used with the shortened meteorological file, since time of day is a determinant of solar radiation in this boundary layer calculation. "Observation" was chosen as the Boundary Layer Type, and the Pasquill-Gifford Stability Class was held constant as "Neutral," or class 4, keeping the mixing height constant at 1000 meters. The dispersion output variations depended on wind direction and velocity only. Upper air profile values were not used, as archived files were not readily available and formatted for ingest into the model. Also, neither precipitation nor deposition were accounted for, keeping the estimates conservative.

After each dispersion model run was complete, a plot was drawn with total integrated surface dosage for the time period. Gridded text files were created while holding grid point coordinates constant between each run so that as tables were created, Map Algebra could be performed in ArcMap. Surface Dosage (kg-sec/m^3) was converted to concentration by dividing by total averaging time, as shown in Equation 7. Applying this equation to the annual plume with the 303-hour weather file results in an average annual concentration.

$$C\left(\frac{\mu g}{m^3}\right) = \frac{Surface\ Dosage\ (kg \cdot sec/m^3)}{t\ (sec)} \times 10^9 \mu g/kg \qquad (7)$$

Finally, special grids were run in SCIPUFF with monitored sampling sites as modeled receptor sites in the dispersion calculation. These values were exported as text files, imported into Excel, and dose was converted to concentration. Concentration between sites was averaged and a positive or negative percent difference from the mean concentration was calculated, and compared to positive or negative percent difference from the mean concentration in monitored results.

Processing in ArcMap

Each gridded file exported from SCIPUFF consisted of 100 points across the Joint Base Balad installation area. Each grid was saved in a georeferenced spreadsheet, and imported as x-y coordinate data into ArcMap, with concentration values as elevation attributes. Interpolation based on concentration data was performed in ArcMap. The ArcMap Radial Basis Function tool, an exact interpolation method, was used to create isoplethed maps, presented in results. Isopleths were broken into 2.5 µm increments of concentration and were not filled, so that continuous interpolated monitoring layers could be seen in the same map as interpolated dispersion layers and areas of modeled higher and lower concentration areas could be compared. Combined dispersion modeled and geospatial modeled maps were exported into Google Earth format to view satellite imagery for possible receptor areas. Number of samples per site was displayed on ArcMap and Google Earth to visualize areas that have been less-sampled, along with modeled concentration in those areas.

Assumptions

Assumptions are inherent in environmental modeling. When modeling exposures that have occurred in the past, additional assumptions are often necessary, since models are limited by existing data, or lack thereof. This section summarizes the assumptions in the methodology for this study.

Monitoring data are assumed to be of reasonable quality with reasonable levels of error, but this may not always be the case. For example, the National Research Council's review of the Enhanced Particulate Matter Surveillance Program (EPMSP) report noted that the MiniVol, which was used to sample PM10, has not been validated in areas where ambient concentrations are excessive, resulting in possibility of sampling artifacts" (National Research Council, 2010). Also, replicate sampling was not accomplished, making it difficult to determine how accurately measurements reflect actual concentrations. Regardless, models must be run with the data that exists, not the data for which a researcher wishes.

Another assumption in the interpolation modeling is that the monitored mean values reasonably reflect the true long-term underlying average. This assumption is also questionable due to the high temporal variability in particulate and low sample size for some sites; random sampling may not be the case with the existing monitoring data.

Spatial autocorrelation is also assumed in the interpolated models, but high between-day variability and changes higher concentration areas over time suggest independence in the sites, in which a number of unknown influencing sources acts upon each site in different ways at different times.

In the dispersion model, a constant emission rate is assumed, based on municipal waste emission factors and reported activity rates. This is expected to be the greatest

source of error in the dispersion modeling, as waste composition, burn characteristics, and actual emissions for each burn are unknown. This limitation prevents justification of a high-resolution dispersion modeling method for characterizing exposures until emissions can be clarified. Also, a constant burn rate and a constant plume height are implied by constant emission rates, though for this study, two separate heights were modeled. Since on-site METAR meteorology was used, it is assumed that the meteorological values reported apply to the entire base. This is a reasonable assumption, as the base is quite flat, and there are few land features that indicate severe terrain effects in highly local meteorological patterns. It is also assumed that the METAR reported values are reasonably accurate.

Meteorological values are taken at hourly increments, and these values are assumed to be constant over the entire hourly period. A problem with this assumption is that high levels of peak burning that contribute significantly to the time-averaged concentrations may be released over a short period of time, and if the reported value is different for a single value, then up to two hours of exposure can be modeled incorrectly.

Though there are many assumptions made in these models, even with significant error in exposure estimates, a reasonable determination of areas of relatively higher concentration and risk may be determined. Also, this study can be considered a "screening" survey, using worst-case long-term estimates, based on conservative buoyant plume rise heights, and full consumption of estimated average mass burned. This research may be refined with future determined emission factors and collaboration with weather and/or air modeling professionals in preparation of meteorological files for other

refined air dispersion models, such as AERMOD, CALPUFF, or refined SCIPUFF modeling.

IV. Results and Analysis

Exploratory analysis of the monitoring data, results from the spatial interpolation in GIS, dispersion model results, and combined maps showing results from both models for comparison are presented. Analysis of each type of modeling result and of the combined maps are also provided, along with attempts to answer each of the initial research questions.

The stated objective of this research was to delineate retrospective exposure zones using spatially interpolated particulate air sampling point data from Joint Base Balad, create burn pit exposure isopleths from dispersion model outputs, and merge into a combined exposure model in GIS.

To accomplish these objectives, specific maps were created by interpolating monitored data from 2007-2008 and SCIPUFF-generated isopleths were created with climatological mean data from the weather station KQTO at Joint Base Balad. These were merged into a combined map, and specific features within a high exposure 1-km buffer around the burn pit identified as well.

Specific research questions and short answers are as follows:

1. Determine spatial and temporal patterns with monitored particulate data. This is determined through Inverse Distance Weighting interpolation of monitored data, after thorough exploration of the existing monitored PM10 data set for Joint Base Balad.

2. Model burn pit ambient exposure zones with a dispersion model. First, SCIPUFF was used to create isopleths representing successively increasing exposure zones. Next, loose-coupling of dispersion model results into ArcMap was performed.
3. Estimate relative burn pit contribution to overall exposure, and determine whether modeled dispersion concentration differences predict monitored concentration differences. This was accomplished by using SCIPUFF to model annual averaged concentration at each ambient air monitoring site, and determining the dispersion modeled PM10 as a percentage of the monitored average PM10 at each site.
4. Identify sampling needs to improve spatial modeling. This is accomplished in the exploratory data analysis to determine temporal completeness, and in creating sampling location maps with sample sizes displayed at each site and in relation to receptor areas to highlight possible weaknesses in the sampling network.
5. Create a method to model relative source-specific ambient exposures for individuals or similar environmental exposure groups. A mathematical exposure model is offered based on modeling results and isopleths created with SCIPUFF and ArcMap.

Exploratory Data Analysis

A large number of particulate matter samples were collected at Balad while the burn pits were operational, but the spatial and temporal distribution of sampling was uneven. Figure 7 shows the number of sampling sites used per month over the 2003-2009 sampling campaign.

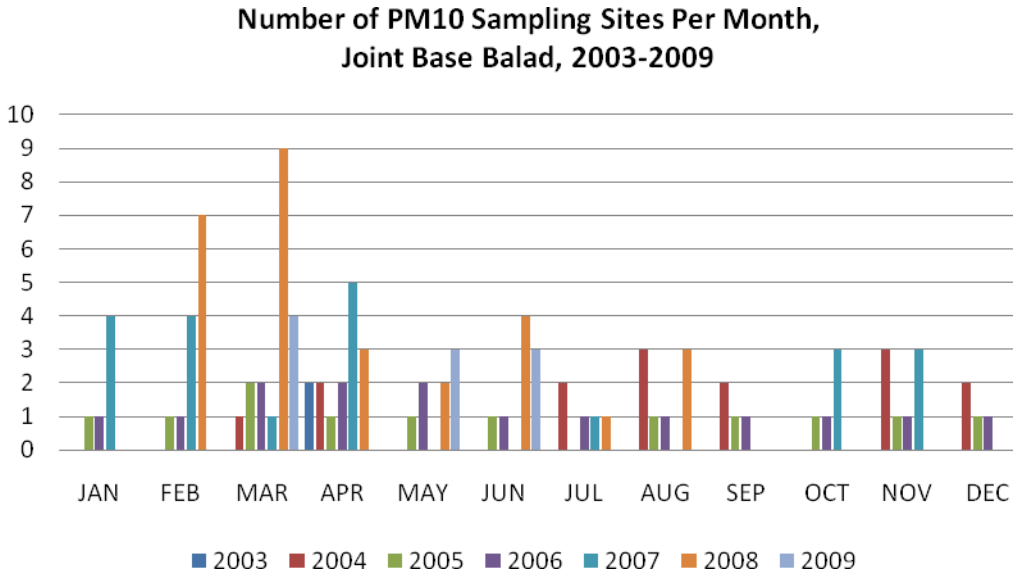

Figure 7: Number of Joint Base Balad PM10 Sampling Sites Per Month, 2003-2009

Averaging across all years would be valid if between-year variability in particulate is insignificant, but this cannot be determined without having sampled each month over several years. One site per month was sampled for each month in 2005 and 2006, but troop levels significantly increased between 2007 and 2008 in Iraq, and several months went unsampled in each of those years. Unfortunately, between-year variability is unknown for the PM10 data set. But, it is likely that the dynamic nature of military

operations over time results in changing air pollution levels and patterns. Thus, between-year averaging may be invalid and may create a dilution effect of possible higher concentrations in high tempo or high troop level years. But, the sparse nature of theater ambient air sampling may require averaging across years to perform basic statistics.

A descriptive statistics summary created from the list of georeferenced 2007-2008 samples, for those sites in which at least three samples were collected, is in Table 3.

Table 3: Descriptive Statistics Summary, Balad Georeferenced PM10 Samples, 2007-2008

Descriptive Summary Statistics, Joint Base Balad Georeferenced PM10 Samples, 2007-2008	
Mean (µg/m^3)	286.5
Standard Error	30.3
Median (µg/m^3)	158
Mode (µg/m^3)	136
Standard Deviation	396.4
Sample Variance	157146.8
Geometric Mean (µg/m^3)	172.1
Geometric Standard Deviation	2.56
Range	2835
Minimum (µg/m^3)	2
Maximum (µg/m^3)	2837
Sum	48995
Count	171

The distribution of the 2007-2008 dataset, created with the JMP statistical software package, is pictured in Figure 8. The data are clearly not normally distributed, as would be expected with ambient environmental data. There is a large number of values below 250 µg/m^3 and most values fall below 500 µg/m^3. There is a small peak between 1000 and 1250 and there are two outlying values above 2750. These values are over six standard deviations away from the mean. These, and other values significantly

greater than the mean, are likely from intense dust storms. The mean value itself is likely influenced heavily by dust storms, which occur frequently in the area. See Figure 9 for the average number of blowing sand and dust days recorded at the weather station (KQTO) at Joint Base Balad. There is no indication of the intensity of these storms, but samples collected on dust storm days could be considered a separate population from those days on which dust storms did not occur. Occurrence of "dust events" may not be a binary issue; in other words, the issue may not be reducible to "there was" or "there was not" a dust event on a given day. Regional events may vary in intensity, and even those events that do not highly reduce visibility and go unrecorded by meteorological stations, may still significantly increase particulate levels, thus influencing sample results.

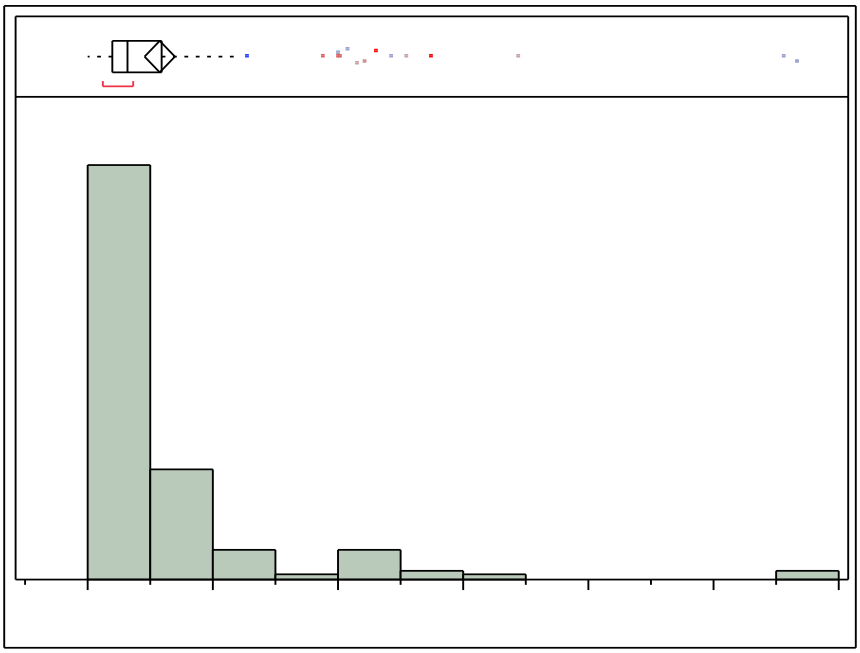

Figure 8: PM10 Frequency Distribution at Balad Sites (N≥3), 2007-2008 (USAPHC, 2010)

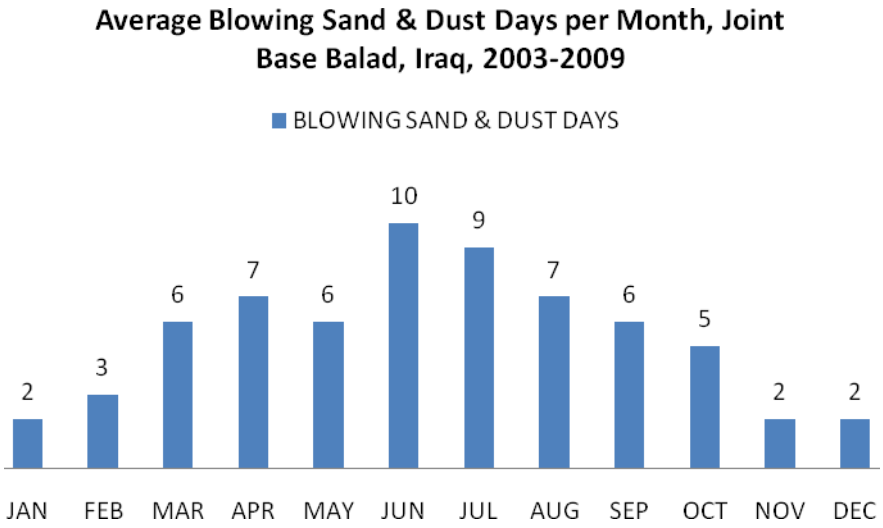

Figure 9: Average Monthly Dust Storm Frequency,Joint Base Balad (14WS, 2010)

The variability in monthly dust storm frequency indicates that between-month variability in average particulate concentration exists and that annual results should probably not be averaged and interpolated to determine total particulate exposure to shorter-length deployments. Examination of a one-way analysis graph and a time-series graph (Appendix D) indicates that actual monitoring results reflect the dust storm frequency averages, with high variability and means in June and July. March of 2008 differs significantly from March 2007. Inspection of the METAR data for the March 2008 outliers (13-14 March) reveal high winds and thunderstorms on the evening of 13 March. Average wind speed for the day was 12 mph, with hourly reported values up to 36.8 mph, and gusts up to 58 mph. It is possible that stirred dust contributed to a significant percentage of the high values for that day. Since moisture slows burning and increases the likelihood of smoldering conditions and meteorological conditions, including high winds, may limit vertical plume rise, then burn pit smoke may also have

been increased at this time. Gravimetric analyses will not provide insight into the sources.

The annual prevailing wind direction is from the northwest to west-northwest, with a minor secondary wind from the southeast (Figure 10), but distinct wind patterns differ, depending on time of year (Figure 11). Wind roses for winter months show increased frequencies of calm winds, with northwestern winds dominating, but with a secondary southeastern wind. Wind roses for summer months show higher wind speeds and a dominating west-northwest direction. Worst case winds to the base from the burn pit would be north northeast to north northwest. It is difficult to determine which months would result in greater burn pit exposure. Greater frequencies of northern direction would result in higher exposures, but so would higher windspeeds. It is clear, however, that just as there are seasonal differences in dust storm frequency, there are also seasonal differences in wind direction and frequency, reinforcing the notion that monitoring should be accomplished randomly throughout the year, and that annual averaged sampling results should not be averaged, unless the period of deployment is one year.

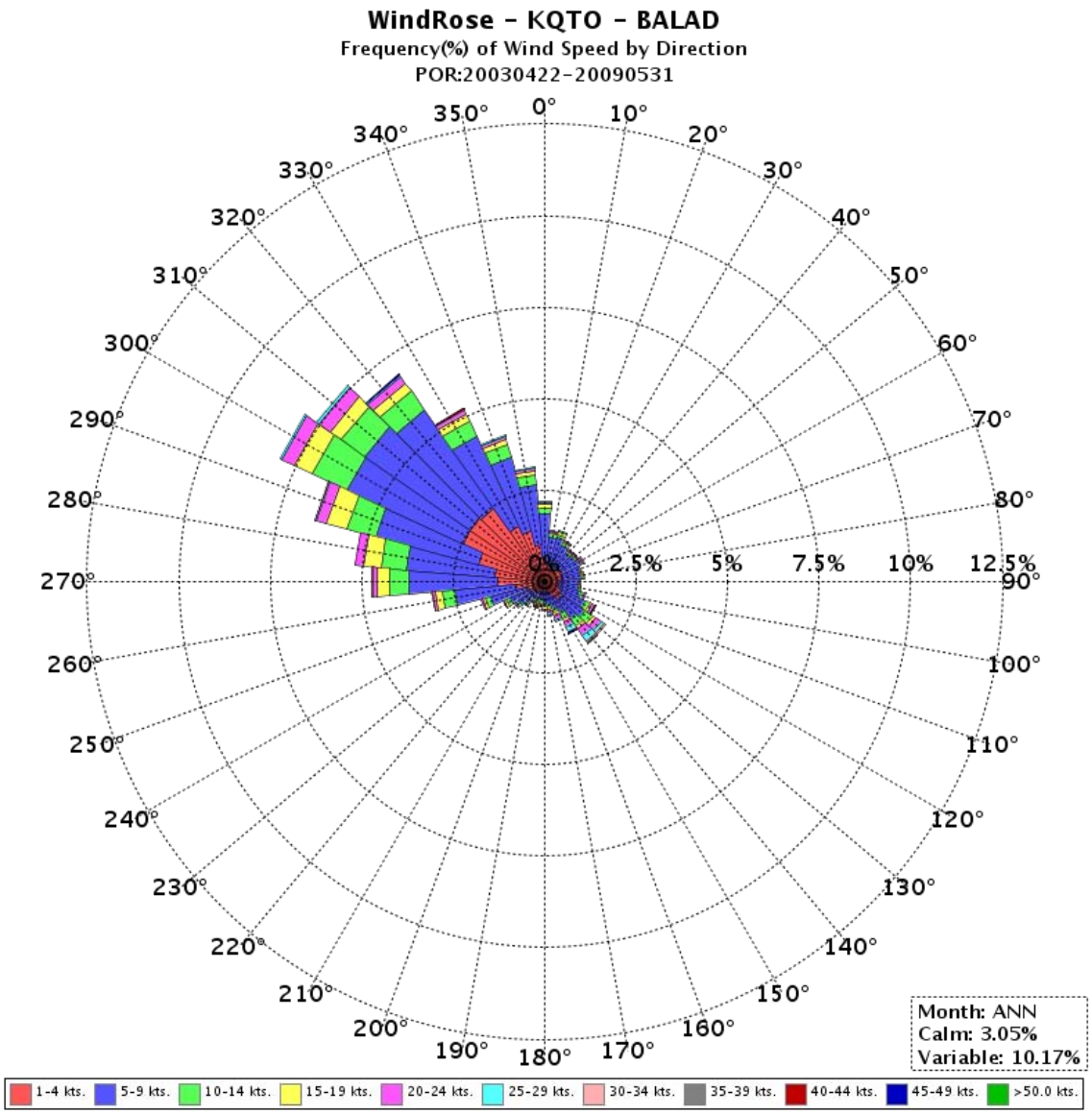

Figure 10: Annual Wind Rose, Based on KQTO Balad 2003-2009 Wind Frequency Data (14WS, 2010)

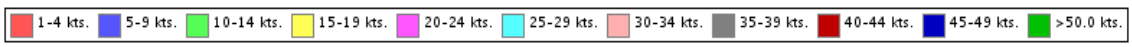

Figure 11: Monthly Wind Roses, KQTO, Balad, 2003-2009 Wind Frequency Data (14WS, 2010)

In addition to high overall temporal variability, there is also a large range of geometric means across sites. Geometric means for each 2007-2008 site with n≥3 are listed in Table 4. The values range from 73 µg/m^3 to 976 µg/m^3.

Table 4: Geometric Means for Joint Base Balad Sampling Sites (n≥3), 2007-2008

Latitude	Longitude	Site	Geometric Mean (µg/m^3)
33.929533	44.361928	2	976
33.929642	44.355283	3	349
33.930314	44.359519	4	408
33.935606	44.333597	5	363
33.935664	44.344417	6	274
33.940622	44.389794	11	759
33.940925	44.335061	12	416
33.941303	44.389011	13	202
33.9441	44.3871	16	127
33.947664	44.328764	18	259
33.950381	44.371389	H-6 Housing	73
33.95045	44.381739	24	194
33.951464	44.380878	25	170
33.952397	44.374408	28	268
33.954667	44.3758	CASF	129
33.955511	44.367967	31	140
33.960533	44.367533	Transportation Field	94
33.962931	44.364167	35	714
33.963603	44.366478	37	287
33.9671	44.368483	Guard Tower	84
33.967117	44.349633	Mortar Pit (Background)	122

Spatial Analysis

Prior to performing spatial interpolation and dispersion modeling, terrain was analyzed to determine whether it was flat enough to be modeled without terrain

processing in a dispersion model. Deep valleys, ridges, and mountains should be considered prior to assuming an even, homogeneous wind field. Elevation isopleths available from the Air Combat Command GeoBase were used to create a simple elevation map that shows a surface that very gently slopes downward toward the west, with an elevation range of ten meters across the base (38-48 meters), which is approximately 20 square kilometers in area. It appears that the burn pit is located at a relatively high elevation on the base (Figure 12).

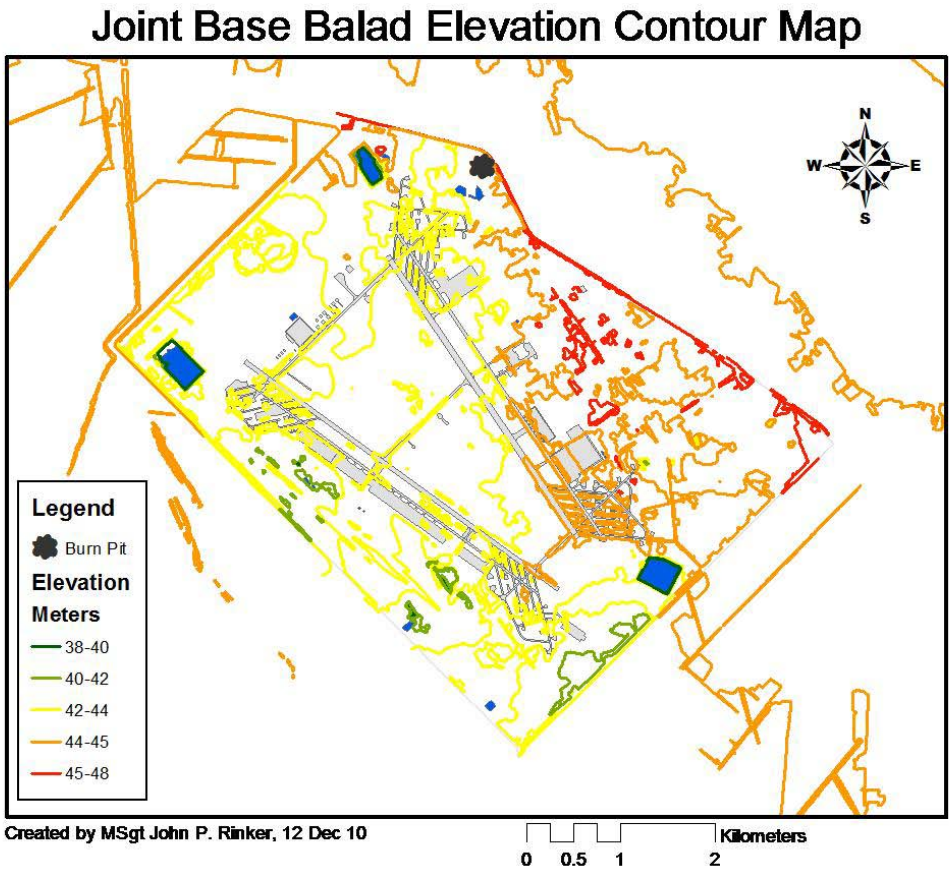

Figure 12: Joint Base Balad Elevation Map

A map of 2007-2008 (n≥3) sampling sites was also created in ArcMap, with total number of samples taken at each site during the period displayed on the map (Figure 13). The northern corner of base has been sampled with a greater frequency than the rest of the base. Mapping sample points with graduated symbols and sample numbers provides the same numerical data as simple table, but visualization of the data in space immediately reveals opportunities to strengthen the sampling effort.

-

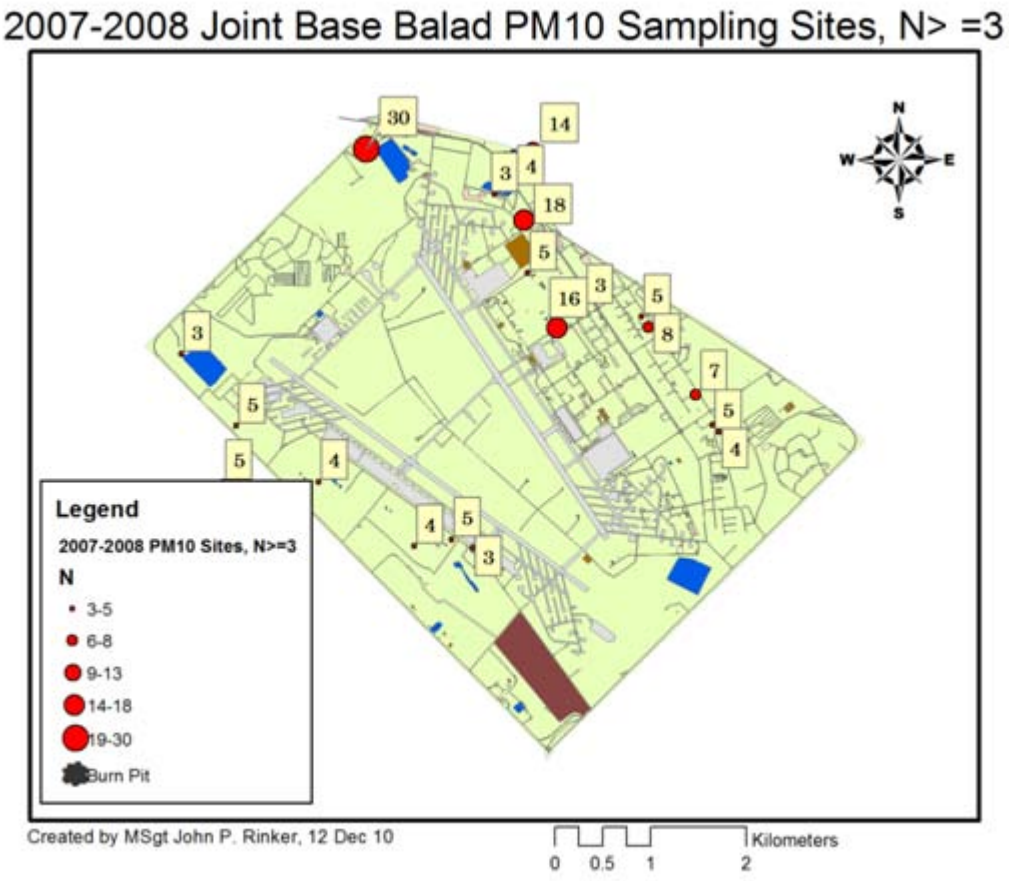

Figure 13: Joint Base Balad PM10 Sampling Site Map with Numbers of Samples, 2007-2008

The first interpolation performed was inverse distance weighting on 2007-2008 averaged PM10 geometric means (Figure 14). Concentrations ranged from 72.6 to 975.8 $\mu g/m^3$. Higher concentrations were modeled toward the southern and western sides of base and southwest of the burn pit. High concentrations appear to be associated with low number of sampling points. Temporal variability issues are likely causing the high weighting toward the south and west. The highest number of samples taken on the west side of base is five and is not enough for high confidence in the mean values with the high temporal variability issue. The map, therefore, is not trustworthy because of this issue. Still, interpolation of the surface and simultaneously displaying the number of samples shows areas where hazard and risk characterization might be improved by increased monitoring. For example, since it is already known that there are monthly differences in PM10, any site with less than 12 samples is suspect, and to be able to complete within-month statistics, a minimum number of samples per month per site should be determined. The concentration field on the entire west side of base is suspect due to the simple fact that sample numbers reflect non-random temporal sampling. Also, since interpolation methods determine unsampled points by weighting neighboring points, there may be error in the unsampled surface between the west and east sides. Personnel who may work in these areas, such as flightline workers, maybe misclassified as to their ambient particulate exposure. Simultaneous monitoring across the entire space would improve the exposure estimation.

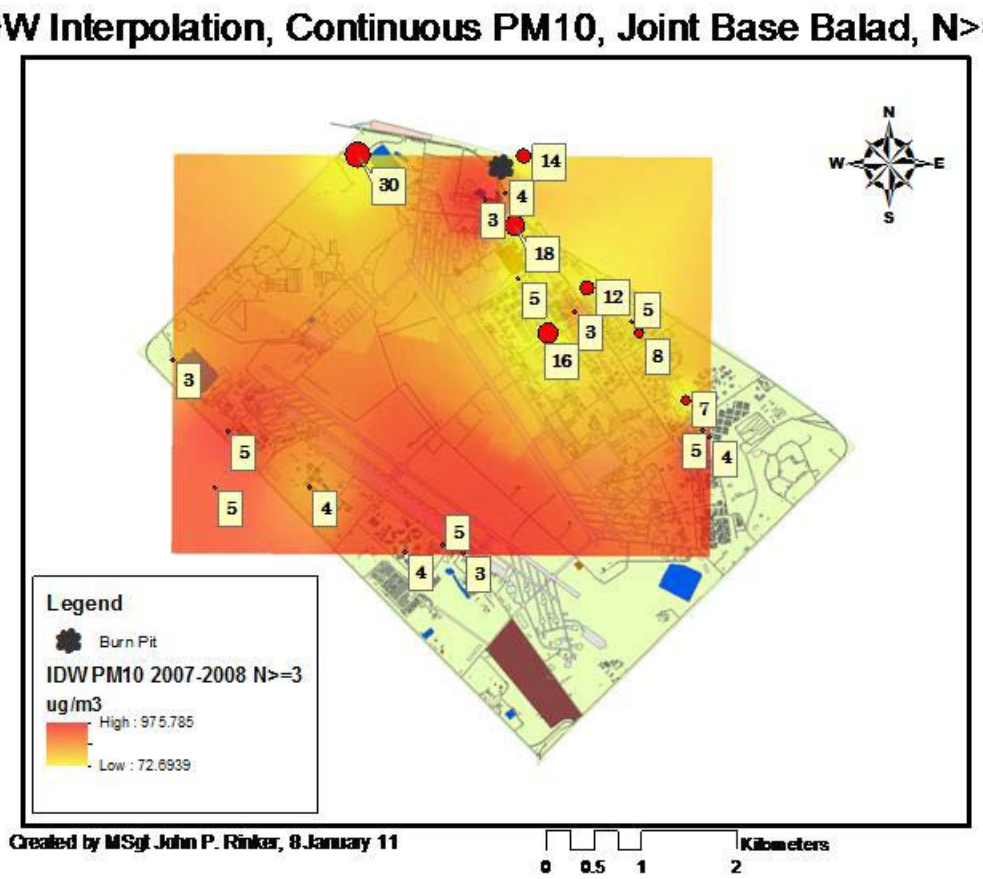

Figure 14: Inverse Distance Weighting Interpolation: Continuous Concentration Surface of PM10, Joint Base Balad, 2007-2008

A isopleth map was also created with the Inverse Distance Weighting interpolation tool, with isopleth intervals defined as <200 µg/m^3, 200-300 µg/m^3, 301-400 µg/m^3, and >400 µg/m^3 selected for isopleth values (Figure 15).

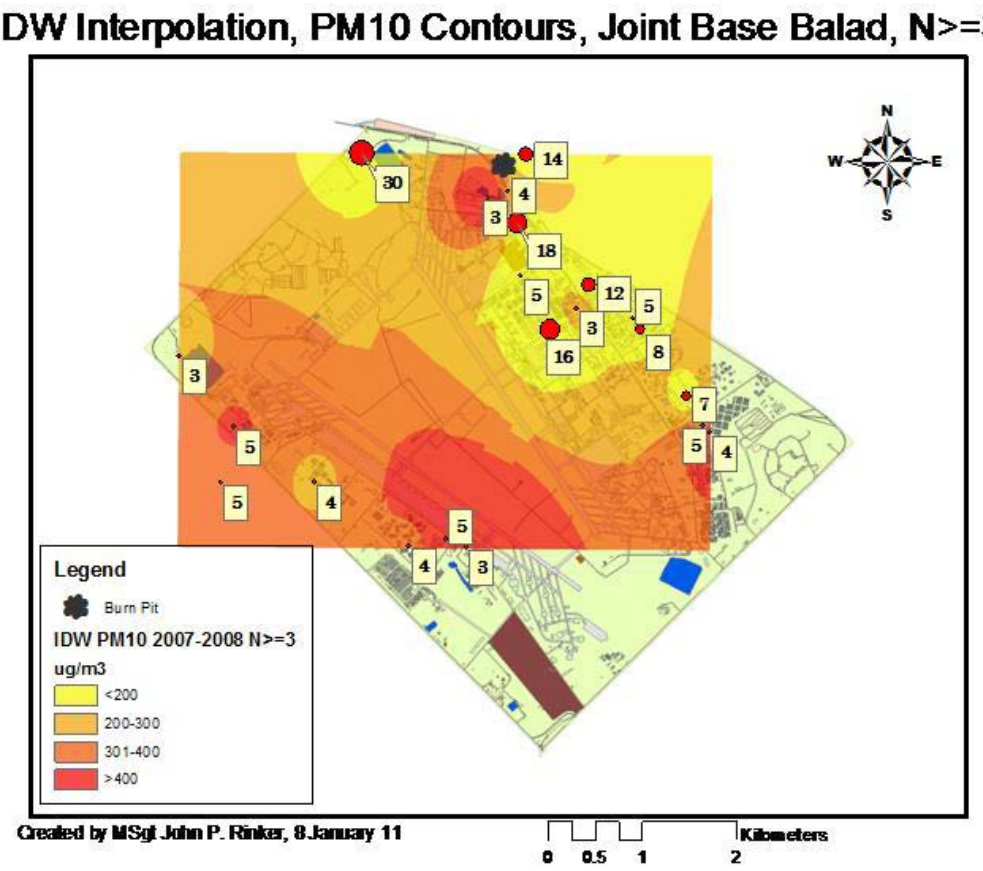

Figure 15: Inverse Distance Weighting Interpolation: Isoplethed Concentration Surface of PM10, Joint Base Balad, 2007-2008

If the confidence in the mean values at each site can be strengthened, then the isopleth map and the continuous exposure surface map could be used to designate areas within isopleths as areas of differing relative risk for year-long deployments, and personnel working or living in those areas could be tagged with an identifier in a geodatabase. Health effects between zones could be compared, linking exposures with modeled concentrations. Red zones, for instance, may be considered as high exposure areas, and yellow zones as low exposure areas. Determination of risk based on these surfaces are best accomplished by a combination of environmental scientists or industrial

hygienists, epidemiologists, and physicians, as well as selection of isopleth division levels. There are many ways that isopleth levels could be selected, but consideration of dose-response effects should be part of that interdisciplinary process. For example, if a linear, no-threshold concentration-response curve is observed for a pollutant for levels up to 50 $\mu g/m^3$ at which point the response (and risk) levels off, then it may make sense to set isopleths for every 10 $\mu g/m^3$ of concentration. It might not make sense to create isopleths at all, if all measured concentrations exceed 50 $\mu g/m^3$.

Once isopleths or exposure areas are defined, queries can be performed in ArcMap to determine features that exist within those isopleths, such as buildings, or if personnel or exposure groups are georeferenced with work and/or living locations, personnel locations. If personnel locations are georeferenced, health effects may be able to be tied to locations, and cluster analyses can then be performed in GIS and viewed simultaneously with exposure maps. Or, relative risk can be determined by comparing incidence among those with health effects who live or work within high exposure zones versus those who do not.

Using satellite imagery from Google Earth and converting exposure surface shapefiles to the Google Earth .kmz file type with the ArcMap Conversion Tool "Layer to KML," monitored exposures can be visualized with actual imagery, with possible population exposure zones viewed with impressive detail. For example, if one wishes to zoom in to a boundary area between modeled zones to see what is there, satellite imagery provides a clear picture (Figure 16), and preserves the exposure surface shapefile scale, as long as the export scale is designated within the "Layer to KML" tool.

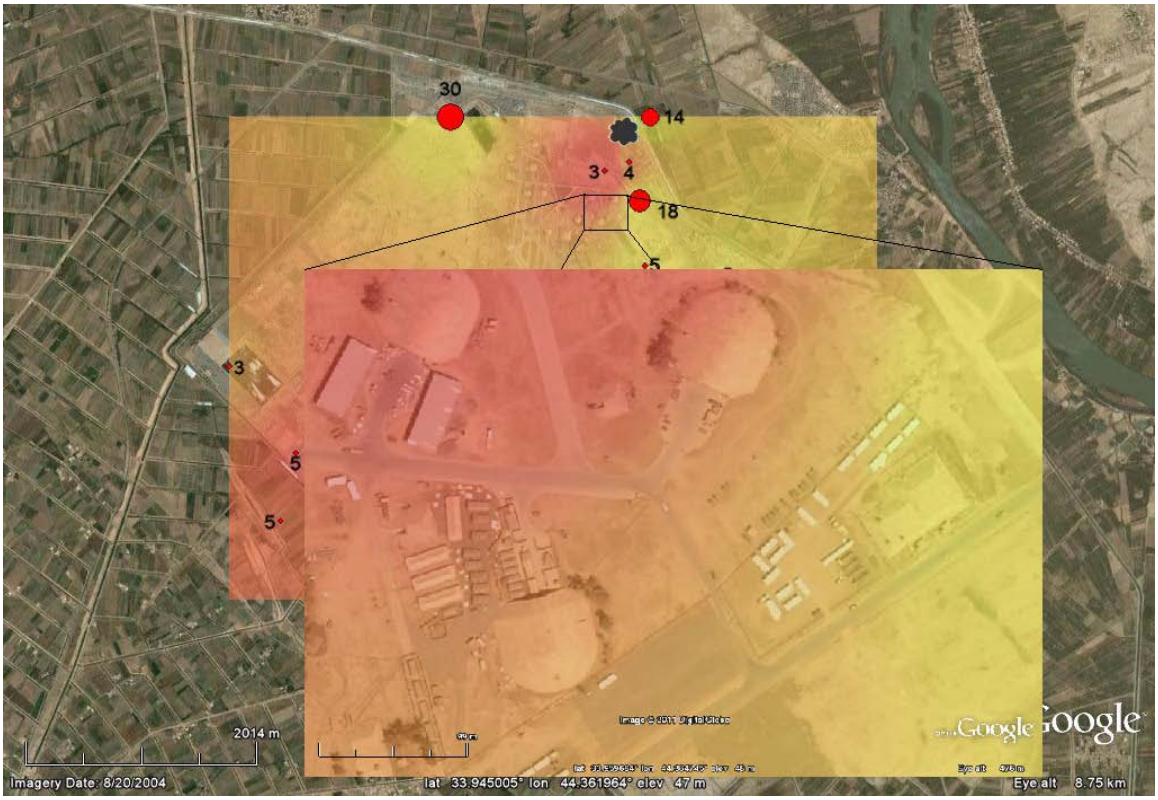

Figure 16: Overlaying Continuous Exposure Surface Layer in Google Earth

Straight-line distance from the burn pit location was determined by creating a map with site name identifiers (Figure 17) and using the "measure" tool in ArcMap. Results are Table 5.

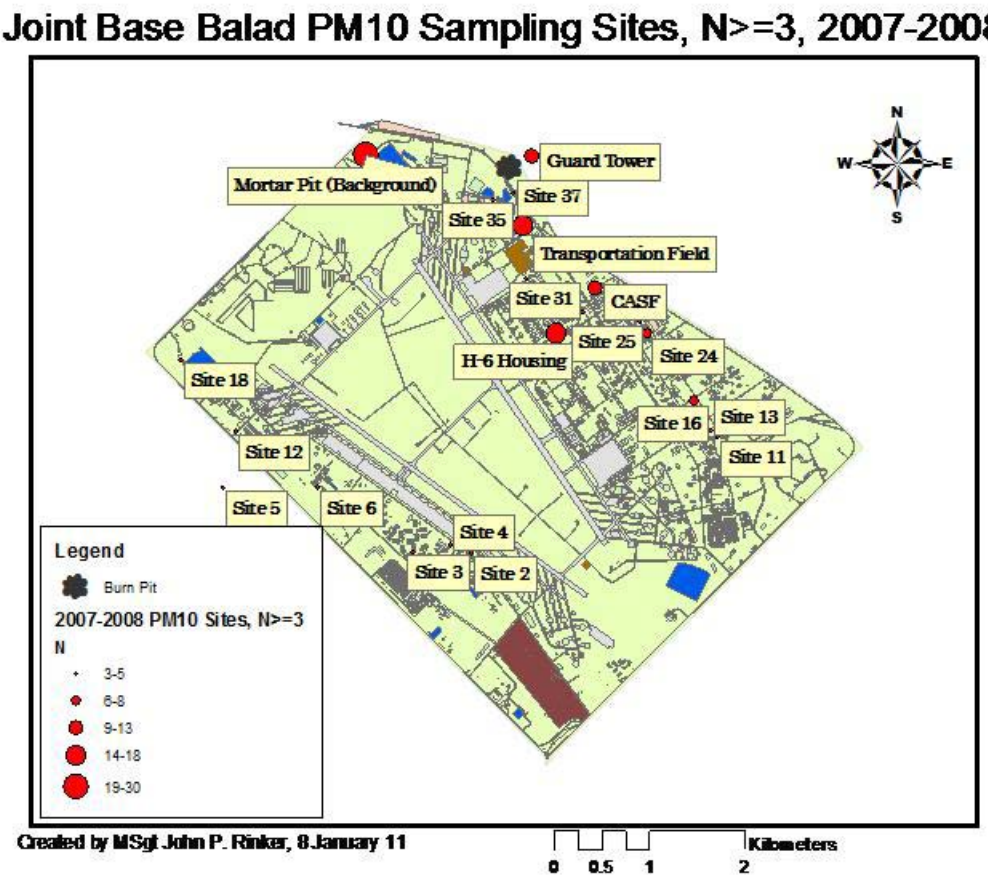

Figure 17: Joint Base Balad PM10 Sampling Sites, 2007-2008, N≥3

Table 5: Distance From Burn Pit to Balad PM10 Sampling Sites (n≥3), 2007-2008

SITE	Distance (km)	Inverse Distance	GM Concentration (µg/m^3)
2	4.06	0.246305419	976
3	4.15	0.240963855	349
4	4	0.25	408
5	4.51	0.22172949	363
6	3.91	0.255754476	274
11	3.57	0.280112045	759
12	3.99	0.250626566	416
13	3.47	0.288184438	202
16	3.12	0.320512821	127
18	4	0.25	259
H-6 Housing	1.8	0.555555556	73
24	2.26	0.442477876	194
25	2.12	0.471698113	170
28	1.7	0.588235294	268
CASF	1.55	0.64516129	129
31	1.18	0.847457627	140
Transportation Field	0.62	1.612903226	94
35	0.38	2.631578947	714
37	0.27	3.703703704	287
Guard Tower	0.26	3.846153846	84
Mortar Pit (Background)	1.52	0.657894737	122

Geometric means of PM10 concentration (µg/m^3) per site were plotted against inverse distance (1/[km]), in Figure 18. If distance, or "proximity," is a proxy for increased exposure, then the inverse of distance should be associated with increased concentrations of PM10. The monitored results do not show this relationship. In fact, there is a slight negative relationship between inverse distance and concentration. Proximity to the burn pit appears to be associated with lower PM10 concentration. Again, however, the problem of low sample numbers at distant sites combined with high temporal variation reduces confidence in the mean concentrations at less-sampled sites.

This variation is reflected in the distances of geometric sites from the line. If distance were the major variable influencing concentration, points would be expected to be closer to the line.

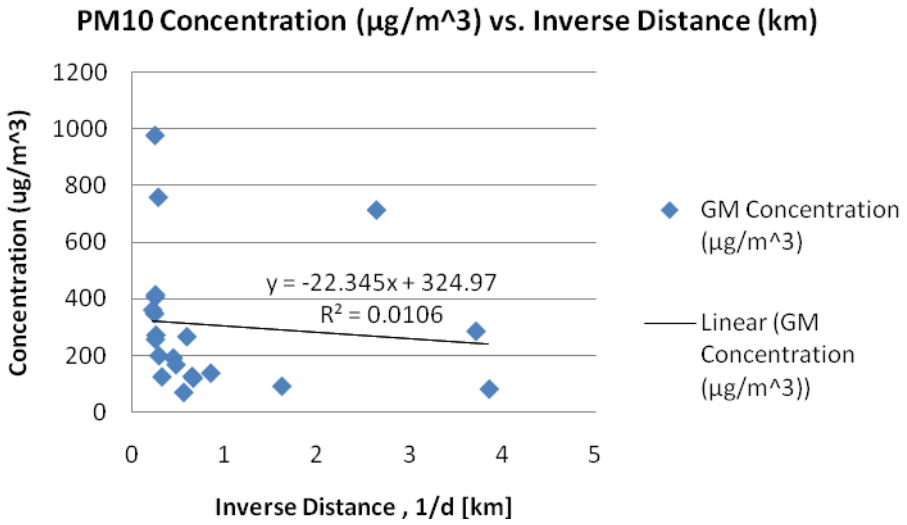

Figure 18: Joint Base Balad PM10 Sampling Sites, 2007-2008, N≥3

Dispersion Modeling Results and Analysis

According to SASEM, the calculated plume centerline height ranged from 92 meters, in fair to good stability with gusting winds of 27 knots, to 2482 meters, in excellent stability conditions and calm (one knot) winds. According to Air Force Weather Agency Operational Climatic Data Summary historical data between 2003 and 2008, the average wind speed for Balad, Iraq, for the months of May and June, is 8 knots (14 WS (US Air Force 14th Weather Squadron), 2010). The calculated plume rise centerline for 8-knot winds under good and fair stability conditions is 310 meters. The SASEM output file, which contains maximum concentrations, plume height, and distance to maximum concentrations, is in Appendix E.

Burn rates and heat release rates change over time, and therefore, emission rates change over time (Tran & White, 1992). Most mass emissions will occur during higher burn rate and heat release rate stages, including particulate matter, but since the temperature is also higher at this time, combustion byproducts, including dioxins and PAH, would be expected to be lower at this point. For this reason, greater dioxin and PAH emissions are expected in lower temperature smoldering phases. Also, during the higher mass emission periods, plume rise would be expected to be higher. Risk from byproducts may be higher at lower burn temperatures, when plume rise is relatively low, and when wind speeds are higher (Carroll, Miller, & Thompson, 1977). In addition, if more smaller piles of trash are burned, then temperatures and buoyancy would be lower. To be conservative, a value of 100 meters was used as the release height for the flaming, high-temperature phase, and a height of 10 meters was used as the release height for the low-temperature, neutrally buoyant, smoldering phase.

The surface dosage plumes created with PC-SCIPUFF, using wind frequency data from the Air Force Weather Agency as described in the methodology section, are pictured in Figures 19 and 20 for the flaming (100 meter release height) and smoldering (10 meter release height) fractions, respectively. As described in the methodology, each plume was created based on 200 tons of total mass burned per day, temperature held constant at the annual average value, and a constant 1000 meter mixing layer height. Equation 8, using 303 hours as the averaging time, can be used to determine average annual concentration from the plumes.

Though the flaming phase plume was created with an emission rate of 108 kg/hr and the smoldering phase plume was created with an emission rate of 36 kg/hr, surface

dose from the smoldering phase is significantly greater than the flaming-phase contribution. Again, the 100-meter plume height is conservative; the modeled plume rise for average winds is over three times the 100-meter release height.

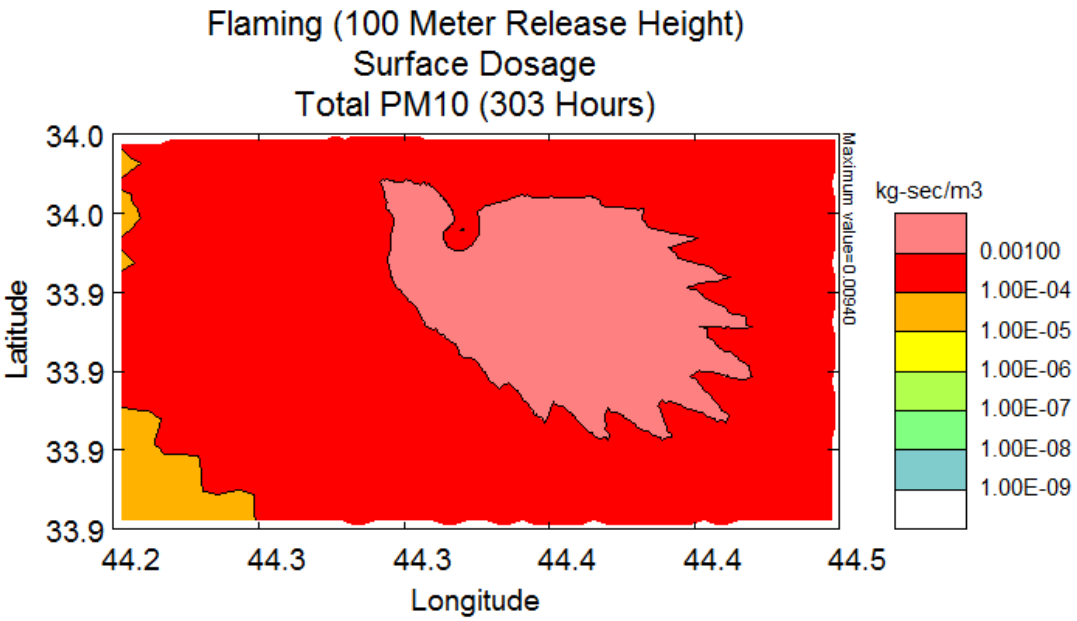

Figure 19: Annual PM10 Surface Dosage From Joint Base Balad Burn Pit

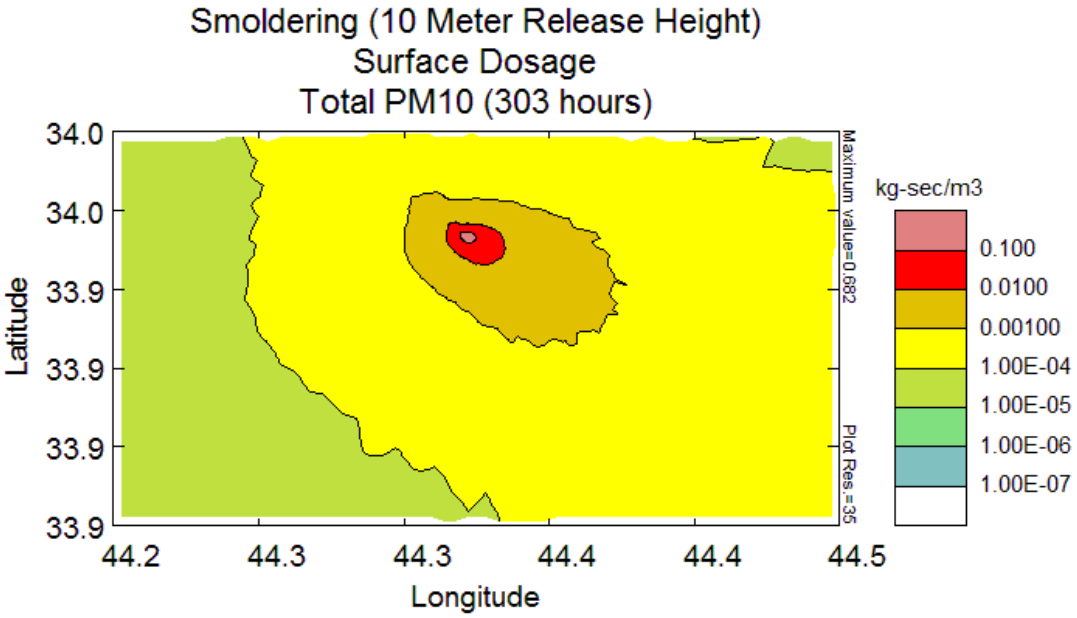

Figure 20: Annual PM10 Surface Dosage From Joint Base Balad Burn Pit

Results from each dispersion run in SCIPUFF were exported into gridded ASCII text files, with a rectangular grid of 10 x 10 points to be modeled across the installation area. The grid, with modeled points identified as evenly spaced dots, is pictured in Figure 21.

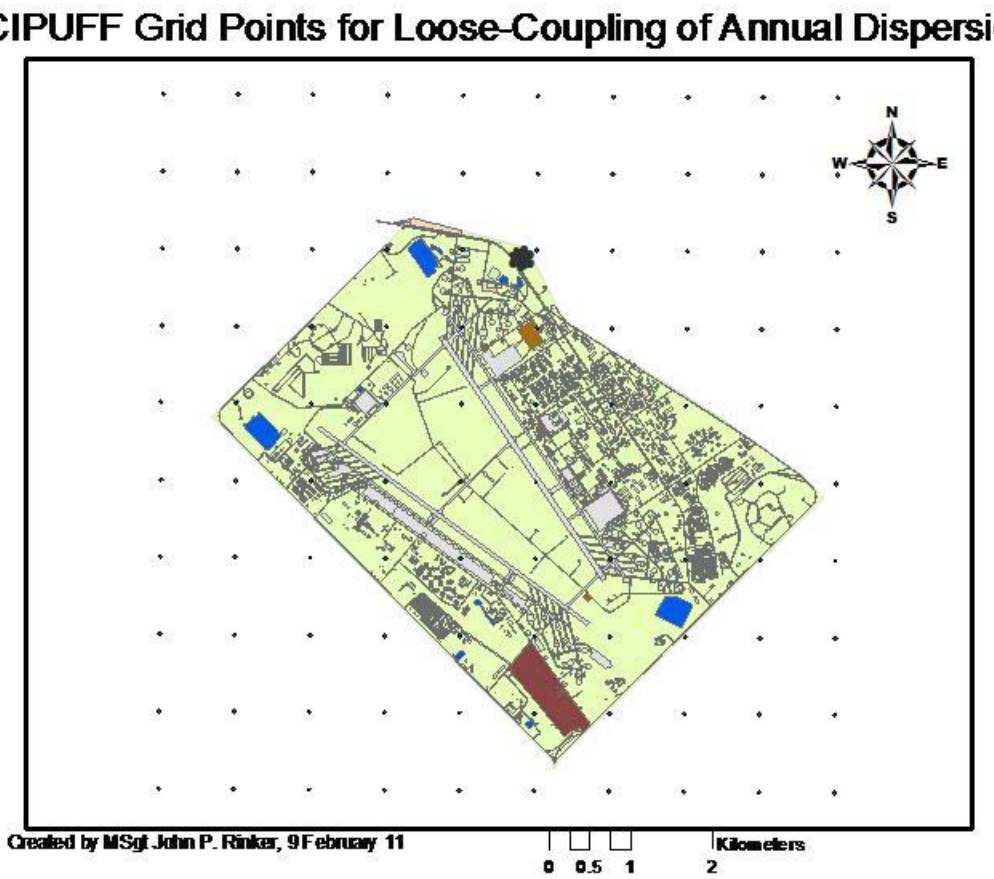

Figure 21: SCIPUFF Dispersion Modeling Export Grid for Loose-Coupling in GIS

Dispersion modeled burn pit PM10 concentrations, created by performing Radial Basis Function interpolation on imported SCIPUFF grid values in ArcMap, are pictured in Figure 22 for the flaming contribution and Figure 23 for the smoldering contribution. Radial Basis Function summed grid concentration values resulted in combined flaming and smoldering concentrations, representing total burn pit dispersion modeled concentration. The total dispersion concentration model (flaming plus smoldering) is pictured in Figure 24.

Concentration isopleths were based on documentation of increases of cardiovascular disease mortality and cardiovascular disease hospital emissions with successive increases of 10 $\mu g/m^3$ in PM10 concentration (Dominici, Zonabetti, Zeger,

Schwartz, & Samet, 2005). Isopleths were also created at 2 $\mu g/m^3$ intervals below 10 $\mu g/m^3$ to allow visualization of the flaming contribution dispersion.

It must be stressed that these maps and models have been created with assumptions that are likely erroneous, such as emission rates based on municipal waste burning in barrels, constant burning and emission conditions, constant burn rates and temperatures, constant mixing height of 1000 meters, constant temperature, and constant plume rise for smoldering and flaming conditions. Due to probable gross errors in concentration estimations caused by "garbage in," these maps should not be used for actual exposure assessment. They are intended to be tools in establishing methodology by which exposures can be determined, given improved input data. Also, the SCIPUFF dispersion model maps model source-specific dispersion from burn pits only. Other sources are not considered in these maps.

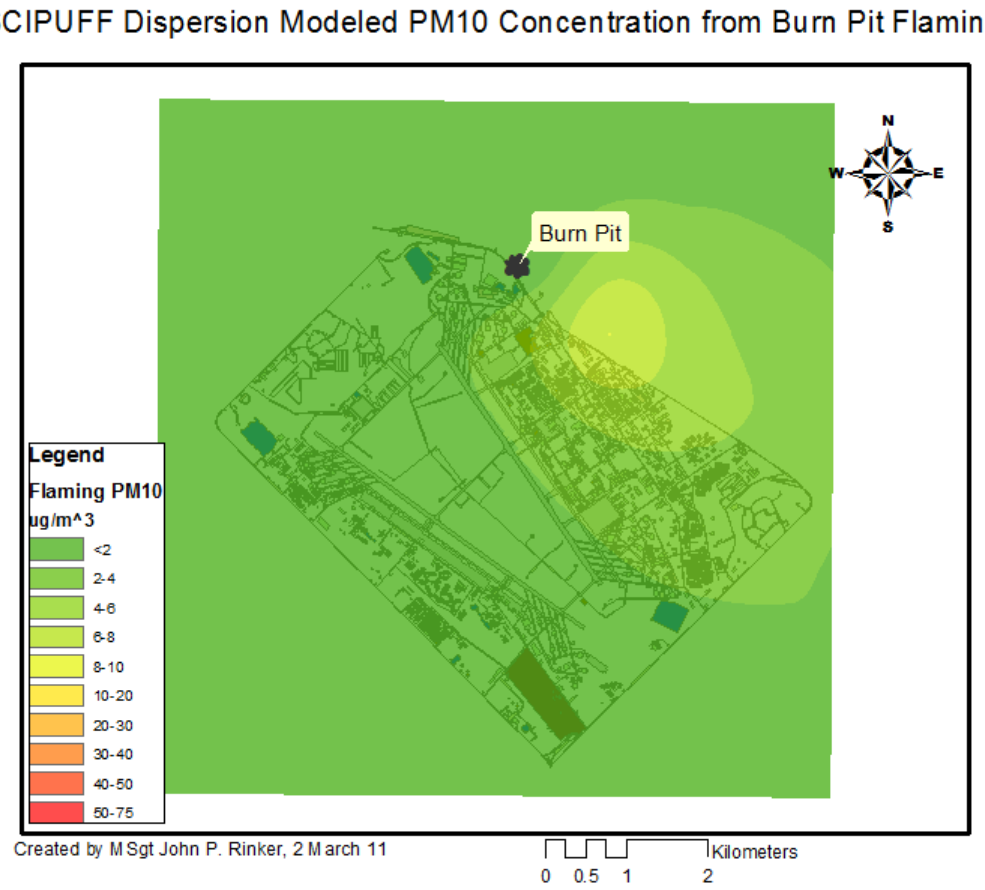

Figure 22: Dispersion Modeled Flaming PM10 Concentration

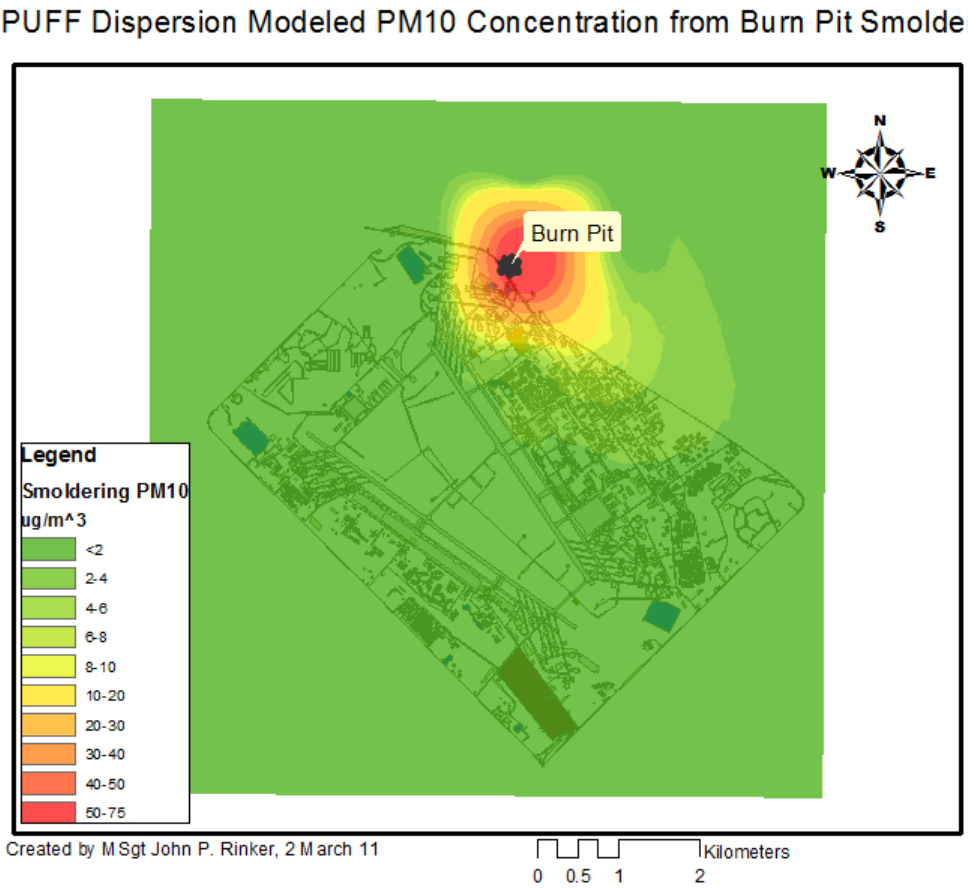

Figure 23: Dispersion Modeled Smoldering PM10 Concentration

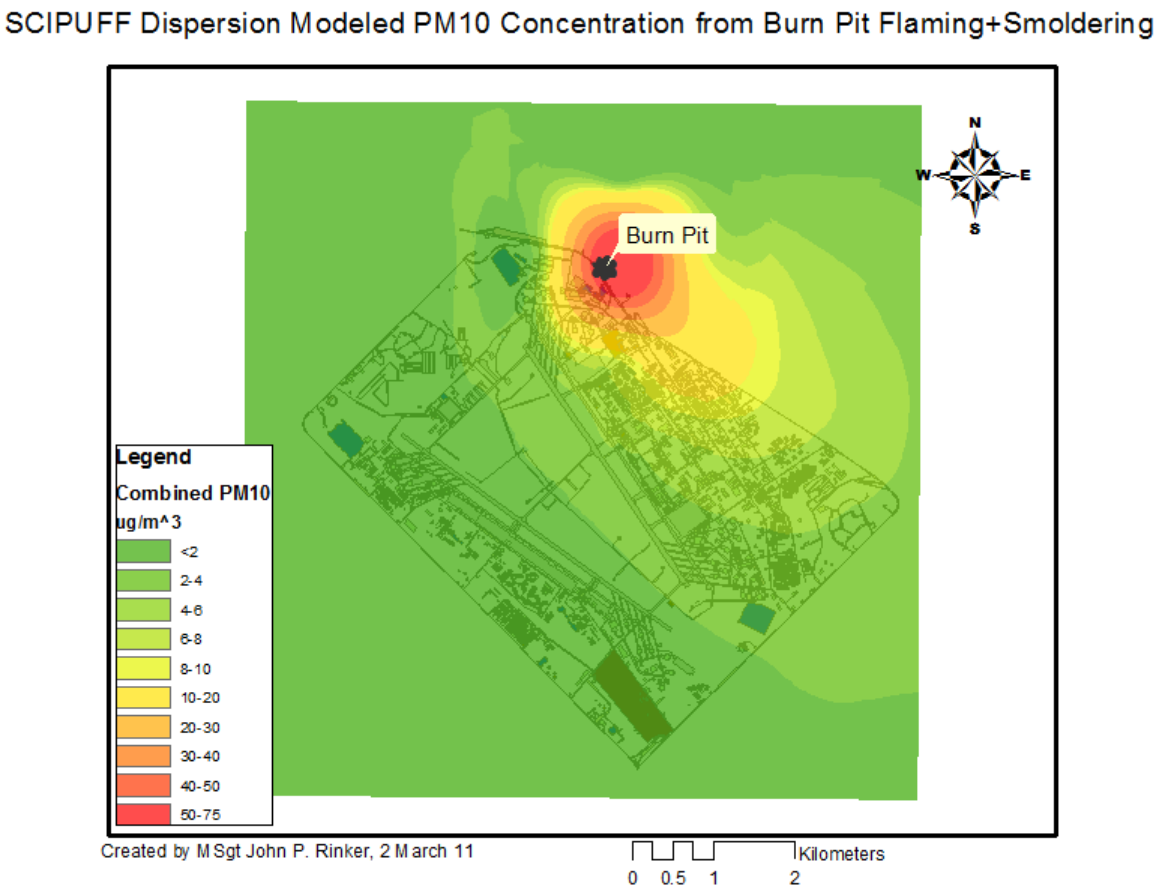

Figure 24: Dispersion Modeled Flaming + Smoldering PM10 Concentration

Concentration from the flaming burn pit contribution ranges from 0.06 µg/m^3 to 8 µg/m^3. Areas immediately adjacent to the burn pit site, such as the Guard Tower, appear to receive significantly less than areas downwind, with peak concentrations just downwind from the Transportation Field, in the vicinity of the CASF area. Overall, the most populated area of base, from the Transportation Field to southwest of the eastern corner of base, receive greater amounts of flaming PM10. According to the dispersion model, the south and west sides of base receives little PM10 from the flaming fraction. The model suggests at least two different exposure areas for flaming PM10.

Note that in the smoldering dispersion model, relative concentrations are higher closer to the burn pit when compared with the flaming contribution. This is expected, since plume rise associated with the flaming contribution acts as an effective stack, resulting in dispersion at greater downwind distances. Again, concentrations on the east side of base are higher than concentrations south and west. This indicates that the east side of base and areas closer and downwind from the burn pit, receive significantly higher fractions of PM10 from smoldering emissions.

The map with total dispersion modeled PM10 from burn pit (Figure 24) was interpolated from the summation of smoldering and flaming concentration values at the same grid points used to create those maps. The total PM10 dispersion pattern (Figure 24) closely resembles the smoldering map pattern (Figure 23), since the modeled concentration from smoldering is significantly greater than the flaming contribution. Like the smoldering and flaming maps, the combined map indicates increased exposure on the northern and western areas of base. Modeled concentrations range from <0.387 $\mu g/m^3$ to 75.2 $\mu g/m^3$. Of the sampling sites, the Guard Tower, sites 35 and 37, the Transportation Field, and CASF appear to receive significantly larger burn pit concentrations than all of the sites on the west side of base. According to the dispersion model, the Mortar Pit area is also relatively low in concentration.

Isopleths were drawn at 2.5 $\mu g/m^3$ intervals from the total PM10 dispersion modeled map. These isopleths were overlaid on the IDW interpolated continuous concentration surface of 2007-2008 measured concentrations (Figure 25). The interpolated model shows higher PM10 on the western side of base, in contrast to the

dispersion modeling isopleths, which show higher concentrations on the eastern and norther sides of base.

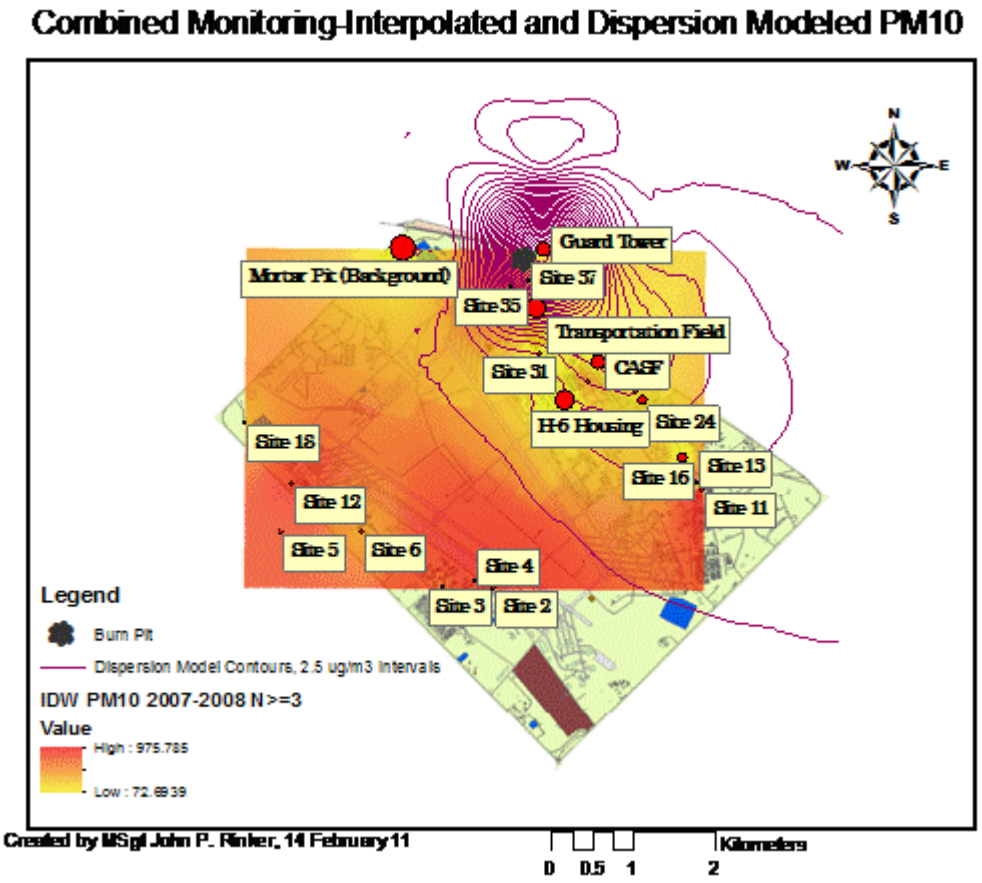

Figure 25: Dispersion Modeled Smoldering PM10 Concentration

The interpolated results from monitoring data represent the sum of PM10 concentration from all sources at all scales, including regional, urban, local, and neighborhood scales. Dispersion modeled isopleths represent modeled PM10 solely from the burn pit source. As previously mentioned, the low sampling numbers on the west side of base result in low confidence in the mean values. Consistent sampling through the year may bring the average down if the current means are skewed high. Alternatively, they may reinforce high mean values on that side of base. To model spatial differences, adequate sample size at each monitoring site across the appropriate

temporal scale is necessary. Increasing the number of samples per site per month will increase confidence in results.

In addition to possible skewing introduced due to temporally inconsistent sampling, there may be local source contributions explaining the local variability in concentration. Mapping pollutant sources and overlaying a source layer on interpolated concentration surface layers may provide insight into the cause of higher concentrations, as well as how to assign and control exposures.

Finally, revisiting the temporal sampling inconsistency issue may provide some insight and correcting such inconsistencies can perhaps increase confidence in interpolation of monitored results.. An example of such inconsistencies was that none of the sampling sites that were sampled in 2007 were sampled in 2008, and vice versa. Also, the entire west side of base (sites 2, 3, 4, 5, 6, 12, and 18) was not sampled in 2007. Six of twelve months were very poorly represented for both years. Table 6 summarizes the distribution of samples per month over time. Site numbers highlighted in yellow are located on the west side of base.

Table 6: Balad PM10 Sample Frequencies Per Site Per Month, 2007-2008

	MONTH											
SITE	JAN	FEB	MAR	APR	MAY	JUN	JUL	AUG	SEP	OCT	NOV	DEC
2					1	2						
3			4									
4			5									
5			4	1								
6			2	2								
11					1	2	1					
12			2	3								
13		5										
16	3	2	2									
18		3										
H6	8			3							5	

24		8										
25		4										
28		3										
CASF	2			5						5		
31		4	1									
Trans. Field		10		3							5	
35						2		1				
37		4										
Guard Tower	3			6						5		
Mortar Pit	1	9		10						5	5	
TOTAL	17	52	20	33	2	6	1	1	0	15	15	0
EAST	17	49	3	27	1	4	1	1	0	15	15	0
WEST	0	3	17	6	1	2	0	0	0	0	0	0

Distribution of samples per site per year are summarized in Table 8.

Table 7: Balad PM10 Sample Frequencies Per Site Per Year, 2007-2008

	YEAR	
SITE	2007	2008
2		3
3		4
4		5
5		5
6		4
11		4
12		5
13		5
16	7	
18		3
H6	16	
24		8
25		5
28		3
CASF	12	
31		5
Trans. Field	18	
35		3
37	4	
Guard	14	

Tower		
Mortar Pit	30	
TOTAL	101	62

Distribution of 2007 and 2008 sampling sites can be seen in the map in Figure 26, with the interpolated 2007-2008 concentration surface from monitored data is included as a layer. In this map, the 2007 sites, labeled as white circles, are generally lower in concentration (yellow), as compared to the 2008 sites.

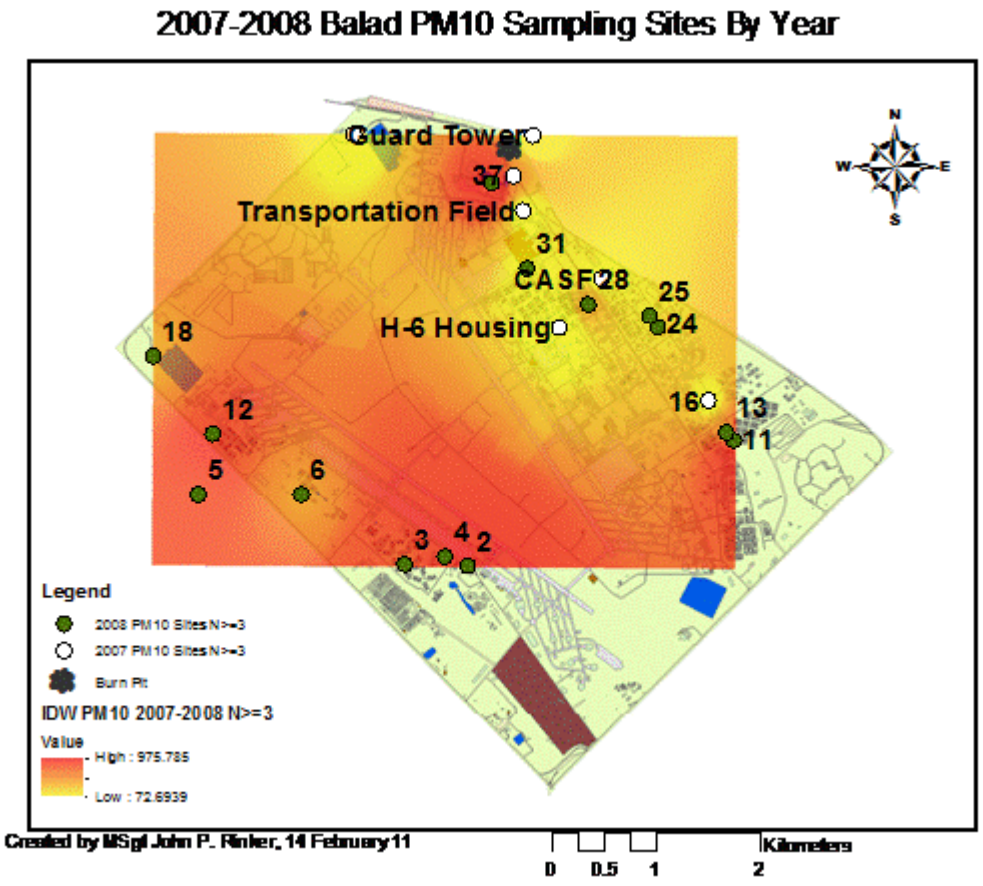

Figure 26: Balad PM10 Sampling Sites By Year, 2007-2008, With PM10 IDW Interpolation

Though the spatial coverage is not as complete and sample size is significantly lower for each year, an interpolated map was created for both 2007 (Figure 27) and 2008 (Figure 28), using only geometric means for sites sampled in the applicable year.

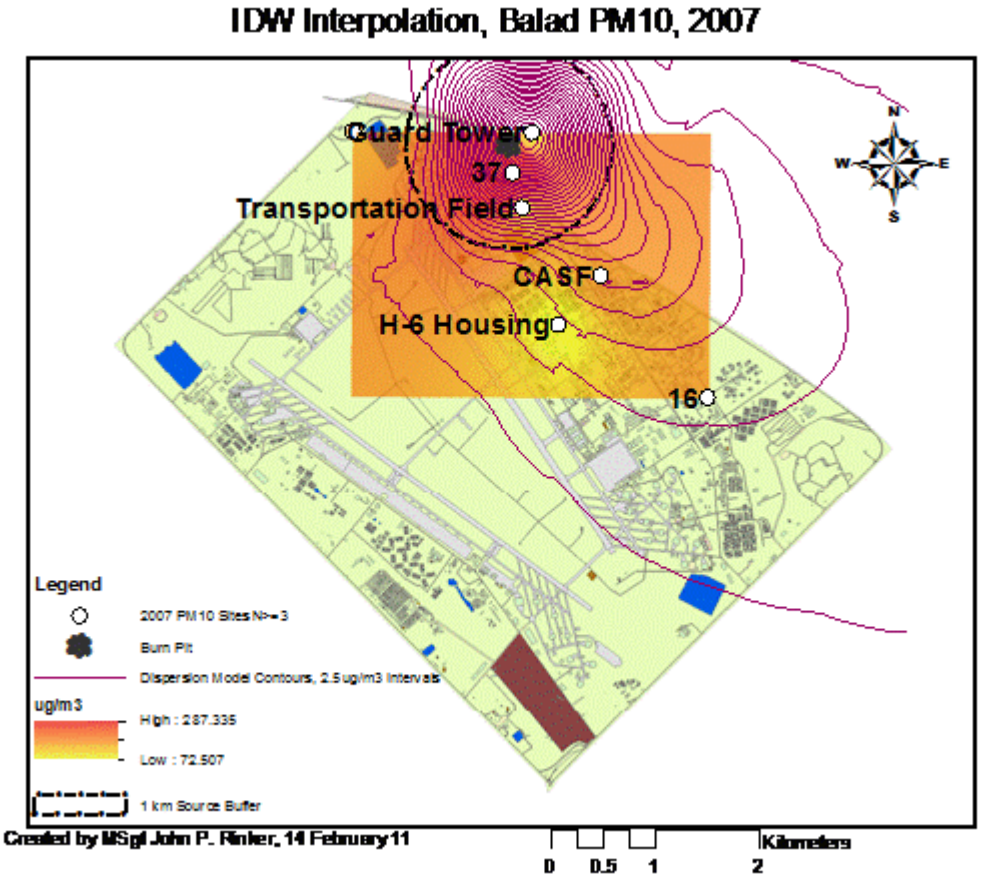

Figure 27: Inverse Distance Weighting Interpolation, Ambient PM10, Balad, 2007

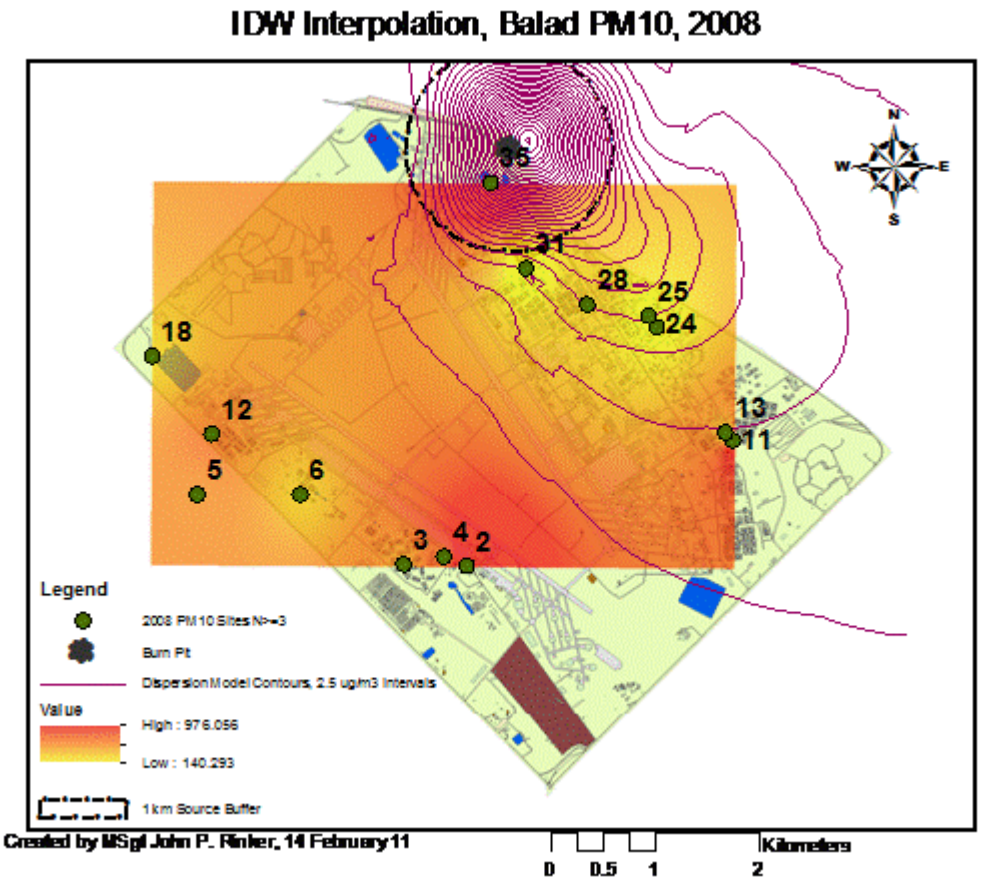

Figure 28: Inverse Distance Weighting Interpolation, Ambient PM10, Balad, 2008

The 2008 surface ranges between 140 and 976 µg/m^3, while the 2007 surface ranges between 72 and 287 µg/m^3. The spatial coverage for 2008 is greater, but more samples were taken in 2007 than in 2008 (n=97 vs. n=65, respectively). In both surfaces, high concentrations are associated with immediate downwind proximity to the burn pit; both "hot spot" areas around the burn pit are within a 1 km buffer, though the entire buffered area is not a "hot spot," as the guard tower concentrations are low in the 2007 map.

Since samples on the west side of base were all taken in 2008 and the combined map shows higher interpolated concentrations on the west side of base, a subsequent question is whether concentrations are higher in the interpolation model due to spatial

differences (are there higher PM10 concentrations on the west side of base), or due to temporal differences (was the PM10 across the entire base higher in 2008 than 2007, with the west side was represented well in 2008, but not 2007). A look at the variability chart of PM10 (Figure 29) shows visibly higher variability in 2008 than in 2007 and a higher mean in 2008, as well (purple line).

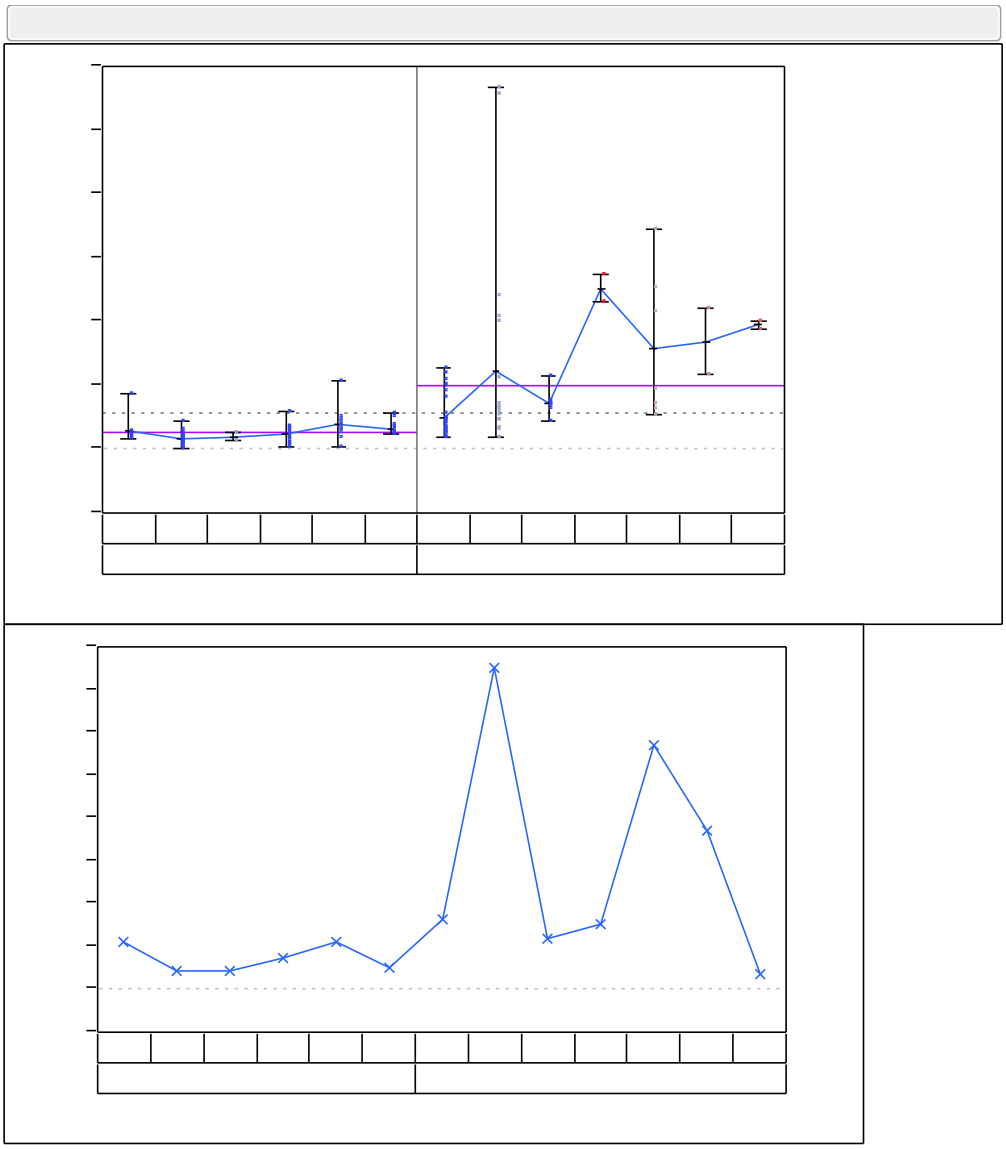

Figure 29: Month Within Year Variability Chart, Balad PM10, 2007-2008

Looking at the chart alone (Figure 29), it would appear that 2008 concentrations were higher than 2007. But, looking at the 2007-2008 interpolated map alone (Figure 28), it would appear that the west side of base is higher than the east side. Therefore, it is difficult to determine completely accurate results, due to the inconsistent spatial and temporal sampling. Higher 2008 concentrations are supported, however, by documentation of higher frequencies of dust storms in that year due to an extreme drought in the 2007-2008 winter (Crisp, 2008). Notes on daily conditions in a sampling database would help link concentrations to sources.

Assuming that concentrations within a 1 km buffer from the burn pit are relatively high, as modeled by both 2007 and 2008 interpolated monitoring surfaces and the dispersion model, an "intersection" geoprocessing operation was performed in ArcMap, using the 1-kilometer source buffer created during this research and the "existing structures" layer obtained from the ACC GeoBase, which contains building details on base. From the intersection, a map was created showing the buildings located in the buffer zone, along with the interpolated 2007-2008 PM10 concentration surface and the SCIPUFF annual concentration isopleths (Figure 30). Both models indicate that this is an area of relatively higher concentration of both PM10 and burn pit-specific PM10.

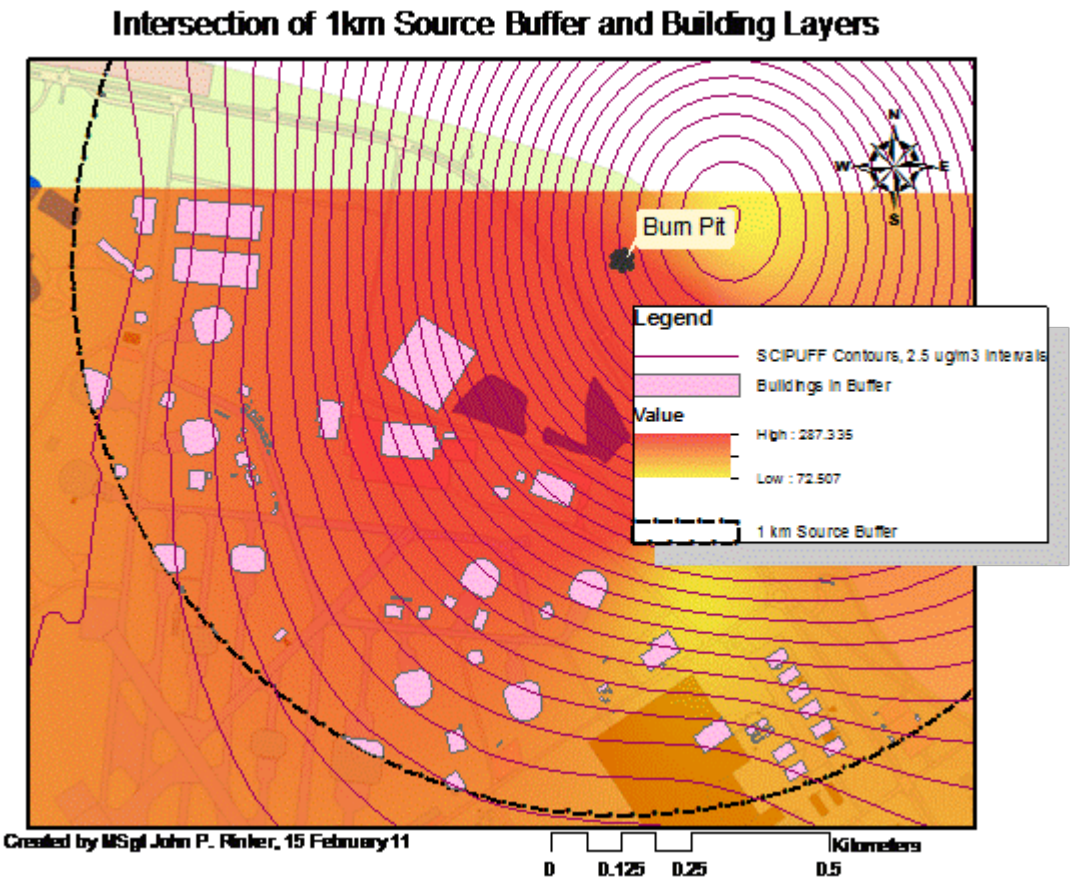

Figure 30: Identification of Buildings Within 1 km of Burn Pit Source

The attribute table for the buffer-structure intersection layer contains 109 features, with many of them being buildings or other structures, such as bunkers. A section of the table with structure attribute values can be seen in Figure 31. Each of these structures can be selected and highlighted by table selection in ArcMap, as well as identified individually directly on the map with the identification tool. Attributes for each feature can be viewed (e.g., building name, building number, structural use, and number of occupants).For security reasons, several values are labeled “null” (presumably).

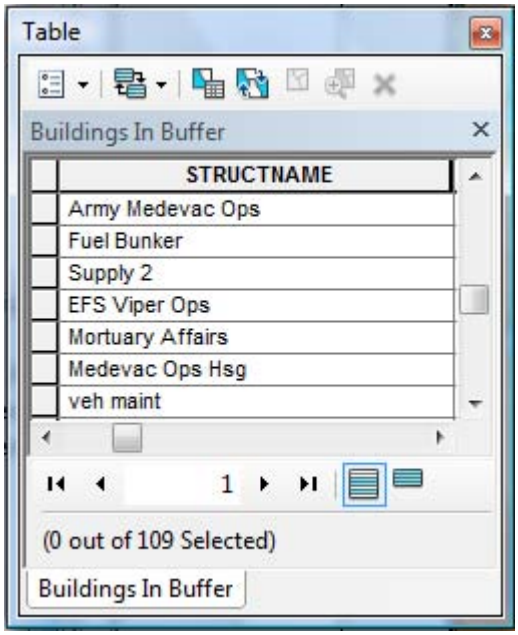

Figure 31: Attribute Table for 1 km Buffer-Buildings Intersection Layer

Sampling site, building-buffer intersection, IDW-interpolated 2007-2008 monitored concentration, and dispersion modeled isopleth layers were exported from ArcMap to Google Earth with the conversion tool "Layer to KML." This allows visualization of geographical exposure information at a high resolution without the need for the ArcMap software. It also simplifies visualization of possible receptor areas off base. A screen shot of the combined map is in Figure 32, and an example of off-base receptor site identification is in Figure 33. In addition, in Figure 32, structures are visible on the west side of base, indicating possible worker activity. This, in conjunction with low sample size numbers, shows potential for improving the monitoring network. Also, confidence intervals could be displayed directly on the maps to provide additional information regarding uncertainty.

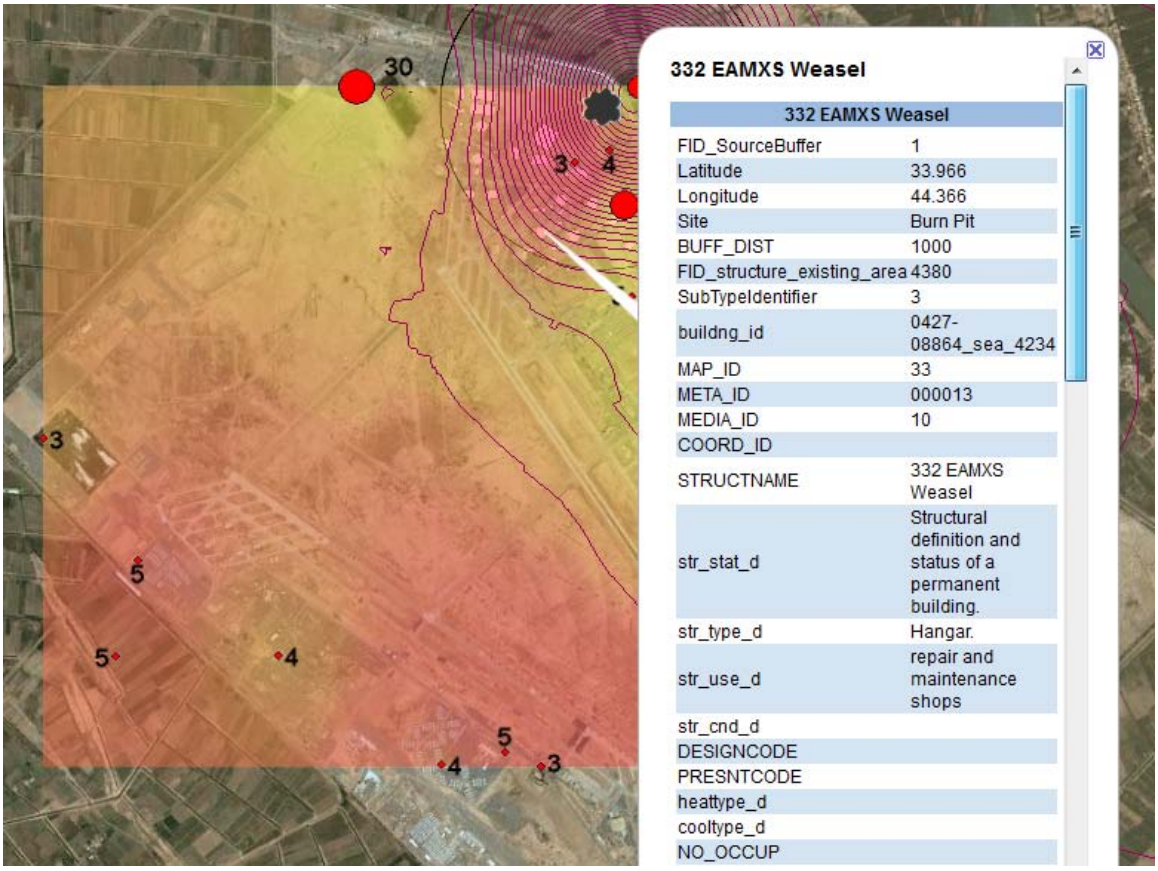

Figure 32: ArcMap Layers in Google Earth

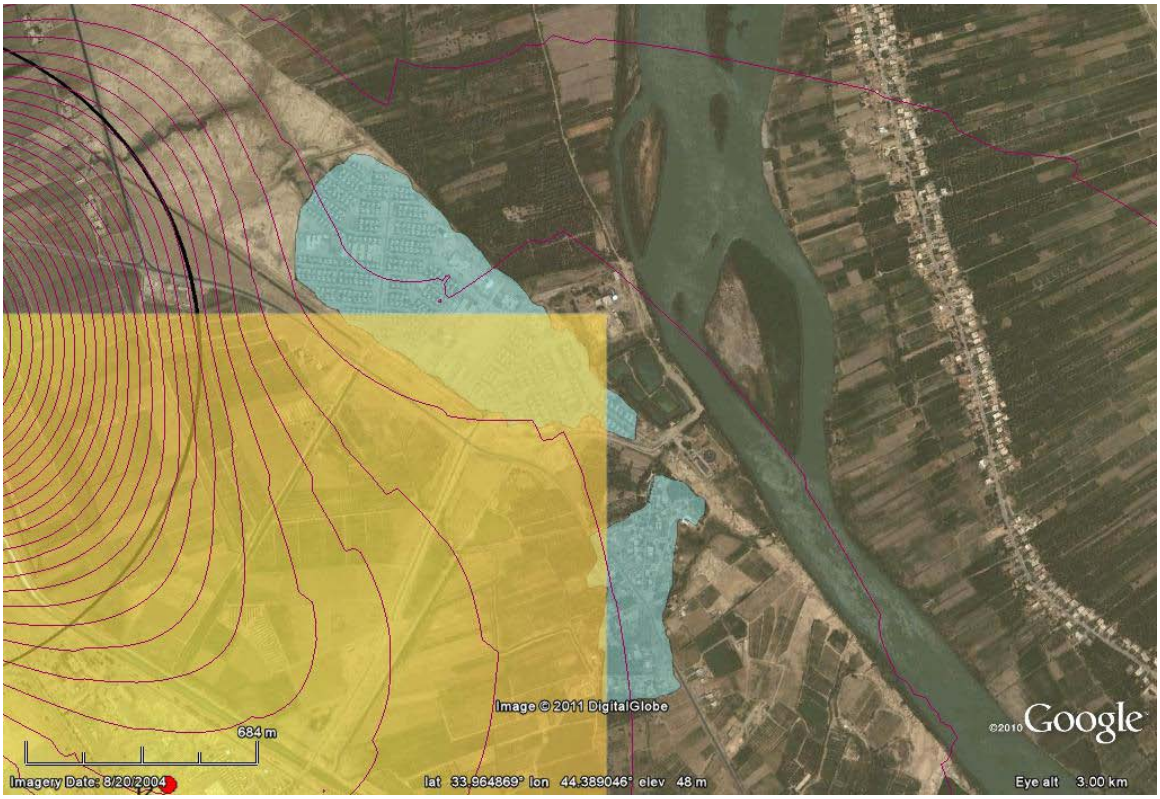

Figure 33: Identification of Off-Base Receptor Areas in Google Earth (Light Blue)

To determine burn pit contribution to total PM10, concentrations for each individual sampling site were modeled in SCIPUFF for the flaming, smoldering, and summed contributions. A determination of the dispersion modeled burn pit PM10 contribution to the monitored PM10 was calculated. Results are in Table 8.

Table 8: Dispersion Modeled Burn Pit-Contributed PM10 Concentration and Percentage of Monitored Concentration at Balad Sampling Sites

SITE	Geo Mean Conc (µg/m^3)	SCIPUFF Flaming Dose (kg*s/m3)	SCIPUFF Flaming Conc (ug/m3)	SCIPUFF Smolder Dose (kg*3/m3)	SCIPUFF Smolder Conc (ug/m3)	SCIPUFF Smoldering + Flaming Conc (ug/m3)	Burn Pit Contributed % of Total PM10 Conc (%)
2	976	8.99E-04	0.82	4.14E-04	0.38	1.20	0.12
3	349	7.75E-04	0.71	3.58E-04	0.33	1.04	0.30
4	408	8.84E-04	0.81	4.21E-04	0.39	1.20	0.29
5	363	5.43E-04	0.50	2.37E-04	0.22	0.72	0.20
6	274	7.05E-04	0.65	3.29E-04	0.30	0.95	0.35

11	759	3.61E-03	3.31	1.69E-03	1.55	4.86	0.64
12	416	6.36E-04	0.58	2.88E-04	0.26	0.85	0.20
13	202	3.66E-03	3.35	1.76E-03	1.62	4.97	2.47
16	127	4.45E-03	4.08	2.17E-03	1.99	6.06	4.76
18	259	6.21E-04	0.57	2.86E-04	0.26	0.83	0.32
H-6 Housing	73	4.15E-03	3.80	3.79E-03	3.48	7.28	10.04
24	194	5.82E-03	5.33	3.81E-03	3.50	8.83	4.55
25	170	6.11E-03	5.60	4.21E-03	3.86	9.47	5.58
28	268	5.99E-03	5.49	5.40E-03	4.95	10.44	3.89
CASF	129	7.11E-03	6.52	7.51E-03	6.89	13.41	10.42
31	140	4.58E-03	4.20	7.13E-03	6.54	10.74	7.66
Transport Field	94	2.96E-03	2.71	2.53E-02	23.22	25.93	27.48
35	714	5.73E-04	0.53	2.91E-02	26.66	27.18	3.81
37	287	5.96E-04	0.55	0.101582	93.13	93.67	32.60
Guard Tower	84	3.89E-04	0.36	5.89E-02	54.02	54.38	64.67
Mortar Pit (Back-ground)	122	1.44E-03	1.32	1.44E-03	1.32	2.63	2.15

The highest dispersion modeled concentrations for ambient sampling points were at site 37 (94 µg/m^3), the Guard Tower (54 µg/m^3), site 35 (27 µg/m^3), and the Transportation Field (26 µg/m^3). The CASF concentration was modeled as 13 µg/m^3, and the H6 Housing concentration as 7.28 µg/m^3.

In contrast to the interpolated PM10 from monitored sampling locations, there is a linear relationship between dispersion modeled PM10 and inverse distance (R^2=0.85) (Figure 34). As inverse distance increases, the linear fit is not as good, which is likely due to the directional effects of wind on pollutant levels near the source in the model.

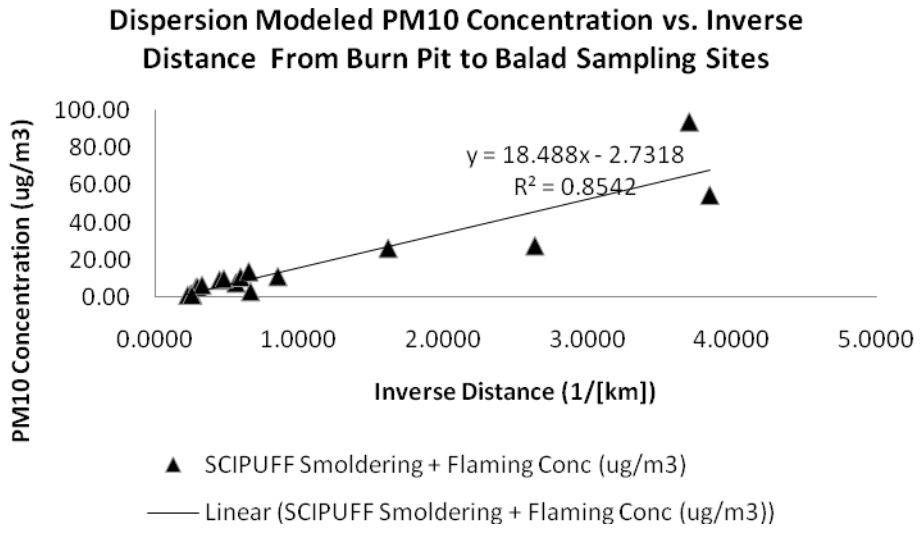

Figure 34: Dispersion Modeled Burn Pit-Specific Total PM10 Concentration vs. Inverse Distance from Sampling Sites to Burn Pit

Dividing the dispersion modeled concentrations by the total monitored concentrations for each site, the highest contribution of PM10 from burn pit as a percentage of total PM10 are at the Guard Tower (64.7%), "Site 37," (32.6%), and the Transportation Field (27.48%). All other sites were at ten percent or lower.

There are several implications for these results. For example, if burn pit emissions are different in composition, or if their particle size distributions differ from other ambient sources, then the percent composition of burn pit-specific compounds in the total PM10 should increase with increasing concentrations of burn pit-specific emissions. If particulate compositional analyses were to be accomplished, percent composition would vary highly depending on where the samples were taken, according to the dispersion models. Samples taken from the CASF or the H6 Housing area, for instance, would be expected to be composed of approximately 90% ambient and 10% burn pit-specific particulate (minus whatever is lost in the collection method). The

Enhanced Particulate Matter Surveillance Program sampling site on Balad was site 16 (Building 4149), which has a modeled 4.76 percent burn pit contribution to total PM10. Assigning this composition of ambient particulate to the entire base would be erroneous.

An improved way to do compositional analyses would be to model source-specific contributions to total ambient concentrations, determine which geographical sections are expected to be compositionally different, and randomly sample within those zones. This should not only result in better characterization of hazard to subpopulations, but it would also help to validate the modeling.

It is also important to note that increased risk at lower levels of exposure were seen in a 20-city study of daily mortality associated with PM10, as increasing levels of PM10 were found to increase mortality, with no minimum threshold concentration (Daniels, Dominici, Samet, & Zeger, 2000). These are short-term effects, but long-term averaging can provide information on most-likely geographical areas for higher concentrations of pollutant. Also, the burn pit-contributed concentration may be more biologically important (bioavailable) than the regional background ambient concentration and is at least likely to be compositionally different. For these reasons, it is important to determine individual or population exposures not only to total ambient particulate, but also to source-specific particulate, such as burn pit emissions and other combustion emissions.

Exposure Modeling With Exposure Maps

Exposure mapping combined with personal or similar exposure group exposure modeling methods provides a refined method for estimating exposures to individuals or exposure groups, compared to assigning one worst-case value to an entire population.

Personal exposure to air pollutants has been expressed as shown in Equation 8. The units are usually expressed as $\mu g \cdot d/m^3$. (Zou, Wilson, Zhan, & Zeng, 2009).

$$E_i = \sum_j^J C_j t_{ij} \quad (8)$$

where:

E_i =the exposure for person *i* over the time period of interest

C_j = concentration of the pollutant of concern in area *j*

t_{ij} = time, usually expressed in days, spent by person *i* in area *j*

J =the number of areas

The concentration term can be divided into scale-specific terms, and broken into microenvironmental categories, as well. For example, $C_j = C_{outdoor\ ambient} + C_{indoor}$, and the outdoor ambient contribution to total concentration can be further broken into $C_{outdoor} = C_{j(regional\ sources)} + C_{j(urban\ sources)} + C_{j(local\ sources)}$, and so forth. Each one of these may have its own toxic pathway, depending on factors such as composition, size, and morphology. In characterizing exposure to particulate matter, it is common practice to assign total concentration, without differentiating between sources. This may be unhelpful in completing longitudinal health effects studies, in which epidemiologists wish to investigate source-specific exposures to health effects.

To demonstrate the determination of daily exposure using an exposure map, first considerthe exposure of interest as being ambient outdoor burn pit PM10 exposures. The map of dispersion modeled PM10 isopleths across base (Figure 35) without interpolated PM10 concentrations will suffice, since we are not interested in other source

contributions. For map-based exposure modeling with separate exposure zones, the following equation can be used:

$$E_i = \sum_z^Z C_z t_{iz} \quad (9)$$

where:

E_i = exposure to individual *i*

C_z = concentration in zone *z*

t_{iz} = time spent by individual *i* in zone *z*

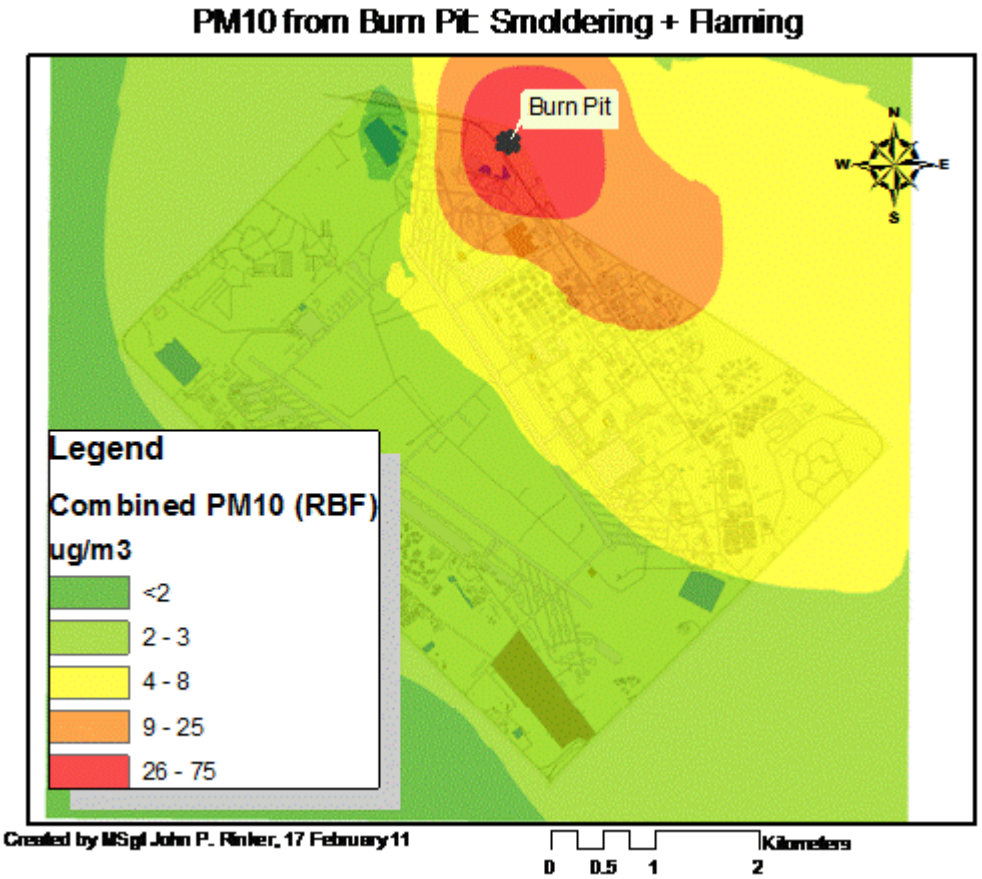

Figure 35: Dispersion Modeled Smoldering + Flaming PM10

Next, assuming that an individual's work and residence locations are georeferenced in a geodatabase, then upon querying the database, it is noted that this

person works outdoors between two buildings on the west side of base 12 hours per day (light green area, 2-3 µg/m^3) and sleeps on the east side of base in the orange area (9-25 µg/m^3) and in a building in which there is 100 percent infiltration of outdoor air. His expected daily exposure to burn pit PM10, in concentration units, would range between $(C_{residence}T_{residence} + C_{work}T_{work})_{min}/T$ = (2 µg/m^3 x 0.5d + 9 µg/m^3 x 0.5d)/1d = 5.5 µg/m^3, as a minimum, to $(C_{residence}T_{residence} + C_{work}T_{work})_{max}/T$ = (3 µg/m^3 x 0.5d + 25 µg/m^3 x 0.5d)/1d = 14 µg/m^3, as a maximum expected average. This individual might be considered to be in a separate exposure group than people who, for example, both live and sleep in the orange area on the east side of base. This estimate assumes 24 hours of outdoor time. If building infiltration of outdoor air is known, multipliers can be added to the exposure concentrations.

Limitations and Uncertainty

An effort was made to explain limitations and uncertainty throughout the Methodology and Results sections. This section will summarize major limitations and uncertainties in this study.

The greatest single source of error in the dispersion modeling portion may be in determination of emissions, with the overarching assumption that burning and emissions are released in a steady-state, continuous manner with a constant emission rate. Emissions were determined using emission factors from small-scale burning of household waste in barrels, which may be very different than actual burn emissions from a military burn pit.

Potential error in the meteorology input to the dispersion models also acknowledged. A 1000 meter mixing height was used as a constant, as well as a constant

average temperature, making dispersion variations dependent on wind direction and frequency. The actual mixing height probably varied diurnally and inversions likely kept actual heights low for periods of time. Lower mixing heights would result in higher average concentrations. Creation of the annual meteorological file with sequential determination of Pasquill-Gifford stability categories for input into the dispersion model would have required creation of a file with nearly 90,000 data values across nearly 9,000 lines and would have required days, rather than hours, for computational run time. This would have taken much more time than was available for completion of this research, without the benefit of known increased accuracy since large error is expected in emissions and burn patterns are unknown.

There is also expected error in loose-coupling the dispersion model into GIS using interpolated gridded values. A finer grid with more than 100 points or an adaptive grid with finer scale at higher concentrations could have been used, but again, the error in the emissions estimate and assumption of steady state burning would likely not overcome translational errors from loose-coupling.

The determination of plume height and assumption of two constant release heights is not likely to reflect reality. Without knowledge of composition and amounts of each burn, plume height is at best a guess. Conservative estimates compared to modeled values were used in this study.

The dispersion model output is based on the full annual frequencies of wind speeds and direction. As shown in the Results section, there are pronounced seasonal differences in wind patterns and exposures are likely to be different depending on the time frame that a member is deployed. The dispersion isopleths created in this study, if

accurate, represent annual average concentration, and would apply to annual deployments. Also, actual conditions may differ from climatological means, and even when monitoring station measurements are used, there may be both measurement errors and error in assuming that hourly measurements apply to the next unmeasured 59 minutes.

There are also uncertainties in the monitoring data. Large temporal differences in concentration from both local and regional sources create uncertainty in the monitored interpolation. Monthly sampling at each site is necessary to approach good estimates of the mean when considering the changing frequency of dust events throughout the year, coupled with possible source-specific differences at multiple scales, such as regional-scale agricultural burning. Since some time periods in each year were not represented with samples, it is likely that the mean concentration was not accurately estimated.

Measurement error may also be a problem. The MiniVol was not validated for sampling in areas with very high ambient particulate, but was used in theater without replicate sampling. There was no estimated error provided with sample results.

There is also uncertainty in georeferencing of sample sites. There is no documentation of georeferencing methodology, so measurement error in sampling site coordinate determination is unknown. This error would be reflected in the interpolated sampling surface. It is probable, however, that this error is minor compared to the error from temporally sparse sampling.

Translating exposure to risk must be done with caution. According to Technical Guide 230, which establishes Military Exposure Guidelines (MEGs), there is no long-term PM10 MEG. Rather, only a short-term 24-hour MEG applies and the guide states

that long-term averaging of PM10 is not recommended (USACHPPM, 2003). Risk is to be determined according to estimated daily levels of PM10 only. According to these guidelines, the exposure maps presented in this study, which are long-term averages, should not be used to determine risk. In practice, long-term averages *are* currently used in estimation of risk, as single-site averages are assigned to the entire base. As previously explained, this is a simple interpolation in which one point defines uniform exposure across an area.

There is currently on-going research on toxic effects of burn pit smoke, results of which may strengthen risk assessments. In the absence of complete toxicity testing, a precautionary approach includes consideration of both short-term, and the possibility of long-term effects of burn pit smoke.The current lack of a long-term MEG is based on EPA's revoking of a PM10 National Ambient Air Quality Standard (NAAQS). EPA revoked the PM10 NAAQS based on the absence of definitive health effects research. Toxicological studies, however, have not yet been concluded on burn pit-generated particulate matter, and long-term effects may not be determined for years.

Finally, the modeling in this study applies to ambient outdoor exposures only. A significant fraction of daily inhalational exposures may occur indoors. A complete exposure model should include outdoor ambient exposure, indoor residential exposure, and occupational exposure.

V. Conclusions

Burn pit exposure continues to be a problem while deployed and the difficulty in determining personnel exposures from open burning has prevented confirming (or disproving) linkages between exposure and health effects. The purpose of this research was to delineate retrospective exposure zones using spatially interpolated particulate air sampling point data from Joint Base Balad, create burn pit exposure isopleths from dispersion model outputs, and merge into a combined exposure model in GIS. This was accomplished by following the process described in the Introduction and pictured in Figure 1. The process was:

1. Collect, georeference, and perform initial analysis on monitoring data
2. Perform spatial analysis and create interpolated exposure maps with monitoring data
3. Determine or estimate emission rates
4. Model plume rise and dispersion; estimate specific source contribution
5. Overlay drawn dispersion modeled isopleths over interpolated exposure maps
6. Determine high exposure intersections between monitored and modeled data

Maps were created by interpolating monitored data from 2007-2008, and SCIPUFF-generated isopleths were created with climatological mean data from the weather station KQTO at Joint Base Balad. These were merged into a combined map, with a high exposure area and specific features identified.

Specific research problems and study results were:

1. Determine spatial and temporal patterns with monitored particulate data.

Expected temporal patterns in ambient particulate were examined in the exploratory data analysis. Climatic data summaries show significantly greater frequencies of dust storms in the summer months, moderate frequencies in the spring and fall months, and low frequencies in the winter months. High temporal variability is expected and it was stated that random sampling throughout the year is required at each site to appropriately estimate mean values and determine spatial patterns in concentration across base. Since this was not done, there is low confidence in interpolated mapping and attempts to determine spatial concentration patterns for an annual time scale. Focusing on shorter time periods, such as seasons or months, may provide higher confidence if sufficient sample numbers per site are available, but temporal variability problems will remain as long simultaneous sampling data and background concentrations are lacking, since between-day variability is also high. Nevertheless, interpolated maps were created to visualize the concentrations estimated by monitoring across space, and to view geographical areas in which sample size was low. Also, the PM10 average for 2008 was significantly higher than the 2007 average, but since all of the sample sites in 2008 differed from those in 2007, it could not be determined whether the difference was due to temporal regional influences or local spatial patterns from point sources.

Interpolated maps were created for the entire 2007-2008 period, as well as for each separate year. A consistent feature and significant finding of each map was a high interpolated concentration within a 1 km buffer of the burn pit source.

2. Model burn pit ambient exposure zones with a dispersion model.

SCIPUFF was used to create isopleths representing successively increasing exposure zones, by first inserting loose-coupling dispersion model results into ArcMap. Areas of higher modeled concentration generally followed the direction of prevailing winds, per the annual wind rose for the Balad meteorological station. Modeling of the north and east areas of base indicated higher levels of PM10 than the south and west areas. Highest modeled concentration could be found within a one kilometer buffer of the burn pit source. Modeled PM10 contribution from smoldering combustion was significantly higher than from flaming combustion. Reducing smoldering combustion by keeping the flame hot, the moisture content low, and ensuring adequate supply of air to the fire should reduce exposures locally.

3. Estimate relative burn pit contribution to overall exposure, and determine whether modeled dispersion concentration differences predict monitored concentration differences.

This was accomplished by using SCIPUFF to model annual averaged concentration at each ambient air monitoring site and determining the dispersion modeled PM10 as a percentage of the monitored average PM10 at each site. Results differed depending on sampling site location, but ranged from less than 5 percent to greater than 60 percent of total monitored PM10. Modeled concentration differences did not accurately predict monitored differences and monitored PM10 concentrations did not show a linear increase with inverse distance. However, dispersion modeled PM10 concentrations did show the linear relationship with inverse distance.

4. Identify sampling needs to improve spatial modeling.

This was accomplished by creating sampling location maps with sample sizes displayed at each site and in relation to receptor areas to highlight possible weaknesses in the sampling network. The west side of base was under-represented with inadequate sample sizes to characterize exposure. Several receptor areas could be seen with satellite imagery and with the GIS existing structure layer, indicating personnel activity in those areas. The measurements that were taken on the west side are associated with higher PM10 compared to the east side. Source identification and additional measurements may clarify the reasons for higher monitored concentrations in this area.

As mentioned in the Introduction, the monitored data represented summation of all sources to the sampling filter, whether at the regional, urban, or local scale. If ambient regional background was known, it could be subtracted to reveal local contributions to the total. This would result in better exposure maps of local source-contributed pollution without confounding influences of high-concentration, temporally variable regional sources. Local sources and pollutant transportation from those sources should be considered to determine possible sites for background monitors. The use of one background monitor is discouraged, as changing wind patterns affect source dispersion. Background monitors should be placed upwind of all local sources that may confound results.

5. Create a method to model relative source-specific ambient exposures for individuals or similar environmental exposure groups. A mathematical exposure model was provided, based on modeling results and isopleths created with SCIPUFF and ArcMap. Refined dispersion modeling will increase confidence in the exposure model estimates.

Suggested Methodology Improvements

The greatest methodology improvements can be made in the dispersion modeling, which will increase confidence in exposure estimates and improve the exposure maps. First, the dispersion model was run with the assumption that municipal waste emissions apply to military waste. Determination of emission factors for military waste will increase the confidence in the estimates. It is important that any field studies that mimic theater burning attempt to use the same composition, quantities, and configurations used in theater, as these parameters are determinants of emissions and may cause high variations in concentration. Questionnaires or surveys to burn pit operators or preventive medicine personnel may assist in collection of this information.

With increased confidence in emission estimates, it may also be worthwhile to refine the model itself. AERMOD and CALPUFF could be used with an improved meteorological input file with stratified wind data, improving mixing layer estimates, plume rise estimates, and increasing accuracy in the dispersion output. This would require significant work in formatting and quality checking the meteorology input files, as well as hands-on user training.

On the other hand, lack of knowledge in burn patterns will limit accuracy. According to the METAR reports, most days in which "smoke" was reported as a condition did show the condition for a period of several hours, rather than an entire day. Burn logs would have been helpful, but tracking of open burning generally did not occur. GAO recommended stronger management of burn pit operations, including waste type documentation and logs. Perhaps these could be reviewed and from this documentation,

estimations of burn time, emission time, and refined short-term modeling could be accomplished.

Strengths and Limitations

There are strengths and limitations associated with any environmental research study. This section explicity describes the greatest strengths and limitations of this study.

Strengths

The greatest strength of this study is that, while concentration estimates are probably erroneous, it provides a process to determine source-specific contributions to total pollutant concentration. This methodology can be applied to any point source, including burn pits. It also provides better resolution in exposure determination than the current method of assigning a worst-case value to the entire base or to large portions of the base, without regard for pollutant movement. Exposure epidemiology depends on identification of differentially exposed individuals (i.e., similar exposure groups), and this study provides a means to do that, by providing the ability to define areas of relative exposure.

Limitations

As stressed throughout this study, there are two significant limitations in this study. First, there is the uncertainty in emissions due to unknown waste composition, burn patterns, and emissions from the open burning of military waste in burn pits. Several assumptions had to be made to complete the modeling and since successive modeling occurred, significant error propagation is likely. Significant error in the

original emission estimate and burn patterns would result in high error in dispersion estimates and the loose-coupling of dispersion estimates into GIS likely results in additional translational error. Assuming constant mixing burn rates, mixing heights, and plume rise are simplifying assumptions that can also significantly affect modeled concentration; high-resolution meteorological and dispersion modeling may be justified when more accurate estimations of emissions are available.

The second major limitation is in the creation of exposure surfaces based heavily on estimates of site-specific mean concentrations. The temporally sparse, non-random sampling at some sites, especially those on the west side of base, may have skewed the mean values at those sites toward the average concentration for the months sampled. Additionally, high between-day variability could have resulted in one site sampled during a severe dust storm, while others were not, making it appear that that site has a higher annual average. Same-day sampling and background accounting should reduce this problem. Confidence in the means, and in the resulting exposure surface, would be increased if each site were sampled simultaneously throughout the year.

There are also general limitations in applying the methodology in this study. Exposure depends on the physical interaction of a person with a pollutant in an environment. Personal movement greatly influences exposure, and tracking movements can be highly difficult. To achieve a good estimate of personal exposure, knowledge of sources and concentrations in a person's environment throughout each microenvironment in which he moves is necessary. Simply assigning concentrations based on annual estimated isopleths does not achieve a high level of accuracy in determining personal

exposure. Indeed, personal sampling is the gold standard in determining personal exposure, but note also that the individual's exposure may not apply to others.

This method as accomplished in this study also has temporal limitations. Since the averaging time was a year, it applies only to annual deployments. Average concentrations may be higher if an individual is deployed in the summer and may be lower if an individual is deployed only in the winter. Though the specific model created in this study applies to annual concentrations, it can be scaled down to seasonal, monthly, daily, or hourly intervals of time, or for whatever period of time is of interest, as long as input data for the models are available for those time periods.

Recommendations for Future Research

Expansion of This Study

Following procedures in the methodology section and the GIS Procedure Log as a in Appendix F as a procedural model, this research can be easily re-accomplished with updated data. Confidence in hazard characterization of burn pit exposures will likely remain low until emissions testing and toxicity testing are completed. Emissions testing has been planned for completion in 2011 and toxicity testing is also in progress. Emissions testing can then be used to refine the dispersion model and toxicity testing may provide insight into what levels to use as cutoff points for concentration isopleths.

Another obvious expansion area for this study is to model other pollutants. PM2.5 data are also available, as are data for PAH, acrolein, metals, and other pollutants. PM10:PM2.5 ratio could also be modeled. This may be important if the particulate emitted from the burn pit has a different size distribution than ambient particulate. If the burn pit has greater fine fraction (<2.5 µm) than ambient, then the PM10:PM2.5 ratio

would be expected to be lower in modeled high-concentration areas from the burn pit. Determining size distribution differences from ambient at different sites may give insight into pollutant source. Dispersion and interpolation could also be performed with datasets from other bases. Further, predictive models could be created with proposed burn pit areas and GIS layers.

Modeling at different temporal scales could also be performed. Using METAR or climatological mean data for seasons, for example, one could quantify differences in expected exposures for a summer versus a winter deployment. Since daily (24-hour) sampling data is available, single-day plumes could be created and compared to individual site results to see whether burn pit predicted plumes explain within-day variability between sites.

Multivariate regression modeling could also be performed, using meteorological observations, source data, and monitored data. Effects of the interactions of averaged wind speed, maximum winds, stability classes, wind direction, and proximity to points within an area, on pollutant concentration, could be modeled.

Finally, a field sampling study to assess exposures by determining the exposure surface could be accomplished. Exposure assessments can be performed for several reasons, including, but not limited to, determining compliance with established limits, quantifying total exposures to a pollutant, regardless of source, defining similar exposure groups, investigating complaints, evaluating controls, allocating pollutant sources, and setting up epidemiological or health effects studies. If there are several reasons to complete an exposure assessment, several strategies may be required, and these strategies may involve sampling, modeling, biomonitoring, or other methods, and a combination of

methods may also be used. Therefore, no attempt will be made to prescribe "the one best sampling strategy" for burn pit or PM10 exposures. Rather, these paragraphs will suggest methods to improve on existing sampling strategies.

To achieve a statistically defensible spatial model of concentration, a large, evenly spaced grid of many samplers is required, so that kriging can be performed, and a semivariogram fitted to the data. A robust grid of many sampling sites is needed to interpolate by kriging, and to achieve a high level of confidence in the model.

For a study investigating cadmium-contaminated soil, 140 sites were needed to achieve reliable predictions with kriging. Using Bayesian kriging, 60 sites were required for adequate predictions (Cui, Stein, & Myers, 1995). To determine within-site error, collocated sampling might also be required. Thus, to set up a grid for kriging analysis, at least 280 samples would be required, and for Bayesian kriging, at least 120. Additionally, to capture temporal variability, simultaneous sampling should occur several days during each month. This can be prohibitively expensive and would likely exceed the capabilities of already highly tasked environmental health sampling technicians. Reducing the number of sites would increase error, but would be an improved method over using a single monitor and extrapolating to the entire area. An iterative approach could also be used, where an increasing number of simultaneously sampled sites are used until a desired confidence is achieved. Also, this approach would be useful if the purpose of sampling is to determine total concentrations from multiple sources of a pollutant across a geographical area, but might not be of value if source-specific exposures need to be determined.

For example, if high variations in concentration are caused by highly localized sources, such as personnel activity, vehicular traffic, or airfield operations, and one is interested in spatial variations caused by a single source, such as a burn pit, that may cause a fraction of the variability on most days, then the burn pit exposures will be extremely difficult to determine. Even with simultaneous sampling on a robust grid, highly variable local confounders may obscure smaller variations caused by single sources. As previously mentioned, the concentration surface of particulate matter has been found to be highly heterogeneous at highly localized intra-urban scales.

It must be stressed that the purpose of sampling must be determined prior to establishing a sampling strategy. If the exposure assessment purpose is to determine spatial differences in a pollutant based on contributions from all sources, then a gridded network of samplers that do not discriminate between sources may be an appropriate choice. If, on the other hand, the purpose of the exposure assessment is to determine exposure to specific sources (such as burn pits), or to differentiate between personnel with higher and lower exposures to a single source so that epidemiological studies can be completed, then a gridded network may not provide the answers, especially if confounding sources are present. If samplers can be placed so that only the source of concern is sampled, and confounding sources will not affect results, then spatial gridded sampling may provide good information on source-specific exposures. This type of strategic placement of samplers, however, makes it challenging to maintain the integrity of a grid.

One way to remove the influence of confounders on samples during exposure assessments is to re-create the pollutant emission and dispersion scenario in an area that

is relatively free of confounders. Instead of attempting to determine burn pit exposures by sampling in theater, where regional ambient variability may be in the hundreds of micrograms per cubic meter, and operational activity adds further significant variability, it may be desirable to set up a mock burn pit, using the same waste, with the same burn conditions, in similar terrain, but in an area where there is low ambient background and a lack of local pollutant-generating activity. A range of meteorological conditions should be sampled, including inversions and varieties of wind conditions. Ideally, an area is selected in which daily temperature profiles match the case in theater.

A suggested methodology is as follows. First, waste composition, burn conditions, and emission rates should be determined, as well as local terrain characteristics. A suitable site that matches the local terrain should be selected, relatively isolated from confounding sources. Then, using a high-resolution dispersion model with high-resolution meteorological forecast input, the release and dispersion can be predicted. The selected dispersion model should have the ability to export concentrations at specific receptor sites, and ideally has the capability to create a grid given coordinate boundaries, so that monitoring results can be directly compared to modeled concentrations. The burn site could be completely surrounded by a grid, but a dispersion model can provide information on where areas of non-detects may be found, so that the sampling grid can be focused on the plume extent rather than clean areas upwind. GIS can be used to create a sampling grid, preferably of at least thirty sampling sites, per the Law of Large Numbers, within the desired prioritized area predicted by the dispersion model.

Software packages such as ArcGIS, and other environmental sampling software packages, may also provide suggested sampling grids to maximize network efficiency.

ArcGIS contains a geoprocessing tool, "Create Spatially Balanced Points," that is designed to maximize independence between samples and create a more efficient network, and may assist in optimizing a network based on limited resources. Another technique may be to export a desired number of dispersion modeled point results from a dispersion model, and interpolate these points by kriging in GIS. A concentration surface and error would be predicted as though the modeled points were monitored. For example, if 33 monitors are available, and a plume is modeled such that coverage is possible with a 6 x 5 grid plus three background monitors, those grid points could be extracted from the dispersion model, the coordinates and modeled concentration values can be imported into GIS. Kriging could then be performed on the modeled values, and the resulting concentration surface compared with the dispersion model output at a desired number of points. If results are acceptable, a decision may be made to employ this grid, and if unacceptable, increased numbers of sampling points or a different sampling point distribution could be tried. Prediction error could also be viewed based on the modeled results. This will differ from the actual results, but could be used as a tool to get a first rough guess of results prior to sampling.

Though software packages can be helpful in setting up a sampling grid, ground realities must always be considered. Keeping sites away from interfering sources is paramount in determination of spatial patterns.

Supposing that the purpose of sampling is to determine a concentration surface from all sources, the costs and difficulties of using a dense network of gridded samplers can be prohibitive, and prioritization of areas to be characterized may be necessary. Rather than sampling the entire extent of contamination across an entire geographical

area, health professionals may determine that it is more important to characterize areas that are most likely to exceed a limit or level of concern. Dispersion models, regression models, or some combination of models can be used to inform conceptual site models, defining areas of predicted higher risk, and shrinking targeted grid areas to manageable sizes. It remains important to determine background concentrations so that regional contributions, such as dust storms, can be subtracted if desired. Background monitors should be placed in upwind locations at distances from local sources at which they will not receive local contributions. A minimum of three background sites with collocated samplers is recommended, so that variability and error can be determined.

Time scales are extremely important when assessing exposures to ambient pollutants. Exposure modeling and monitoring must reflect the exposure for the time period for which a member is deployed. An annual average may be much different than the averaged concentration for a shorter period of time. Determination of whether pollutants present acute or chronic effects must also be considered. Monitoring must be representative of the entire time period for the assessed exposure. Simultaneous random sampling that captures temporal variability is necessary for accurate exposure assessments. Since periods of deployment are spread throughout the year and last for differing periods of time, and there are expected seasonal and monthly variations in ambient concentration, sampling should be performed throughout the year.

Air pollution dispersion is highly dependent on meteorological patterns and terrain complexity. Combining dispersion models and source locations in GIS can greatly assist in determining optimal sampling locations, and also in ruling out poor ones. There are many different ways to set up a sampling strategy. Modeling within a GIS

framework can help to prevent wasteful sampling that costs much and provides few answers to the critical questions.

Additional Research Areas

There are several additional research opportunities implicated by this study. An obvious one is to model total exposure, including indoor and outdoor sources, as well as determining contributions at different geographical scales (neighborhood, local, regional). This would require information to determine indoor concentrations.

A reliable method for modeling regional exposure would greatly help in differentiating between local point source and regional source pollutants. There are remote sensing products available from the National Oceanic and Atmospheric Association and NASA, that could aid in modeling background. If correlations in values on these products can be made with surface particulate concentrations, this would not only improve accuracy of determining local source contributions, but it could also result in substantial cost savings in requiring background ambient sampling only to validate the correlation.

As discussed in the introduction, there has been congressional interest in the exposure of off-base populations. Long-range dispersion model products are available and through the use of existing emission factors for municipal waste, a first guess of long-range exposure could be determined. With military-specific waste emission factors, refined exposure modeling could be determined and combinational effects from several burning sources could be simultaneously modeled.

Developing a format for an exposure geodatabase would be of great value to environmental scientists and epidemiologists, as well as personnel who require

information in order to assess and control exposures to populations. If geocoded monitored environmental data from a previous location were available to a deploying health professional to that same location at a future time, a map could be created prior to deployment, with possible hot spots and sources identified. This could help identify a sampling and environmental reconnaissance plan, or site arrangements to mitigate exposures.

Epidemiological studies could also be performed with refined dispersion modeling. This would require knowledge of the spatial distribution of disease, and an ability to geocode personnel locations.

Particle size distribution of burn pit waste would assist in dispersion modeling, and may also enhance sampling strategies. If the size distribution of burn pit emissions differs significantly from ambient and other local sources, then specific size ranges can be targeted for sampling, and results mapped in GIS, providing sampling verification of models.

Finally, and perhaps most important, combinations of emissions and dispersion modeling could be used to create predictive models and provide information on optimal burning conditions, or conditions during which burning should not occur, to reduce exposures to personnel. Larger burn piles, minimized smoldering, and modeling during specific meteorological conditions could be modeled, and for each condition, resulting exposure maps can give insight into "worst-case" or "best-case" burning conditions. For example, it may be determined that avoiding night smoldering, when winds are predicted to remain steady from an upwind direction, and atmospheric inversion layers keep the mixing height low, provides the greatest percentage of total exposure. In other words,

that condition may be modeled to be the greatest determinant of total exposure. If that is the case, then by avoiding those burning conditions when meteorological forecasts predict those weather patterns, exposures could be significantly reduced.

Exposure to environmental agents will be a part of war as long as boots continue to be on the ground, with Soldiers, Sailors, Airmen, and Marines remain in intimate contact with the air, water, and soil from which they fight, and the problem of war trash will remain as long as supplies are consumed. As Geographical Information Systems, GPS, and environmental modeling software continue to become more practical and useful, the critical linkage that links exposures to specific populations or individuals can finally be made. Our servicemembers deserve no less than the best environmental exposure assessments and environmental controls that technology and expertise can provide.

Appendix A: Balad Particulate Monitoring Results, 2003-2010 (USAPHC, 2010)

The following PM10 dataset for Joint Base Balad/Logistical Staging Area Anaconda, 2003-2010, includes results that were not georeferenced. Two negative values were reported in 2009, but these were not included in the selected range for modeling and data analysis.

PM10 Results

Sample Date	PM10 (µg/m^3)	Latitude	Longitude
22-Apr-03	73.15	33.954069	44.372431
24-Apr-03	248.19	33.954069	44.372431
28-Apr-03	71.79	33.939831	44.405661
29-Apr-03	73.87	33.939831	44.405661
31-Mar-04	82.99	33.956211	44.365439
1-Apr-04	246.36	33.943331	44.361389
1-Apr-04	131.46	33.956211	44.365439
2-Apr-04	264.40	33.943331	44.361389
2-Apr-04	329.69	33.956211	44.365439
3-Apr-04	161.62	33.943331	44.361389
3-Apr-04	127.80	33.956211	44.365439
4-Apr-04	81.84	33.943331	44.361389
4-Apr-04	64.93	33.956211	44.365439
5-Apr-04	122.59	33.943331	44.361389
5-Apr-04	107.46	33.956211	44.365439
6-Apr-04	113.24	33.943331	44.361389
6-Apr-04	104.28	33.956211	44.365439
5-Jul-04	267.85	33.951669	44.378839
9-Jul-04	290.86	33.951669	44.378839
13-Jul-04	210.97	33.951669	44.378839
17-Jul-04	177.15	33.951669	44.378839
29-Jul-04	152.98	33.951669	44.378839
2-Aug-04	180.41	33.951669	44.378839
4-Aug-04	184.16	33.950381	44.371389
5-Aug-04	296.46	33.950381	44.371389
6-Aug-04	226.70	33.950381	44.371389
6-Aug-04	172.45	33.951669	44.378839
7-Aug-04	237.07	33.950381	44.371389
8-Aug-04	248.44	33.950381	44.371389
9-Aug-04	163.32	33.950381	44.371389
10-Aug-04	221.01	33.950381	44.371389

11-Aug-04	157.37	33.950381	44.371389
12-Aug-04	208.08	33.950381	44.371389
13-Aug-04	172.78	33.950381	44.371389
14-Aug-04	183.58	33.950381	44.371389
14-Aug-04	243.28	33.951669	44.378839
15-Aug-04	298.73	33.950381	44.371389
16-Aug-04	199.18	33.950381	44.371389
17-Aug-04	191.64	33.950381	44.371389
22-Aug-04	174.20	33.951669	44.378839
26-Aug-04	244.51	33.950381	44.371389
26-Aug-04	243.72	33.950381	44.371389
27-Aug-04	212.23	33.951669	44.378839
30-Aug-04	224.98	33.950381	44.371389
31-Aug-04	223.51	33.951669	44.378839
3-Sep-04	284.70	33.950381	44.371389
3-Sep-04	222.37	33.951669	44.378839
8-Sep-04	231.12	33.951669	44.378839
11-Sep-04	190.55	33.950381	44.371389
11-Sep-04	232.57	33.951669	44.378839
17-Sep-04	126.69	33.950381	44.371389
18-Sep-04	369.35	33.951669	44.378839
18-Sep-04	149.69	33.951669	44.378839
20-Sep-04	196.41	33.951669	44.378839
20-Sep-04	254.93	33.950381	44.371389
21-Sep-04	347.42	33.950381	44.371389
23-Sep-04	228.88	33.951669	44.378839
27-Sep-04	338.70	33.951669	44.378839
1-Oct-04	237.86	33.943331	44.361389
1-Oct-04	323.84	33.951669	44.378839
5-Oct-04	311.04	33.951669	44.378839
7-Oct-04	134.64	33.943331	44.361389
12-Oct-04	219.07	33.943331	44.361389
14-Oct-04	176.28	33.951669	44.378839
15-Oct-04	287.05	33.943331	44.361389
15-Oct-04	38.31	33.943331	44.361389
22-Oct-04	272.00	33.943331	44.361389
25-Oct-04	302.41	33.951669	44.378839
27-Oct-04	567.42	33.943331	44.361389
29-Oct-04	346.28	33.951669	44.378839
1-Nov-04	56.30	33.943331	44.361389
2-Nov-04	36.88	33.951669	44.378839
6-Nov-04	132.10	33.943331	44.361389
6-Nov-04	55.01	33.951669	44.378839
11-Nov-04	392.64	33.95	44.37
11-Nov-04	413.63	33.943331	44.361389
15-Nov-04	171.71	33.943331	44.361389
21-Nov-04	233.84	33.943331	44.361389
22-Nov-04	111.19	33.95	44.37

26-Nov-04	139.77	33.95	44.37
26-Nov-04	144.82	33.943331	44.361389
2-Dec-04	173.34	33.943331	44.361389
9-Dec-04	101.44	33.95	44.37
9-Dec-04	118.22	33.943331	44.361389
14-Dec-04	38.39	33.943331	44.361389
20-Dec-04	118.21	33.95	44.37
23-Dec-04	14.80	33.943331	44.361389
28-Dec-04	92.65	33.95	44.37
1-Jan-05	206.13	33.95	44.37
5-Jan-05	66.22	33.95	44.37
7-Jan-05	244.50	33.95	44.37
13-Jan-05	169.33	33.95	44.37
17-Jan-05	81.38	33.95	44.37
8-Feb-05	41.53	33.95	44.37
11-Feb-05	322.18	33.95	44.37
15-Feb-05	145.37	33.95	44.37
19-Feb-05	213.31	33.95	44.37
23-Feb-05	99.35	33.95	44.37
28-Feb-05	245.38	33.95	44.37
3-Mar-05	271.75	33.95	44.37
7-Mar-05	138.35	33.95	44.37
14-Mar-05	249.17	33.95	44.37
14-Mar-05	43.75	33.95	44.37
16-Mar-05	291.78	33.95	44.37
16-Mar-05	210.03	33.95	44.37
17-Mar-05	274.71	33.95	44.37
17-Mar-05	467.09	33.96295	44.3694
18-Mar-05	208.29	33.95	44.37
18-Mar-05	331.39	33.95	44.37
21-Mar-05	428.73	33.95	44.37
21-Mar-05	251.85	33.95	44.37
22-Mar-05	135.08	33.95	44.37
28-Mar-05	296.92	33.95	44.37
29-Mar-05	262.76	33.95	44.37
1-Apr-05	247.10	33.95	44.37
4-Apr-05	183.34	33.95	44.37
7-Apr-05	95.49	33.95	44.37
12-Apr-05	191.48	33.95	44.37
18-Apr-05	190.37	33.95	44.37
19-Apr-05	205.79	33.95	44.37
20-Apr-05	237.76	33.95	44.37
25-Apr-05	226.16	33.95	44.37
27-Apr-05	177.06	33.95	44.37
28-Apr-05	95.18	33.95	44.37
2-May-05	739.94	33.95	44.37
5-May-05	209.55	33.95	44.37
12-May-05	283.62	33.95	44.37

14-May-05	321.75	33.95	44.37
18-May-05	241.36	33.95	44.37
18-May-05	157.55	33.95	44.37
21-May-05	137.68	33.95	44.37
25-May-05	152.14	33.95	44.37
26-May-05	364.45	33.95	44.37
30-May-05	282.30	33.95	44.37
1-Jun-05	178.93	33.95	44.37
2-Jun-05	252.56	33.95	44.37
8-Jun-05	212.72	33.95	44.37
15-Jun-05	330.64	33.95	44.37
22-Jun-05	385.30	33.95	44.37
29-Jun-05	149.01	33.95	44.37
6-Jul-05	303.53	33.95	44.37
13-Jul-05	1228.30	33.95	44.37
20-Jul-05	140.72	33.95	44.37
27-Jul-05	351.00	33.95	44.37
3-Aug-05	287.34	33.95	44.37
3-Aug-05	280.34	33.95	44.37
5-Aug-05	1376.10	33.95	44.37
8-Aug-05	4204.56	33.95	44.37
8-Aug-05	4822.32	33.95	44.37
9-Aug-05	1687.08	33.95	44.37
10-Aug-05	1389.20	33.95	44.37
10-Aug-05	856.26	33.95	44.37
11-Aug-05	1360.82	33.95	44.37
17-Aug-05	562.33	33.95	44.37
18-Aug-05	430.56	33.95	44.37
23-Aug-05	197.42	33.95	44.37
30-Aug-05	287.68	33.95	44.37
31-Aug-05	296.14	33.95	44.37
3-Sep-05	179.24	33.95	44.37
7-Sep-05	551.16	33.95	44.37
12-Sep-05	300.57	33.95	44.37
12-Sep-05	210.41	33.95	44.37
16-Sep-05	252.70	33.95	44.37
19-Sep-05	303.78	33.95	44.37
26-Sep-05	314.30	33.95	44.37
3-Oct-05	158.96	33.95	44.37
4-Oct-05	152.12	33.95	44.37
6-Oct-05	237.14	33.95	44.37
7-Oct-05	418.48	33.95	44.37
8-Oct-05	246.11	33.95	44.37
17-Oct-05	2712.03	33.95	44.37
20-Oct-05	259.99	33.95	44.37
28-Nov-05	222.79	33.95	44.37
5-Dec-05	217.25	33.95	44.37
12-Dec-05	271.81	33.95	44.37

20-Dec-05	101.48	33.95	44.37
26-Dec-05	175.70	33.95	44.37
2-Jan-06	89.54	33.95	44.37
9-Jan-06	60.15	33.95	44.37
18-Jan-06	88.94	33.95	44.37
23-Jan-06	472.40	33.95	44.37
1-Feb-06	55.20	33.95	44.37
21-Feb-06	114.69	33.95	44.37
4-Mar-06	90.28	33.95	44.37
14-Mar-06	243.90	33.95	44.37
16-Mar-06	91.04	33.9441	44.3871
22-Mar-06	126.67	33.9441	44.3871
23-Mar-06	128.46	33.95	44.37
30-Mar-06	112.66	33.95	44.37
3-Apr-06	82.80	33.9441	44.3871
5-Apr-06	384.27	33.95	44.37
9-Apr-06	172.58	33.9441	44.3871
14-Apr-06	93.35	33.95	44.37
15-Apr-06	176.22	33.9441	44.3871
21-Apr-06	158.45	33.9441	44.3871
25-Apr-06	152.80	33.95	44.37
29-Apr-06	170.58	33.95	44.37
4-May-06	444.11	33.9441	44.3871
10-May-06	150.55	33.9441	44.3871
11-May-06	106.60	33.950381	44.371389
18-May-06	125.42	33.950381	44.371389
25-May-06	135.46	33.950381	44.371389
3-Jun-06	392.60	33.9441	44.3871
9-Jun-06	170.35	33.9441	44.3871
15-Jun-06	197.97	33.9441	44.3871
21-Jun-06	152.62	33.9441	44.3871
3-Jul-06	393.66	33.9441	44.3871
9-Jul-06	157.39	33.9441	44.3871
15-Jul-06	180.39	33.9441	44.3871
21-Jul-06	286.15	33.9441	44.3871
25-Jul-06	149.62		
26-Jul-06	93.42		
27-Jul-06	104.89		
29-Jul-06	539.10		
30-Jul-06	344.19		
1-Aug-06	160.09		
2-Aug-06	189.46	33.9441	44.3871
3-Aug-06	477.35		
8-Aug-06	227.89	33.9441	44.3871
14-Aug-06	311.63	33.9441	44.3871
17-Aug-06	315.69		
19-Aug-06	411.85		
20-Aug-06	420.98		

20-Aug-06	462.50	33.9441	44.3871
21-Aug-06	870.27		
22-Aug-06	348.34		
23-Aug-06	497.32		
24-Aug-06	295.57		
1-Sep-06	170.12	33.9441	44.3871
7-Sep-06	200.94	33.9441	44.3871
13-Sep-06	157.67	33.9441	44.3871
19-Sep-06	172.77	33.9441	44.3871
1-Oct-06	238.27	33.9441	44.3871
7-Oct-06	160.86	33.9441	44.3871
13-Oct-06	39.14	33.9441	44.3871
19-Oct-06	203.02	33.9441	44.3871
31-Oct-06	159.57	33.9441	44.3871
6-Nov-06	108.61	33.9441	44.3871
12-Nov-06	138.99	33.9441	44.3871
12-Dec-06	161.81	33.9441	44.3871
2-Jan-07	99.98		
2-Jan-07	123.47		
2-Jan-07	78.34		
3-Jan-07	134.43		
3-Jan-07	143.35		
3-Jan-07	89.94		
10-Jan-07	76.00	33.9441	44.3871
16-Jan-07	110.55	33.9441	44.3871
28-Jan-07	434.43	33.9441	44.3871
8-Feb-07	109.67		
8-Feb-07	54.29		
8-Feb-07	1.98		
9-Feb-07	101.19		
9-Feb-07	122.40		
9-Feb-07	41.46		
10-Feb-07	93.98		
10-Feb-07	69.95		
10-Feb-07	220.88		
10-Feb-07	106.03	33.9441	44.3871
14-Feb-07	105.07	33.95	44.366667
14-Feb-07	80.92	33.95	44.366667
15-Feb-07	97.64	33.966667	44.333333
15-Feb-07	53.08	33.95	44.366667
16-Feb-07	67.37	33.95	44.366667
16-Feb-07	28.27	33.95	44.366667
16-Feb-07	60.31	33.966667	44.333333
17-Feb-07	62.12	33.966667	44.333333
17-Feb-07	18.42	33.95	44.366667
20-Feb-07	134.62	33.966667	44.333333
20-Feb-07	74.71	33.95	44.366667
20-Feb-07	79.22	33.95	44.366667

21-Feb-07	133.04	33.966667	44.333333
21-Feb-07	118.88	33.95	44.366667
21-Feb-07	82.28	33.95	44.366667
22-Feb-07	41.77	33.966667	44.333333
22-Feb-07	80.15	33.95	44.366667
22-Feb-07	63.52	33.95	44.366667
27-Feb-07	163.42	33.9441	44.3871
11-Mar-07	129.17	33.9441	44.3871
17-Mar-07	66.25	33.9441	44.3871
9-Apr-07	151.07	33.966667	44.333333
9-Apr-07	11.60	33.95	44.366667
9-Apr-07	182.51	33.95	44.366667
10-Apr-07	164.92	33.966667	44.333333
10-Apr-07	13.06	33.95	44.366667
11-Apr-07	61.87		
11-Apr-07	32.32		
11-Apr-07	46.50		
13-Apr-07	78.00		
13-Apr-07	89.07		
14-Apr-07	53.84		
14-Apr-07	72.90		
14-Apr-07	85.07		
17-Apr-07	130.43		
17-Apr-07	97.90		
17-Apr-07	112.33		
18-Apr-07	294.38		
18-Apr-07	298.02		
18-Apr-07	126.55		
19-Apr-07	159.67		
19-Apr-07	165.03		
20-Apr-07	170.33		
20-Apr-07	76.43		
20-Apr-07	95.50		
20-Apr-07	48.35		
21-Apr-07	112.82		
21-Apr-07	146.13		
18-Oct-07	136.63		
18-Oct-07	217.34		
18-Oct-07	535.36		
19-Oct-07	98.90		
19-Oct-07	18.53		
19-Oct-07	154.11		
20-Oct-07	222.36		
20-Oct-07	200.12		
20-Oct-07	181.07		
21-Oct-07	235.43		
21-Oct-07	180.54		
21-Oct-07	162.42		

22-Oct-07	252.76		
22-Oct-07	233.26		
22-Oct-07	136.13		
21-Nov-07	283.21		
21-Nov-07	257.03		
21-Nov-07	170.19		
22-Nov-07	189.92		
22-Nov-07	178.66		
22-Nov-07	135.85		
23-Nov-07	173.87		
23-Nov-07	147.85		
23-Nov-07	116.43		
24-Nov-07	130.61		
24-Nov-07	125.81		
24-Nov-07	121.93		
25-Nov-07	135.52		
25-Nov-07	125.12		
25-Nov-07	115.67		
20-Feb-08	510.37	33.947611	44.328764
20-Feb-08	595.08	33.963603	44.366478
20-Feb-08	552.34	33.952397	44.374408
20-Feb-08	492.66	33.951464	44.380878
21-Feb-08	170.71	33.947664	44.328764
21-Feb-08	164.94	33.963603	44.366478
21-Feb-08	221.11	33.952397	44.374408
21-Feb-08	99.77	33.951464	44.380878
22-Feb-08	287.17	33.963603	44.366478
22-Feb-08	92.04	33.951464	44.380878
23-Feb-08	241.86	33.963603	44.366478
23-Feb-08	199.11	33.947664	44.328764
23-Feb-08	158.44	33.952397	44.374408
23-Feb-08	130.21	33.951464	44.380878
25-Feb-08	458.40	33.941303	44.389011
25-Feb-08	403.55	33.95045	44.381739
25-Feb-08	638.41	33.95045	44.381739
26-Feb-08	224.65	33.955511	44.367967
26-Feb-08	241.41	33.941303	44.389011
26-Feb-08	154.49	33.95045	44.381739
26-Feb-08	148.28	33.95045	44.381739
27-Feb-08	250.21	33.955511	44.367967
27-Feb-08	109.31	33.941303	44.389011
27-Feb-08	96.09	33.95045	44.381739
27-Feb-08	173.38	33.95045	44.381739
28-Feb-08	97.78	33.955511	44.367967
28-Feb-08	127.45	33.941303	44.389011
28-Feb-08	150.19	33.95045	44.381739
29-Feb-08	103.51	33.955511	44.367967
29-Feb-08	215.67	33.941303	44.389011

29-Feb-08	134.81	33.95045	44.381739
1-Mar-08	95.18	33.955511	44.367967
11-Mar-08	320.84	33.947892	44.329119
11-Mar-08	238.14	33.951464	44.380878
11-Mar-08	317.79	33.952308	44.374917
14-Mar-08	2836.60	33.947892	44.329119
14-Mar-08	2783.55	33.952308	44.374917
20-Mar-08	314.69	33.932172	44.362967
20-Mar-08	297.96	33.930314	44.359519
22-Mar-08	360.83	33.929642	44.355283
22-Mar-08	336.27	33.930314	44.359519
23-Mar-08	172.84	33.929642	44.355283
23-Mar-08	294.13	33.930314	44.359519
23-Mar-08	275.80	33.932172	44.362967
25-Mar-08	1002.60	33.932172	44.362967
25-Mar-08	1211.09	33.930314	44.359519
25-Mar-08	1039.05	33.929642	44.355283
27-Mar-08	335.60	33.932172	44.362967
27-Mar-08	317.40	33.930314	44.359519
27-Mar-08	230.01	33.929642	44.355283
29-Mar-08	156.09	33.935664	44.344417
29-Mar-08	320.38	33.940925	44.335061
31-Mar-08	291.67	33.935664	44.344417
31-Mar-08	566.36	33.940925	44.335061
1-Apr-08	215.07	33.935606	44.333597
1-Apr-08	572.87	33.940925	44.335061
2-Apr-08	347.44	33.935664	44.344417
2-Apr-08	315.92	33.940925	44.335061
3-Apr-08	380.58	33.940925	44.335061
4-Apr-08	357.60	33.935664	44.344417
6-May-08	978.45		
6-May-08	523.17		
6-May-08	820.97		
20-May-08	1150.58	33.929533	44.361928
20-May-08	1369.36	33.940622	44.389794
17-Jun-08	1076.35	33.962931	44.364167
17-Jun-08	1721.00	33.929533	44.361928
17-Jun-08	1269.96	33.940622	44.389794
24-Jun-08	327.48	33.940622	44.389794
24-Jun-08	359.36	33.962931	44.364167
24-Jun-08	270.91	33.947042	44.328692
24-Jun-08	469.78	33.929533	44.361928
9-Jul-08	1104.06	33.947042	44.328692
9-Jul-08	581.63	33.940622	44.389794
4-Aug-08	1171.54		
4-Aug-08	940.68	33.962931	44.364167
4-Aug-08	1008.58	33.938419	44.338736
4-Aug-08	1000.58	33.936253	44.344856

6-Mar-09	145.03	33.962894	44.3642
6-Mar-09	64.26	33.935844	44.351297
6-Mar-09	185.28	33.917611	44.372736
6-Mar-09	71.35	33.943017	44.394431
20-Mar-09	115.41		
20-Mar-09	139.86		
20-Mar-09	98.77		
20-Mar-09	172.87		
27-Mar-09	319.51		
27-Mar-09	365.86		
27-Mar-09	219.96		
3-Apr-09	253.45		
3-Apr-09	229.20		
3-Apr-09	232.55		
3-Apr-09	230.34		
3-Apr-09	216.64		
10-Apr-09	178.98		
10-Apr-09	202.08		
10-Apr-09	156.34		
17-Apr-09	-11463.61		
17-Apr-09	-10610.01		
1-May-09	1178.33		
1-May-09	963.36		
8-May-09	205.02		
8-May-09	466.91		
8-May-09	466.48		
12-May-09	206.80		
12-May-09	198.13		
13-May-09	251.18		
13-May-09	207.93		
13-May-09	227.95		
14-May-09	283.34		
14-May-09	270.35		
15-May-09	227.38		
15-May-09	85.17		
15-May-09	257.60		
16-May-09	477.41		
16-May-09	452.25		
16-May-09	563.40		
17-May-09	205.73		
17-May-09	206.43		
17-May-09	148.26		
18-May-09	342.88		
18-May-09	198.67		
18-May-09	104.23		
19-May-09	221.17		
19-May-09	228.75		
19-May-09	324.36		

20-May-09	266.35		
20-May-09	270.22		
20-May-09	352.26		
10-Jun-09	381.76		
10-Jun-09	391.80		
10-Jun-09	271.11		
11-Jun-09	312.52		
11-Jun-09	341.02		
11-Jun-09	244.75		
12-Jun-09	282.43		
12-Jun-09	287.65		
12-Jun-09	235.40		
13-Jun-09	1562.05		
13-Jun-09	513.38		
13-Jun-09	1800.73		
14-Jun-09	1056.01		
14-Jun-09	943.81		
14-Jun-09	789.41		
15-Jun-09	368.43		
15-Jun-09	317.80		
15-Jun-09	350.69		
16-Jun-09	1295.54		
16-Jun-09	1227.91		
16-Jun-09	1314.99		
17-Jun-09	1950.70		
17-Jun-09	9576.12		
17-Jun-09	2480.85		
18-Jun-09	1096.41		
18-Jun-09	1085.14		
18-Jun-09	1129.61		
19-Jun-09	463.18		
19-Jun-09	617.08		
19-Jun-09	531.50		
25-Sep-09	0.99		
25-Sep-09	172.96		
25-Sep-09	171.71		

Appendix B: Joint Base Balad Sampling Locations with Coordinates

Table 9 is the list of all sampling sites with coordinates provided by the U.S. Army Public Health Command. Not all of these sites were monitored during the 2007-2008 time period. The site numbers were assigned by the author of this study, not by the U.S. Army Public Health Command.

Table 9: Sampling Sites

Latitude	Longitude	SITE
33.917611	44.372736	1
33.929533	44.361928	2
33.929642	44.355283	3
33.930314	44.359519	4
33.935606	44.333597	5
33.935664	44.344417	6
33.935844	44.351297	7
33.936253	44.344856	8
33.938419	44.338736	9
33.939831	44.405661	10
33.940622	44.389794	11
33.940925	44.335061	12
33.941303	44.389011	13
33.943017	44.394431	14
33.943331	44.361389	15
33.9441	44.3871	16
33.947042	44.328692	17
33.947664	44.328764	18
33.947892	44.329119	19
33.95015	44.372717	H-6 Housing
33.95045	44.381739	24
33.951464	44.380878	25
33.951669	44.378839	26
33.952308	44.374917	27
33.952397	44.374408	28
33.954069	44.372431	29
33.954667	44.3758	CASF
33.955511	44.367967	31
33.956211	44.365439	32
33.960533	44.367533	Transportation Field
33.962894	44.3642	34
33.962931	44.364167	35
33.96295	44.3694	36
33.963603	44.366478	37
33.9671	44.368483	Guard Tower

33.967117	44.349633	Mortar Pit (Background)

Appendix C: Meteorological Surface Data File Used in Annual SCIPUFF Plumes

This file was created using wind rose data and climatic data summaries available from the Air Force Weather Agency (14 WS, 2010). Annual frequencies of wind direction and speed were converted from an annual, 365 day file to a 12.6 day file; wind directions and speeds that occurred very infrequently (less than half a day per year) were not included in the surface data file, to maintain the hourly observation format.

```
SURFACE
11
ID     YEAR  MONTH DAY   HOUR   LAT    LON    WDIR   WSPD   T
PGT
                                               DEG    M/S    K

-999
10000 12  1  1  1    33.9501   44.3667    000.0000  1.0000    298.2  4
10000 12  1  1  2    33.9501   44.3667    000.0000  1.0000    298.2  4
10000 12  1  1  3    33.9501   44.3667    000.0000  3.5000    298.2  4
10000 12  1  1  4    33.9501   44.3667    000.0000  3.5000    298.2  4
10000 12  1  1  5    33.9501   44.3667    000.0000  3.5000    298.2  4
10000 12  1  1  6    33.9501   44.3667    000.0000  3.5000    298.2  4
10000 12  1  1  7    33.9501   44.3667    000.0000  1.0000    298.2  4
10000 12  1  1  8    33.9501   44.3667    010.0000  1.0000    298.2  4
10000 12  1  1  9    33.9501   44.3667    010.0000  1.0000    298.2  4
10000 12  1  1 10    33.9501   44.3667    010.0000  3.5000    298.2  4
10000 12  1  1 11    33.9501   44.3667    010.0000  3.5000    298.2  4
10000 12  1  1 12    33.9501   44.3667    010.0000  3.5000    298.2  4
10000 12  1  1 13    33.9501   44.3667    020.0000  1.0000    298.2  4
10000 12  1  1 14    33.9501   44.3667    020.0000  1.0000    298.2  4
10000 12  1  1 15    33.9501   44.3667    020.0000  3.5000    298.2  4
10000 12  1  1 16    33.9501   44.3667    020.0000  3.5000    298.2  4
10000 12  1  1 17    33.9501   44.3667    020.0000  3.5000    298.2  4
10000 12  1  1 18    33.9501   44.3667    030.0000  1.0000    298.2  4
10000 12  1  1 19    33.9501   44.3667    030.0000  1.0000    298.2  4
10000 12  1  1 20    33.9501   44.3667    030.0000  3.5000    298.2  4
10000 12  1  1 21    33.9501   44.3667    030.0000  3.5000    298.2  4
10000 12  1  1 22    33.9501   44.3667    040.0000  1.0000    298.2  4
10000 12  1  1 23    33.9501   44.3667    040.0000  1.0000    298.2  4
10000 12  1  1 24    33.9501   44.3667    040.0000  3.5000    298.2  4
10000 12  1  2  1    33.9501   44.3667    040.0000  3.5000    298.2  4
10000 12  1  2  2    33.9501   44.3667    050.0000  1.0000    298.2  4
10000 12  1  2  3    33.9501   44.3667    050.0000  1.0000    298.2  4
10000 12  1  2  4    33.9501   44.3667    050.0000  3.5000    298.2  4
10000 12  1  2  5    33.9501   44.3667    050.0000  3.5000    298.2  4
10000 12  1  2  6    33.9501   44.3667    060.0000  1.0000    298.2  4
10000 12  1  2  7    33.9501   44.3667    060.0000  1.0000    298.2  4
10000 12  1  2  8    33.9501   44.3667    060.0000  3.5000    298.2  4
10000 12  1  2  9    33.9501   44.3667    060.0000  3.5000    298.2  4
10000 12  1  2 10    33.9501   44.3667    070.0000  1.0000    298.2  4
10000 12  1  2 11    33.9501   44.3667    070.0000  1.0000    298.2  4
10000 12  1  2 12    33.9501   44.3667    070.0000  3.5000    298.2  4
10000 12  1  2 13    33.9501   44.3667    070.0000  3.5000    298.2  4
10000 12  1  2 14    33.9501   44.3667    080.0000  1.0000    298.2  4
```

```
10000 12  1  2 15    33.9501   44.3667    080.0000  1.0000    298.2  4
10000 12  1  2 16    33.9501   44.3667    080.0000  3.5000    298.2  4
10000 12  1  2 17    33.9501   44.3667    080.0000  3.5000    298.2  4
10000 12  1  2 18    33.9501   44.3667    090.0000  1.0000    298.2  4
10000 12  1  2 19    33.9501   44.3667    090.0000  3.5000    298.2  4
10000 12  1  2 20    33.9501   44.3667    090.0000  3.5000    298.2  4
10000 12  1  2 21    33.9501   44.3667    100.0000  1.0000    298.2  4
10000 12  1  2 22    33.9501   44.3667    100.0000  3.5000    298.2  4
10000 12  1  2 23    33.9501   44.3667    100.0000  3.5000    298.2  4
10000 12  1  2 24    33.9501   44.3667    110.0000  1.0000    298.2  4
10000 12  1  3  1    33.9501   44.3667    110.0000  1.0000    298.2  4
10000 12  1  3  2    33.9501   44.3667    110.0000  3.5000    298.2  4
10000 12  1  3  3    33.9501   44.3667    110.0000  3.5000    298.2  4
10000 12  1  3  4    33.9501   44.3667    120.0000  1.0000    298.2  4
10000 12  1  3  5    33.9501   44.3667    120.0000  1.0000    298.2  4
10000 12  1  3  6    33.9501   44.3667    120.0000  3.5000    298.2  4
10000 12  1  3  7    33.9501   44.3667    120.0000  3.5000    298.2  4
10000 12  1  3  8    33.9501   44.3667    120.0000  3.5000    298.2  4
10000 12  1  3  9    33.9501   44.3667    130.0000  1.0000    298.2  4
10000 12  1  3 10    33.9501   44.3667    130.0000  1.0000    298.2  4
10000 12  1  3 11    33.9501   44.3667    130.0000  3.5000    298.2  4
10000 12  1  3 12    33.9501   44.3667    130.0000  3.5000    298.2  4
10000 12  1  3 13    33.9501   44.3667    130.0000  3.5000    298.2  4
10000 12  1  3 14    33.9501   44.3667    130.0000  6.1000    298.2  4
10000 12  1  3 15    33.9501   44.3667    130.0000 11.4000    298.2  4
10000 12  1  3 16    33.9501   44.3667    140.0000  1.0000    298.2  4
10000 12  1  3 17    33.9501   44.3667    140.0000  1.0000    298.2  4
10000 12  1  3 18    33.9501   44.3667    140.0000  3.5000    298.2  4
10000 12  1  3 19    33.9501   44.3667    140.0000  3.5000    298.2  4
10000 12  1  3 20    33.9501   44.3667    140.0000  6.1000    298.2  4
10000 12  1  3 21    33.9501   44.3667    140.0000 11.4000    298.2  4
10000 12  1  3 22    33.9501   44.3667    140.0000 13.5000    298.2  4
10000 12  1  3 23    33.9501   44.3667    150.0000  1.0000    298.2  4
10000 12  1  3 24    33.9501   44.3667    150.0000  1.0000    298.2  4
10000 12  1  4  1    33.9501   44.3667    150.0000  3.5000    298.2  4
10000 12  1  4  2    33.9501   44.3667    150.0000  3.5000    298.2  4
10000 12  1  4  3    33.9501   44.3667    150.0000  6.1000    298.2  4
10000 12  1  4  4    33.9501   44.3667    150.0000 11.4000    298.2  4
10000 12  1  4  5    33.9501   44.3667    160.0000  1.0000    298.2  4
10000 12  1  4  6    33.9501   44.3667    160.0000  3.5000    298.2  4
10000 12  1  4  7    33.9501   44.3667    170.0000  1.0000    298.2  4
10000 12  1  4  8    33.9501   44.3667    170.0000  3.5000    298.2  4
10000 12  1  4  9    33.9501   44.3667    180.0000  1.0000    298.2  4
10000 12  1  4 10    33.9501   44.3667    180.0000  3.5000    298.2  4
10000 12  1  4 11    33.9501   44.3667    190.0000  1.0000    298.2  4
10000 12  1  4 12    33.9501   44.3667    190.0000  3.5000    298.2  4
10000 12  1  4 13    33.9501   44.3667    200.0000  1.0000    298.2  4
10000 12  1  4 14    33.9501   44.3667    200.0000  3.5000    298.2  4
10000 12  1  4 15    33.9501   44.3667    210.0000  1.0000    298.2  4
10000 12  1  4 16    33.9501   44.3667    210.0000  3.5000    298.2  4
10000 12  1  4 17    33.9501   44.3667    220.0000  1.0000    298.2  4
10000 12  1  4 18    33.9501   44.3667    220.0000  3.5000    298.2  4
10000 12  1  4 19    33.9501   44.3667    230.0000  1.0000    298.2  4
10000 12  1  4 20    33.9501   44.3667    230.0000  1.0000    298.2  4
10000 12  1  4 21    33.9501   44.3667    230.0000  3.5000    298.2  4
10000 12  1  4 22    33.9501   44.3667    230.0000  3.5000    298.2  4
10000 12  1  4 23    33.9501   44.3667    240.0000  1.0000    298.2  4
10000 12  1  4 24    33.9501   44.3667    240.0000  1.0000    298.2  4
10000 12  1  5  1    33.9501   44.3667    240.0000  3.5000    298.2  4
10000 12  1  5  2    33.9501   44.3667    240.0000  3.5000    298.2  4
10000 12  1  5  3    33.9501   44.3667    250.0000  1.0000    298.2  4
10000 12  1  5  4    33.9501   44.3667    250.0000  1.0000    298.2  4
10000 12  1  5  5    33.9501   44.3667    250.0000  3.5000    298.2  4
10000 12  1  5  6    33.9501   44.3667    250.0000  3.5000    298.2  4
```

10000	12	1	5	7	33.9501	44.3667	250.0000	3.5000	298.2	4
10000	12	1	5	8	33.9501	44.3667	250.0000	3.5000	298.2	4
10000	12	1	5	9	33.9501	44.3667	250.0000	6.1000	298.2	4
10000	12	1	5	10	33.9501	44.3667	260.0000	1.0000	298.2	4
10000	12	1	5	11	33.9501	44.3667	260.0000	1.0000	298.2	4
10000	12	1	5	12	33.9501	44.3667	260.0000	3.5000	298.2	4
10000	12	1	5	13	33.9501	44.3667	260.0000	3.5000	298.2	4
10000	12	1	5	14	33.9501	44.3667	260.0000	3.5000	298.2	4
10000	12	1	5	15	33.9501	44.3667	260.0000	3.5000	298.2	4
10000	12	1	5	16	33.9501	44.3667	260.0000	3.5000	298.2	4
10000	12	1	5	17	33.9501	44.3667	260.0000	3.5000	298.2	4
10000	12	1	5	18	33.9501	44.3667	260.0000	3.5000	298.2	4
10000	12	1	5	19	33.9501	44.3667	260.0000	6.1000	298.2	4
10000	12	1	5	20	33.9501	44.3667	260.0000	13.5000	298.2	4
10000	12	1	5	21	33.9501	44.3667	270.0000	1.0000	298.2	4
10000	12	1	5	22	33.9501	44.3667	270.0000	1.0000	298.2	4
10000	12	1	5	23	33.9501	44.3667	270.0000	1.0000	298.2	4
10000	12	1	5	24	33.9501	44.3667	270.0000	1.0000	298.2	4
10000	12	1	6	1	33.9501	44.3667	270.0000	1.0000	298.2	4
10000	12	1	6	2	33.9501	44.3667	270.0000	3.5000	298.2	4
10000	12	1	6	3	33.9501	44.3667	270.0000	3.5000	298.2	4
10000	12	1	6	4	33.9501	44.3667	270.0000	3.5000	298.2	4
10000	12	1	6	5	33.9501	44.3667	270.0000	3.5000	298.2	4
10000	12	1	6	6	33.9501	44.3667	270.0000	3.5000	298.2	4
10000	12	1	6	7	33.9501	44.3667	270.0000	3.5000	298.2	4
10000	12	1	6	8	33.9501	44.3667	270.0000	3.5000	298.2	4
10000	12	1	6	9	33.9501	44.3667	270.0000	3.5000	298.2	4
10000	12	1	6	10	33.9501	44.3667	270.0000	3.5000	298.2	4
10000	12	1	6	11	33.9501	44.3667	270.0000	6.1000	298.2	4
10000	12	1	6	12	33.9501	44.3667	270.0000	6.1000	298.2	4
10000	12	1	6	13	33.9501	44.3667	270.0000	13.5000	298.2	4
10000	12	1	6	14	33.9501	44.3667	280.0000	1.0000	298.2	4
10000	12	1	6	15	33.9501	44.3667	280.0000	1.0000	298.2	4
10000	12	1	6	16	33.9501	44.3667	280.0000	1.0000	298.2	4
10000	12	1	6	17	33.9501	44.3667	280.0000	1.0000	298.2	4
10000	12	1	6	18	33.9501	44.3667	280.0000	1.0000	298.2	4
10000	12	1	6	19	33.9501	44.3667	280.0000	3.5000	298.2	4
10000	12	1	6	20	33.9501	44.3667	280.0000	3.5000	298.2	4
10000	12	1	6	21	33.9501	44.3667	280.0000	3.5000	298.2	4
10000	12	1	6	22	33.9501	44.3667	280.0000	3.5000	298.2	4
10000	12	1	6	23	33.9501	44.3667	280.0000	3.5000	298.2	4
10000	12	1	6	24	33.9501	44.3667	280.0000	3.5000	298.2	4
10000	12	1	7	1	33.9501	44.3667	280.0000	3.5000	298.2	4
10000	12	1	7	2	33.9501	44.3667	280.0000	3.5000	298.2	4
10000	12	1	7	3	33.9501	44.3667	280.0000	3.5000	298.2	4
10000	12	1	7	4	33.9501	44.3667	280.0000	6.1000	298.2	4
10000	12	1	7	5	33.9501	44.3667	280.0000	6.1000	298.2	4
10000	12	1	7	6	33.9501	44.3667	280.0000	6.1000	298.2	4
10000	12	1	7	7	33.9501	44.3667	280.0000	13.5000	298.2	4
10000	12	1	7	8	33.9501	44.3667	280.0000	13.5000	298.2	4
10000	12	1	7	9	33.9501	44.3667	280.0000	11.4000	298.2	4
10000	12	1	7	10	33.9501	44.3667	280.0000	11.4000	298.2	4
10000	12	1	7	11	33.9501	44.3667	290.0000	1.0000	298.2	4
10000	12	1	7	12	33.9501	44.3667	290.0000	1.0000	298.2	4
10000	12	1	7	13	33.9501	44.3667	290.0000	1.0000	298.2	4
10000	12	1	7	14	33.9501	44.3667	290.0000	1.0000	298.2	4
10000	12	1	7	15	33.9501	44.3667	290.0000	1.0000	298.2	4
10000	12	1	7	16	33.9501	44.3667	290.0000	1.0000	298.2	4
10000	12	1	7	17	33.9501	44.3667	290.0000	1.0000	298.2	4
10000	12	1	7	18	33.9501	44.3667	290.0000	3.5000	298.2	4
10000	12	1	7	19	33.9501	44.3667	290.0000	3.5000	298.2	4
10000	12	1	7	20	33.9501	44.3667	290.0000	3.5000	298.2	4
10000	12	1	7	21	33.9501	44.3667	290.0000	3.5000	298.2	4
10000	12	1	7	22	33.9501	44.3667	290.0000	3.5000	298.2	4

10000	12	1	7	23	33.9501	44.3667	290.0000	3.5000	298.2	4
10000	12	1	7	24	33.9501	44.3667	290.0000	3.5000	298.2	4
10000	12	1	8	1	33.9501	44.3667	290.0000	3.5000	298.2	4
10000	12	1	8	2	33.9501	44.3667	290.0000	3.5000	298.2	4
10000	12	1	8	3	33.9501	44.3667	290.0000	3.5000	298.2	4
10000	12	1	8	4	33.9501	44.3667	290.0000	3.5000	298.2	4
10000	12	1	8	5	33.9501	44.3667	290.0000	6.1000	298.2	4
10000	12	1	8	6	33.9501	44.3667	290.0000	6.1000	298.2	4
10000	12	1	8	7	33.9501	44.3667	290.0000	6.1000	298.2	4
10000	12	1	8	8	33.9501	44.3667	290.0000	13.5000	298.2	4
10000	12	1	8	9	33.9501	44.3667	290.0000	13.5000	298.2	4
10000	12	1	8	10	33.9501	44.3667	290.0000	11.4000	298.2	4
10000	12	1	8	11	33.9501	44.3667	300.0000	1.0000	298.2	4
10000	12	1	8	12	33.9501	44.3667	300.0000	1.0000	298.2	4
10000	12	1	8	13	33.9501	44.3667	300.0000	1.0000	298.2	4
10000	12	1	8	14	33.9501	44.3667	300.0000	1.0000	298.2	4
10000	12	1	8	15	33.9501	44.3667	300.0000	1.0000	298.2	4
10000	12	1	8	16	33.9501	44.3667	300.0000	1.0000	298.2	4
10000	12	1	8	17	33.9501	44.3667	300.0000	1.0000	298.2	4
10000	12	1	8	18	33.9501	44.3667	300.0000	1.0000	298.2	4
10000	12	1	8	19	33.9501	44.3667	300.0000	1.0000	298.2	4
10000	12	1	8	20	33.9501	44.3667	300.0000	3.5000	298.2	4
10000	12	1	8	21	33.9501	44.3667	300.0000	3.5000	298.2	4
10000	12	1	8	22	33.9501	44.3667	300.0000	3.5000	298.2	4
10000	12	1	8	23	33.9501	44.3667	300.0000	3.5000	298.2	4
10000	12	1	8	24	33.9501	44.3667	300.0000	3.5000	298.2	4
10000	12	1	9	1	33.9501	44.3667	300.0000	3.5000	298.2	4
10000	12	1	9	2	33.9501	44.3667	300.0000	3.5000	298.2	4
10000	12	1	9	3	33.9501	44.3667	300.0000	3.5000	298.2	4
10000	12	1	9	4	33.9501	44.3667	300.0000	3.5000	298.2	4
10000	12	1	9	5	33.9501	44.3667	300.0000	3.5000	298.2	4
10000	12	1	9	6	33.9501	44.3667	300.0000	3.5000	298.2	4
10000	12	1	9	7	33.9501	44.3667	300.0000	3.5000	298.2	4
10000	12	1	9	8	33.9501	44.3667	300.0000	3.5000	298.2	4
10000	12	1	9	9	33.9502	44.3667	300.0000	6.1000	298.2	4
10000	12	1	9	10	33.9501	44.3667	300.0000	6.1000	298.2	4
10000	12	1	9	11	33.9501	44.3667	300.0000	6.1000	298.2	4
10000	12	1	9	12	33.9501	44.3667	300.0000	6.1000	298.2	4
10000	12	1	9	13	33.9501	44.3667	300.0000	13.5000	298.2	4
10000	12	1	9	14	33.9501	44.3667	300.0000	13.5000	298.2	4
10000	12	1	9	15	33.9501	44.3667	300.0000	11.4000	298.2	4
10000	12	1	9	16	33.9501	44.3667	310.0000	1.0000	298.2	4
10000	12	1	9	17	33.9501	44.3667	310.0000	1.0000	298.2	4
10000	12	1	9	18	33.9501	44.3667	310.0000	1.0000	298.2	4
10000	12	1	9	19	33.9501	44.3667	310.0000	1.0000	298.2	4
10000	12	1	9	20	33.9501	44.3667	310.0000	1.0000	298.2	4
10000	12	1	9	21	33.9501	44.3667	310.0000	1.0000	298.2	4
10000	12	1	9	22	33.9501	44.3667	310.0000	1.0000	298.2	4
10000	12	1	9	23	33.9501	44.3667	310.0000	1.0000	298.2	4
10000	12	1	9	24	33.9501	44.3667	310.0000	1.0000	298.2	4
10000	12	1	10	1	33.9501	44.3667	310.0000	3.5000	298.2	4
10000	12	1	10	2	33.9501	44.3667	310.0000	3.5000	298.2	4
10000	12	1	10	3	33.9501	44.3667	310.0000	3.5000	298.2	4
10000	12	1	10	4	33.9501	44.3667	310.0000	3.5000	298.2	4
10000	12	1	10	5	33.9501	44.3667	310.0000	3.5000	298.2	4
10000	12	1	10	6	33.9501	44.3667	310.0000	3.5000	298.2	4
10000	12	1	10	7	33.9501	44.3667	310.0000	3.5000	298.2	4
10000	12	1	10	8	33.9501	44.3667	310.0000	3.5000	298.2	4
10000	12	1	10	9	33.9501	44.3667	310.0000	3.5000	298.2	4
10000	12	1	10	10	33.9501	44.3667	310.0000	3.5000	298.2	4
10000	12	1	10	11	33.9501	44.3667	310.0000	3.5000	298.2	4
10000	12	1	10	12	33.9501	44.3667	310.0000	3.5000	298.2	4
10000	12	1	10	13	33.9501	44.3667	310.0000	3.5000	298.2	4
10000	12	1	10	14	33.9501	44.3667	310.0000	6.1000	298.2	4

10000	12	1	10	15	33.9501	44.3667	310.0000	6.1000	298.2	4
10000	12	1	10	16	33.9501	44.3667	310.0000	6.1000	298.2	4
10000	12	1	10	17	33.9501	44.3667	310.0000	13.5000	298.2	4
10000	12	1	10	18	33.9501	44.3667	310.0000	11.4000	298.2	4
10000	12	1	10	19	33.9501	44.3667	320.0000	1.0000	298.2	4
10000	12	1	10	20	33.9501	44.3667	320.0000	1.0000	298.2	4
10000	12	1	10	21	33.9501	44.3667	320.0000	1.0000	298.2	4
10000	12	1	10	22	33.9501	44.3667	320.0000	1.0000	298.2	4
10000	12	1	10	23	33.9501	44.3667	320.0000	1.0000	298.2	4
10000	12	1	10	24	33.9501	44.3667	320.0000	1.0000	298.2	4
10000	12	1	11	1	33.9501	44.3667	320.0000	1.0000	298.2	4
10000	12	1	11	2	33.9501	44.3667	320.0000	1.0000	298.2	4
10000	12	1	11	3	33.9501	44.3667	320.0000	1.0000	298.2	4
10000	12	1	11	4	33.9501	44.3667	320.0000	3.5000	298.2	4
10000	12	1	11	5	33.9501	44.3667	320.0000	3.5000	298.2	4
10000	12	1	11	6	33.9501	44.3667	320.0000	3.5000	298.2	4
10000	12	1	11	7	33.9501	44.3667	320.0000	3.5000	298.2	4
10000	12	1	11	8	33.9501	44.3667	320.0000	3.5000	298.2	4
10000	12	1	11	9	33.9501	44.3667	320.0000	3.5000	298.2	4
10000	12	1	11	10	33.9501	44.3667	320.0000	3.5000	298.2	4
10000	12	1	11	11	33.9501	44.3667	320.0000	3.5000	298.2	4
10000	12	1	11	12	33.9501	44.3667	320.0000	3.5000	298.2	4
10000	12	1	11	13	33.9501	44.3667	320.0000	3.5000	298.2	4
10000	12	1	11	14	33.9501	44.3667	320.0000	3.5000	298.2	4
10000	12	1	11	15	33.9501	44.3667	320.0000	3.5000	298.2	4
10000	12	1	11	16	33.9501	44.3667	320.0000	6.1000	298.2	4
10000	12	1	11	17	33.9501	44.3667	320.0000	6.1000	298.2	4
10000	12	1	11	18	33.9501	44.3667	320.0000	13.5000	298.2	4
10000	12	1	11	19	33.9501	44.3667	320.0000	11.4000	298.2	4
10000	12	1	11	20	33.9501	44.3667	330.0000	1.0000	298.2	4
10000	12	1	11	21	33.9501	44.3667	330.0000	1.0000	298.2	4
10000	12	1	11	22	33.9501	44.3667	330.0000	1.0000	298.2	4
10000	12	1	11	23	33.9501	44.3667	330.0000	1.0000	298.2	4
10000	12	1	11	24	33.9501	44.3667	330.0000	1.0000	298.2	4
10000	12	1	12	1	33.9501	44.3667	330.0000	1.0000	298.2	4
10000	12	1	12	2	33.9501	44.3667	330.0000	3.5000	298.2	4
10000	12	1	12	3	33.9501	44.3667	330.0000	3.5000	298.2	4
10000	12	1	12	4	33.9501	44.3667	330.0000	3.5000	298.2	4
10000	12	1	12	5	33.9501	44.3667	330.0000	3.5000	298.2	4
10000	12	1	12	6	33.9501	44.3667	330.0000	3.5000	298.2	4
10000	12	1	12	7	33.9501	44.3667	330.0000	3.5000	298.2	4
10000	12	1	12	8	33.9501	44.3667	330.0000	3.5000	298.2	4
10000	12	1	12	9	33.9501	44.3667	330.0000	3.5000	298.2	4
10000	12	1	12	10	33.9501	44.3667	330.0000	3.5000	298.2	4
10000	12	1	12	11	33.9501	44.3667	330.0000	3.5000	298.2	4
10000	12	1	12	12	33.9501	44.3667	330.0000	6.1000	298.2	4
10000	12	1	12	13	33.9501	44.3667	330.0000	6.1000	298.2	4
10000	12	1	12	14	33.9501	44.3667	330.0000	13.5000	298.2	4
10000	12	1	12	15	33.9501	44.3667	340.0000	1.0000	298.2	4
10000	12	1	12	16	33.9501	44.3667	340.0000	1.0000	298.2	4
10000	12	1	12	17	33.9501	44.3667	340.0000	1.0000	298.2	4
10000	12	1	12	18	33.9501	44.3667	340.0000	1.0000	298.2	4
10000	12	1	12	19	33.9501	44.3667	340.0000	1.0000	298.2	4
10000	12	1	12	20	33.9501	44.3667	340.0000	3.5000	298.2	4
10000	12	1	12	21	33.9501	44.3667	340.0000	3.5000	298.2	4
10000	12	1	12	22	33.9501	44.3667	340.0000	3.5000	298.2	4
10000	12	1	12	23	33.9501	44.3667	340.0000	3.5000	298.2	4
10000	12	1	12	24	33.9501	44.3667	340.0000	3.5000	298.2	4
10000	12	1	13	1	33.9501	44.3667	340.0000	3.5000	298.2	4
10000	12	1	13	2	33.9501	44.3667	340.0000	3.5000	298.2	4
10000	12	1	13	3	33.9501	44.3667	340.0000	3.5000	298.2	4
10000	12	1	13	4	33.9501	44.3667	340.0000	6.1000	298.2	4
10000	12	1	13	5	33.9501	44.3667	340.0000	13.5000	298.2	4
10000	12	1	13	6	33.9501	44.3667	350.0000	1.0000	298.2	4

```
10000 12  1 13  7    33.9501   44.3667    350.0000  1.0000    298.2  4
10000 12  1 13  8    33.9501   44.3667    350.0000  1.0000    298.2  4
10000 12  1 13  9    33.9501   44.3667    350.0000  1.0000    298.2  4
10000 12  1 13 10    33.9501   44.3667    350.0000  3.5000    298.2  4
10000 12  1 13 11    33.9501   44.3667    350.0000  3.5000    298.2  4
10000 12  1 13 12    33.9501   44.3667    350.0000  3.5000    298.2  4
10000 12  1 13 13    33.9501   44.3667    350.0000  3.5000    298.2  4
10000 12  1 13 14    33.9501   44.3667    350.0000  3.5000    298.2  4
10000 12  1 13 15    33.9501   44.3667    350.0000  3.5000    298.2  4
10000 12  1 13 16    33.9501   44.3667    350.0000  6.1000    298.2  4
```

Appendix D: One-way Analysis and Variability Charts

Figure 36: Oneway Analysis, Balad – PM10 (µg/m^3) by Month, 2007-2008

Green Diamond Centerlines = Monthly Mean Values
Red Lines = Standard Deviation Markers

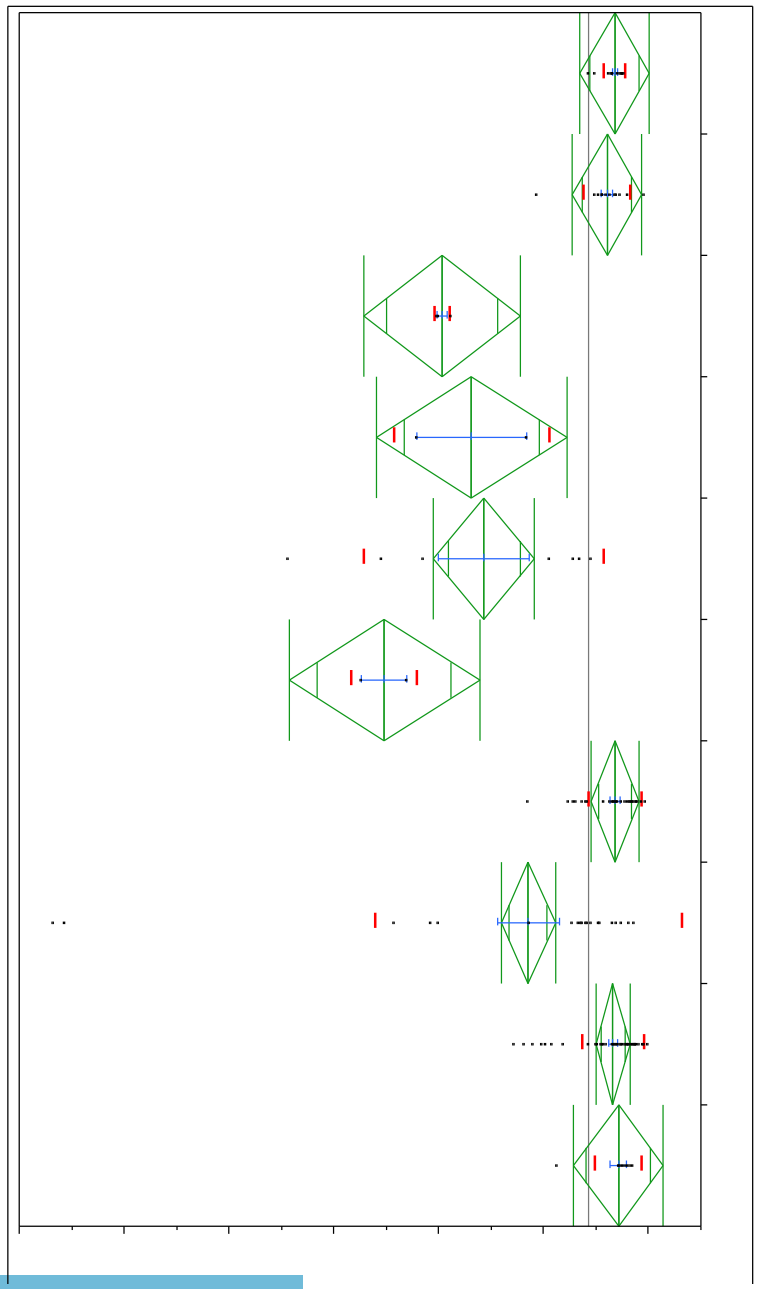

Figure 37: Balad PM10 Variability Charts, January 2007-November 2008

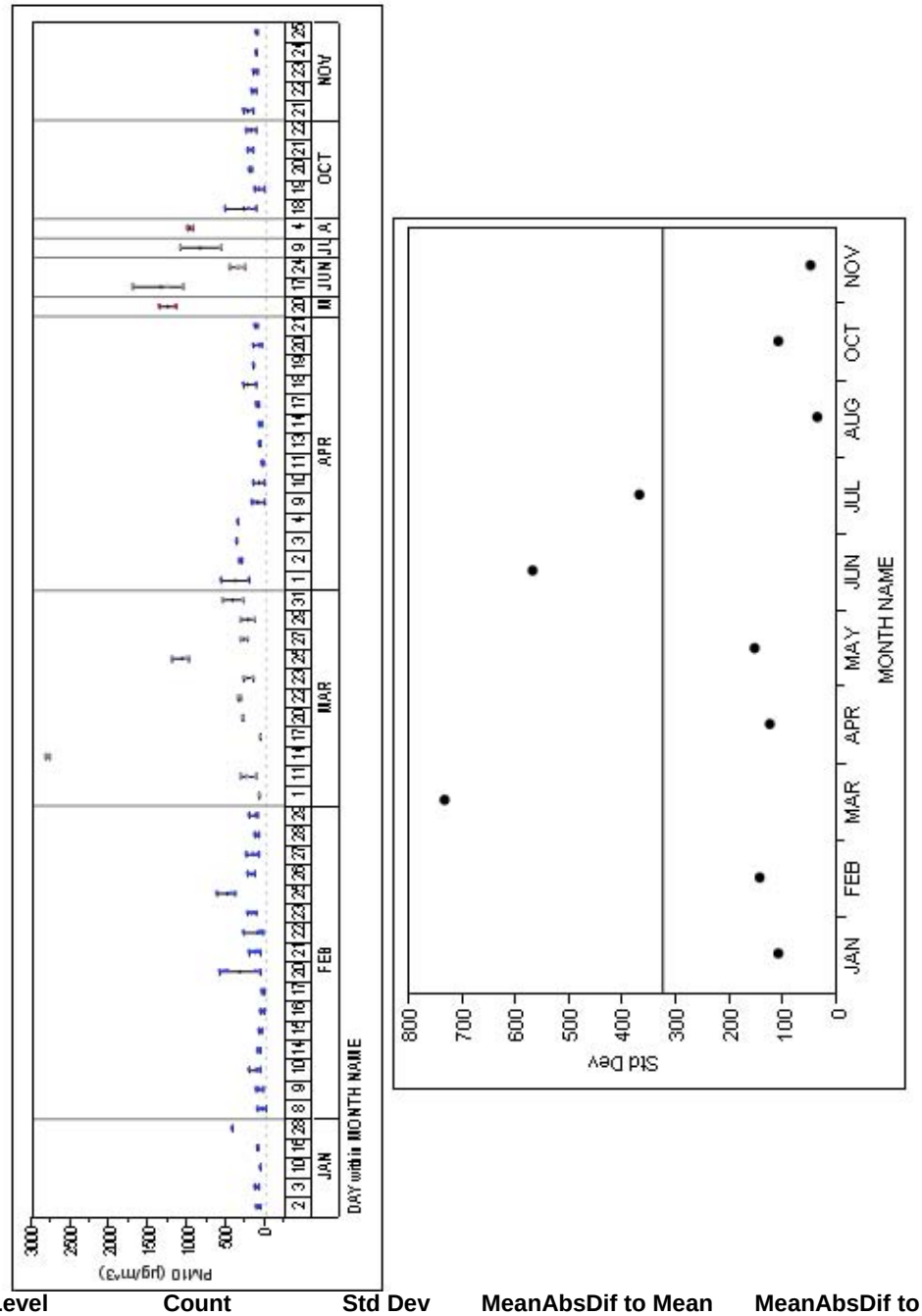

Level	Count	Std Dev	MeanAbsDif to Mean	MeanAbsDif to Median
JAN	9	111.5558	64.6173	55.6667
FEB	60	145.1941	102.1400	92.1000
MAR	25	732.3577	480.9440	354.8400
APR	33	126.4610	93.9945	89.9697
MAY	2	154.1493	109.0000	109.0000
JUN	7	570.1846	489.2653	460.1429
JUL	2	369.1097	261.0000	261.0000
AUG	3	37.1663	28.4444	25.3333
OCT	15	111.2730	68.2400	67.1333
NOV	15	50.6554	38.5867	35.2667

Appendix E: SASEM Output File

This is the plume rise software output, based on input described in methodology. The 100-meter plume rise was based on wind conditions that are much higher than the average wind conditions at Balad, but provides a conservative plume rise estimate, as higher wind speeds result in lower plume rise and greater concentrations. Exceedence values are not applicable and were not used, as they are based on particulate emissions from hardwood burning.

```
Using NewSasem input and calculations.

 Burn Name ........................      burn pit
 Burn Date ........................      4/13/2009
 Burn Type ........................      PILED
 Fuel Model .......................      R
 Burn Duration ....................      4.000 Hr
 Pile Volume ......................      300.000 Cu meters
 Number of Piles ..................      10

 Wind Speed Min ...................      1.0 knots
 Wind Speed Max ...................      27.0 knots
 Wind Speed Inc ...................      1.0 knots
 Wind Direction Min ...............      WNW
 Wind Direction Max ...............      NNW
 Stability Type ...................      Dispersion Day
 Stability Min ....................      Excellent
 Stability Max ....................      Poor
 Mixing Height ....................      1500.0 m
 Met Limitation ...................      Only Valid Combinations

 Number of Receptors ..............      9
 Receptor Name ....................      Rec #1
 Receptor Distance ................      0.50 km
 Receptor Direction ...............      NW
 Receptor Name ....................      Rec # 2
 Receptor Distance ................      1.00 km
 Receptor Direction ...............      NW
 Receptor Name ....................      Rec # 3
 Receptor Distance ................      1.50 km
 Receptor Direction ...............      NW
 Receptor Name ....................      Rec # 4
 Receptor Distance ................      2.00 km
 Receptor Direction ...............      NW
 Receptor Name ....................      Rec # 5
 Receptor Distance ................      2.50 km
 Receptor Direction ...............      NW
 Receptor Name ....................      Rec # 6
 Receptor Distance ................      3.00 km
 Receptor Direction ...............      NW
 Receptor Name ....................      Rec # 7
 Receptor Distance ................      3.50 km
```

```
Receptor Direction ..............       NW
Receptor Name ...................       Rec # 8
Receptor Distance ...............       4.00 km
Receptor Direction ..............       NW
Receptor Name ...................       Rec # 9
Receptor Distance ...............       4.50 km
Receptor Direction ..............       NW

Total Fuel Consumed .............       15.194 T/A
TSP Emission Factor .............       11.217 g/kg
PM-10 Emission Factor ...........       8.124 g/kg
PM-2.5 Emission Factor ..........       6.863 g/kg
TSP Emission Rate ...............       26.530 g/s/pile
PM-10 Emission Rate .............       19.214 g/s/pile
PM-2.5 Emission Rate ............       16.232 g/s/pile
TSP Total Emissions .............       4.211 T
PM-10 Total Emissions ...........       3.050 T
PM-2.5 Total Emissions ..........       2.577 T
Fireline Length .................       31.37 m
Heat Content of Fuel ............       7000. Btu/lb
Heat Release Rate ...............       9198110. cal/s
Wind Persistence Factor .........       0.167
Portion of smoke which rises ....       90.00 %
```

Stability	Wind Speed (knots)	Maximum Concen (ug/m**3)	Distance to Maximum Concen (mi)	Exceedences Distance From (mi)	Exceedences Distance To (mi)	Plume Rise (m)
EXC	1.0	4.3	7.56	No Exceedence		2482.
EXC	2.0	7.6	4.06	No Exceedence		1241.
EXC	3.0	10.6	2.82	No Exceedence		827.
EXC	4.0	13.5	2.18	No Exceedence		620.
GOOD	2.0	4.5	11.32	No Exceedence		1241.
GOOD	3.0	6.7	7.26	No Exceedence		827.
GOOD	4.0	9.0	5.29	No Exceedence		620.
GOOD	5.0	11.2	4.14	No Exceedence		496.
GOOD	6.0	13.4	3.39	No Exceedence		414.
GOOD	7.0	15.7	2.86	No Exceedence		355.
GOOD	8.0	17.9	2.47	No Exceedence		310.
GOOD	9.0	20.1	2.17	No Exceedence		276.
GOOD	10.0	22.3	1.93	No Exceedence		248.
GOOD	11.0	24.5	1.74	No Exceedence		226.
GOOD	12.0	26.7	1.58	No Exceedence		207.
GOOD	13.0	28.9	1.45	No Exceedence		191.
GOOD	14.0	31.1	1.34	No Exceedence		177.
GOOD	15.0	33.3	1.24	No Exceedence		165.
GOOD	16.0	35.5	1.15	No Exceedence		155.
GOOD	17.0	37.7	1.08	No Exceedence		146.
GOOD	18.0	40.2	0.62	No Exceedence		138.
GOOD	19.0	43.3	0.62	No Exceedence		131.
GOOD	20.0	46.2	0.62	No Exceedence		124.
GOOD	21.0	48.9	0.62	No Exceedence		118.
GOOD	22.0	51.4	0.62	No Exceedence		113.
GOOD	23.0	53.7	0.62	No Exceedence		108.
GOOD	24.0	55.7	0.62	No Exceedence		103.
GOOD	25.0	57.6	0.62	No Exceedence		99.
GOOD	26.0	59.2	0.62	No Exceedence		95.
GOOD	27.0	60.6	0.62	No Exceedence		92.
FAIR	3.0	1.6	25.09	No Exceedence		827.

FAIR	4.0	2.5	15.07	No Exceedence	620.
FAIR	5.0	3.6	10.14	No Exceedence	496.
FAIR	6.0	4.8	7.34	No Exceedence	414.
FAIR	7.0	6.1	5.59	No Exceedence	355.
FAIR	8.0	7.6	4.41	No Exceedence	310.
FAIR	9.0	9.1	3.58	No Exceedence	276.
FAIR	10.0	10.7	2.97	No Exceedence	248.
FAIR	11.0	12.1	2.51	No Exceedence	226.
FAIR	12.0	13.4	2.15	No Exceedence	207.
FAIR	13.0	14.8	1.87	No Exceedence	191.
FAIR	14.0	16.2	1.64	No Exceedence	177.
FAIR	15.0	17.6	1.45	No Exceedence	165.
FAIR	16.0	19.0	1.29	No Exceedence	155.
FAIR	17.0	20.4	1.16	No Exceedence	146.
FAIR	18.0	21.9	1.05	No Exceedence	138.
FAIR	19.0	23.3	0.95	No Exceedence	131.
FAIR	20.0	24.7	0.87	No Exceedence	124.
FAIR	21.0	26.2	0.80	No Exceedence	118.
FAIR	22.0	27.7	0.73	No Exceedence	113.
FAIR	23.0	29.1	0.68	No Exceedence	108.
FAIR	24.0	30.6	2.15	No Exceedence	103.
FAIR	25.0	32.9	0.62	No Exceedence	99.
FAIR	26.0	35.5	0.62	No Exceedence	95.
FAIR	27.0	38.1	0.62	No Exceedence	92.
POOR	1.0	65.2	7.60	No Exceedence	240.
POOR	2.0	63.5	4.70	No Exceedence	190.
POOR	3.0	62.5	3.55	No Exceedence	166.
POOR	4.0	60.6	2.91	No Exceedence	151.

* The TSP standard used is 150. micrograms per cubic meter.

Stability	Wind Speed (knots)	Maximum Concen (ug/m**3)	Distance to Maximum Concen (mi)	Exceedences Distance From (mi)	To (mi)	Plume Rise (m)
EXC	1.0	3.1	7.56	No Exceedence		2482.
EXC	2.0	5.5	4.06	No Exceedence		1241.
EXC	3.0	7.7	2.82	No Exceedence		827.
EXC	4.0	9.8	2.18	No Exceedence		620.
GOOD	2.0	3.3	11.32	No Exceedence		1241.
GOOD	3.0	4.9	7.26	No Exceedence		827.
GOOD	4.0	6.5	5.29	No Exceedence		620.
GOOD	5.0	8.1	4.14	No Exceedence		496.
GOOD	6.0	9.7	3.39	No Exceedence		414.
GOOD	7.0	11.3	2.86	No Exceedence		355.
GOOD	8.0	12.9	2.47	No Exceedence		310.
GOOD	9.0	14.5	2.17	No Exceedence		276.
GOOD	10.0	16.1	1.93	No Exceedence		248.
GOOD	11.0	17.7	1.74	No Exceedence		226.
GOOD	12.0	19.3	1.58	No Exceedence		207.
GOOD	13.0	20.9	1.45	No Exceedence		191.
GOOD	14.0	22.5	1.34	No Exceedence		177.
GOOD	15.0	24.1	1.24	No Exceedence		165.
GOOD	16.0	25.7	1.15	No Exceedence		155.
GOOD	17.0	27.3	1.08	No Exceedence		146.
GOOD	18.0	29.1	0.62	No Exceedence		138.
GOOD	19.0	31.4	0.62	No Exceedence		131.
GOOD	20.0	33.5	0.62	No Exceedence		124.
GOOD	21.0	35.4	0.62	No Exceedence		118.
GOOD	22.0	37.2	0.62	No Exceedence		113.

Stability	Wind Speed (knots)	Maximum Concen (ug/m**3)	Distance to Maximum Concen (mi)	Exceedences Distance From (mi)	To (mi)	Plume Rise (m)
GOOD	23.0	38.9	0.62	No Exceedence		108.
GOOD	24.0	40.4	0.62	No Exceedence		103.
GOOD	25.0	41.7	0.62	No Exceedence		99.
GOOD	26.0	42.9	0.62	No Exceedence		95.
GOOD	27.0	43.9	0.62	No Exceedence		92.
FAIR	3.0	1.1	25.09	No Exceedence		827.
FAIR	4.0	1.8	15.07	No Exceedence		620.
FAIR	5.0	2.6	10.14	No Exceedence		496.
FAIR	6.0	3.5	7.34	No Exceedence		414.
FAIR	7.0	4.4	5.59	No Exceedence		355.
FAIR	8.0	5.5	4.41	No Exceedence		310.
FAIR	9.0	6.6	3.58	No Exceedence		276.
FAIR	10.0	7.8	2.97	No Exceedence		248.
FAIR	11.0	8.7	2.51	No Exceedence		226.
FAIR	12.0	9.7	2.15	No Exceedence		207.
FAIR	13.0	10.7	1.87	No Exceedence		191.
FAIR	14.0	11.7	1.64	No Exceedence		177.
FAIR	15.0	12.7	1.45	No Exceedence		165.
FAIR	16.0	13.8	1.29	No Exceedence		155.
FAIR	17.0	14.8	1.16	No Exceedence		146.
FAIR	18.0	15.8	1.05	No Exceedence		138.
FAIR	19.0	16.9	0.95	No Exceedence		131.
FAIR	20.0	17.9	0.87	No Exceedence		124.
FAIR	21.0	19.0	0.80	No Exceedence		118.
FAIR	22.0	20.0	0.73	No Exceedence		113.
FAIR	23.0	21.1	0.68	No Exceedence		108.
FAIR	24.0	22.2	2.15	No Exceedence		103.
FAIR	25.0	23.9	0.62	No Exceedence		99.
FAIR	26.0	25.7	0.62	No Exceedence		95.
FAIR	27.0	27.6	0.62	No Exceedence		92.
POOR	1.0	47.2	7.60	No Exceedence		240.
POOR	2.0	46.0	4.70	No Exceedence		190.
POOR	3.0	45.2	3.55	No Exceedence		166.
POOR	4.0	43.9	2.91	No Exceedence		151.

* The PM-10 standard used is 150. micrograms per cubic meter.

Stability	Wind Speed (knots)	Maximum Concen (ug/m**3)	Distance to Maximum Concen (mi)	Exceedences Distance From (mi)	To (mi)	Plume Rise (m)
EXC	1.0	2.6	7.56	No Exceedence		2482.
EXC	2.0	4.7	4.06	No Exceedence		1241.
EXC	3.0	6.5	2.82	No Exceedence		827.
EXC	4.0	8.3	2.18	No Exceedence		620.
GOOD	2.0	2.8	11.32	No Exceedence		1241.
GOOD	3.0	4.1	7.26	No Exceedence		827.
GOOD	4.0	5.5	5.29	No Exceedence		620.
GOOD	5.0	6.9	4.14	No Exceedence		496.
GOOD	6.0	8.2	3.39	No Exceedence		414.
GOOD	7.0	9.6	2.86	No Exceedence		355.
GOOD	8.0	10.9	2.47	No Exceedence		310.
GOOD	9.0	12.3	2.17	No Exceedence		276.
GOOD	10.0	13.6	1.93	No Exceedence		248.
GOOD	11.0	15.0	1.74	No Exceedence		226.
GOOD	12.0	16.3	1.58	No Exceedence		207.
GOOD	13.0	17.7	1.45	No Exceedence		191.
GOOD	14.0	19.0	1.34	No Exceedence		177.
GOOD	15.0	20.4	1.24	No Exceedence		165.
GOOD	16.0	21.7	1.15	No Exceedence		155.

GOOD	17.0	23.1	1.08	No Exceedence	146.
GOOD	18.0	24.6	0.62	No Exceedence	138.
GOOD	19.0	26.5	0.62	No Exceedence	131.
GOOD	20.0	28.3	0.62	No Exceedence	124.
GOOD	21.0	29.9	0.62	No Exceedence	118.
GOOD	22.0	31.4	0.62	No Exceedence	113.
GOOD	23.0	32.8	0.62	No Exceedence	108.
GOOD	24.0	34.1	0.62	No Exceedence	103.
GOOD	25.0	35.2	0.62	No Exceedence	99.
GOOD	26.0	36.2	0.62	No Exceedence	95.
GOOD	27.0	37.1	0.62	No Exceedence	92.
FAIR	3.0	1.0	25.09	No Exceedence	827.
FAIR	4.0	1.5	15.07	No Exceedence	620.
FAIR	5.0	2.2	10.14	No Exceedence	496.
FAIR	6.0	2.9	7.34	No Exceedence	414.
FAIR	7.0	3.7	5.59	No Exceedence	355.
FAIR	8.0	4.6	4.41	No Exceedence	310.
FAIR	9.0	5.6	3.58	No Exceedence	276.
FAIR	10.0	6.6	2.97	No Exceedence	248.
FAIR	11.0	7.4	2.51	No Exceedence	226.
FAIR	12.0	8.2	2.15	No Exceedence	207.
FAIR	13.0	9.1	1.87	No Exceedence	191.
FAIR	14.0	9.9	1.64	No Exceedence	177.
FAIR	15.0	10.8	1.45	No Exceedence	165.
FAIR	16.0	11.6	1.29	No Exceedence	155.
FAIR	17.0	12.5	1.16	No Exceedence	146.
FAIR	18.0	13.4	1.05	No Exceedence	138.
FAIR	19.0	14.3	0.95	No Exceedence	131.
FAIR	20.0	15.1	0.87	No Exceedence	124.
FAIR	21.0	16.0	0.80	No Exceedence	118.
FAIR	22.0	16.9	0.73	No Exceedence	113.
FAIR	23.0	17.8	0.68	No Exceedence	108.
FAIR	24.0	18.7	2.15	No Exceedence	103.
FAIR	25.0	20.2	0.62	No Exceedence	99.
FAIR	26.0	21.7	0.62	No Exceedence	95.
FAIR	27.0	23.3	0.62	No Exceedence	92.
POOR	1.0	39.9	7.60	No Exceedence	240.
POOR	2.0	38.9	4.70	No Exceedence	190.
POOR	3.0	38.2	3.55	No Exceedence	166.
POOR	4.0	37.1	2.91	No Exceedence	151.

* The PM-2_5 standard used is 65. micrograms per cubic meter.

Appendix F. GIS Data Sources and Procedure Log

This appendix contains the process used to create maps and perform spatial analysis in this research. Its intent is to allow future researchers to reproduce the results achieved in this research, as well as to provide information into step-by-step methodology in achieving research results.

Metadata & Data

1. *Shapefile Properties (all GeoBase Shapefiles)*

XY Coordinate System: WGS_1984_UTM_Zone_38N

Projection: Transverse_Mercator

False_Easting: 500000.000000

False_Northing: 0.000000

Central_Meridian: 45.000000

Scale_Factor: 0.999600

Latitude_Of_Origin: 0.000000

Linear Unit: Meter (1.000000)

Geographic Coordinate System: GCS_WGS_1984

Angular Unit: Degree (0.0174532925199433299)

Prime Meridian: Greenwich (0.000000000000000000)

Datum: D_WGS_1984

Spheroid: WGS_1984

Semimajor Axis: 6378137.000000000000000000

Semiminor Axis: 6356752.314245179300000000

Inverse Flattening: 298.257223563000030000

2. *Data Sources*

Joint Base Balad PM10 Monitoring Results for POEMS, 2003-2010:

U.S. Army Public Health Command, provided by Mr. John Kolivosky

http://phc.amedd.army.mil/Pages/default.aspx

Joint Base Balad PM10 Sampling Location Coordinates:

U.S. Army Public Health Command, provided by Mr. John Kolivosky

http://phc.amedd.army.mil/Pages/default.aspx

Joint Base Balad Base Layers: "balad_southeast_01dec2008_wgs84_utm38n_cip_shp" and "balad_southeast_01dec2008_wgs84_utm38n_cip_pgdb" from:

U.S. Air Force A7ZG - ACC IGI&S GeoBase:

https://www.my.af.mil/gcss-af/USAF/ep/globalTab.do?channelPageId=s6925EC1340060FB5E044080020E329A9

Procedure Log

I. Spatial Interpolation of Monitored PM10, 2007-2008

1. Add ACC GeoBase Layers in ArcMap:

BAAS_installation_area

BAAS_road_area

BAAS_airfield_surface_area

BAAS_slab_area

BAAS_vehicle_parking_area

BAAS_vehicle_driveway_area

Structure_existing_area

Surface_water_body_area

Fuel_farm_area_layer

2. Prepare Monitoring Data Tables

   Sort 2007-2008 PM10 sampling results by coordinates

   Create "Site Name" for unique coordinate pairs

   Calculate geometric and arithmetic mean for unique coordinate pairs

   Create geometric mean table, with individual sites as features, and the following as attributes: geometric mean, year, number of samples

3. Import Monitoring Data Information

   File: Add Data: add geometric mean table created in step 2.

   File: Add Data: Add XY Data: add geometric mean table information, using Latitude and Longitude fields as XY data, and geometric mean attribute as Z field. Edit coordinate system of Input Coordinates: Select a predefined coordinate system: Geographic Coordinate System: World: WGS1984.prj Right Click on Data Layer: Data: Export Data: Use same coordinate system as this source's data layer

4. View semivariogram

   Geostatistical Analyst: Semivariogram/Covariance Cloud

Select 2007-2008 monitoring sites layer

Choose Geometric Mean as attribute

Visual inspection of semivariogram reveals lack of trend, lack of autocorrelation

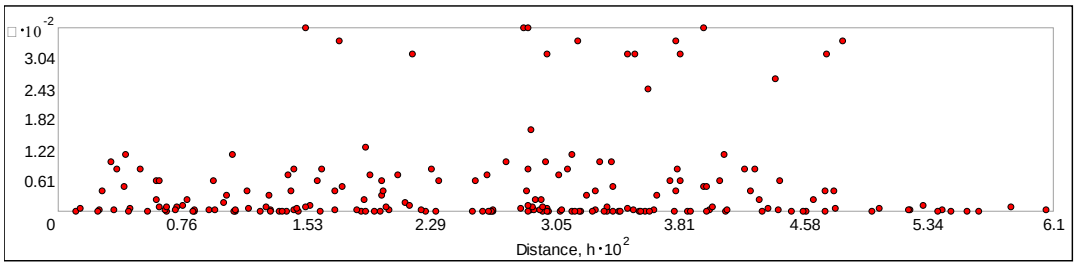

5. IDW Interpolation on Monitored Data

    Select geometric mean layer

    Spatial Analyst Tools: Interpolation: IDW

        Input Point Features: geometric mean layer

        Z value field: Geometric Mean

        Power: 2

        Search Radius Settings: Search Radius-Variable; Number of Points-12

6. Map Creation

    Label sites with number of samples

    Symbology: Stretched (Map 1); Classified (Map 2)

    Transparency 35%

7. Repeat process for each year (2007 & 2008)

II. Loose-Coupled Dispersion Modeling

1. Run dispersion models in PC-SCIPUFF: Flaming, Smoldering

2. Export 100-point georeferenced data as ASCII (WGS1984 is default SCIPUFF projection); keep grid points constant between runs by setting domain as:

Latitude Min 33.907 Latitude Max 33.984

Longitude Min 44.318 Longitude Max 44.408

3. Import georeferenced data into table for both Flaming and Smoldering

4. Create column with sum of Flaming and Smoldering

5. Interpolate 100-point grid with Radial Basis Function using concentration values for each of Flaming, Smoldering, and sum as Z-values; Default output cell size; Search Neigborhood – standard. Output Geostatistical Layer.

6. Open Geostatistical Wizard – Save Method Report. Method report displays as:

Input datasets
-Dataset
Export_Output_43
Location: C:\Users\John\Documents\AFIT\thesis\BaladData\GIS
Type: Feature Class
Data field: Concsum
Records: 100

-Method
Radial Basis Functions
Kernel function: Thin Plate Spline
Parameter: 117.64705882355763

-Searching neighborhood: Standard
Type: Standard
Neighbors to include: 15
Include at least: 10
Sector type: Full
Angle: 0
Major semiaxis: 11836.697011942291
Minor semiaxis: 11836.697011942291

7. Display as “classified”

8. Create Contours

Spatial Analyst Tools: Surface: Contour

Select sum of flaming and smoldering as contour raster

Select 2.5 as contour interval

III. Combined Map

1. Turn on desired Geometric Mean interpolated layer; display as stretched, 35% transparency

2. Turn on Dispersion Model contour layer

3. Compare layers, visualize areas with common high PM10 concentration; all maps show high PM10 within 1 km of burn pit location

IV. Identify Features in High Risk Area

1. Create 1 km buffer containing high risk area

Geoprocessing: Buffer

Select Burn Pit site layer as Input Features

Distance: 1000 meters (or 1 kilometer)

2. Display buffer layer with monitored interpolation and dispersion model layers

3. Geoprocessing: Intersect buffer layer features and *BAAS_existing_structure* layer features

4. Display intersected layer

5. Display attribute table; view structure properties in table to identify building types, occupancy, and other relevant information

VI. Export to KML for viewing in Google Earth

1. Conversion Tools: To KML: Layer to KML
2. Select Intersection layer
3. Export to KML
4. View layer in Google Earth

Bibliography

14 WS (US Air Force 14th Weather Squadron). (2010). *14th Weather Squadron Services*. Retrieved October 15, 2010, from 14th Weather Squadron Web Site: https://notus2.afccc.af.mil/SCISPublic/services.asp

Ainslie, B., & Jackson, P. (2008). The Use of an Atmospheric Dispersion Model to Determine Influence Regions in the Prince George, B.C. Airshed From the Open Burning of Open Wood Waste Piles. *Journal of Environmental Management* , 2393-2401.

Akagi, S. K., Yokelson, R., Wiedinmyer, C., Alvarado, M., Reid, J., Karl, T., et al. (2010). Emission Factors for Open Burning for Use in Atmospheric Models. *Atmospheric Chemistry and Physics Discussions* , 27523-27602.

ArcGIS 10 Desktop. (n.d.). Redlands, CA.
Arizona State University. (n.d.). *OpenGeoDa*. Retrieved February 8, 2011, from Arizona State University Web Site: http://geodacenter.asu.edu/

Armed Forces Health Surveillance Center; Naval Health Research Center; US Army Public Health Command. (2010). *Epidemiological Studies of Health Outcomes among Troops Deployed to Burn Pit Sites.* Washington, DC: Department of Defense.

Army Institute of Public Health. (2010). *Classification/Composition of Solid Waste Found in Operations Iraqi Freedom and Enduring Freedom during 2006-2010.* Aberdeen Proving Ground, MD.

Atwood, S. (2010). *Backtrajectory Analysis for Baghdad, Iraq: Preliminary Results Completed to Date.* Colorado State University.

Barakat, A. (2003). Persistent Organic Pollutants in Smoke Particles Emitted During Open Burning of Municipal Solid Wastes. *Bulletin of Environmental Contamination and Toxicology , 70*, 174–181.

Bellander, T., Jonson, T., Gustavsson, P., Pershagen, G., & Järup, L. (2001). Using Geographic Information Systems to Assess Individual Historical Exposure to Air Pollution from Traffic and House Heating in Stockholm. *Environmental Health Perspectives , 109*, 633-639.

Beyea, J., & Hatch, M. (1999). Geographic Exposure Modeling: A Valuable Extension of Geographic Information Systems for Use in Environmental Epidemiology. *Environmental Health Perspectives , 107, Supplement 1*, 181-190.

Briggs, D. J., Collins, S., Elliott, P., Fischer, P., Kingham, S., Lebret, E., et al. (2001). Mapping Urban Air Pollution Using GIS: a Regression-based Approach. *International Journal of Geographical Information Science , 11* (7).
Briggs, D. (2005). The Role of GIS: Coping With Space (and Time) in Air Pollution Exposure Assessment. *Journal of Toxicology and Environmental Health, Part A , 68*, 1243-1261.

Carroll, J. J., Miller, G. E., & Thompson, J. F. (1977). The Dependence of Open Field Burning Emissions and Plume Concentrations on Meteorology, Field Conditions and Ignition Technique. *Atmospheric Environment , 11* (11), 1037-1050.

Cheng, M., Horng, C., Sua, Y., Lin, L., Lin, Y., & Chou, C. (2009). Particulate Matter Characteristics During Agricultural Waste Burning in Taichung City, Taiwan. *Journal of Hazardous Materials , 165*, pp. 187-192.

Clench-Aas, J., Bartonova, A., Bøhler, T., Grønskei, K. E., Sivertsen, B., & Larssen, S. (1999). Air Pollution Exposure Monitoring and Estimating. *Journal of Environmental Monitoring* (1), 313-319.

Code of Federal Regulations, Title 40, Part 51. (2005, November 9). Revision to the Guideline on Air Quality Models: Adoption of a Preferred General Purpose (Flat and Complex Terrain) Dispersion Model and Other Revisions; Final Rule. *Title 40 (Protection of Environment), Part 51* . Washington, D.C.: Environmental Protection Agency.

Crabbe, H., Hamilton, R., & Machin, N. (2000). Using GIS and Dispersion Modeling Tools to Assess the Effect of the Environment on Health. *Transactions in GIS , 4* (3), 235-244.

Crisp, J. (2008, July 27). *The Dirt Behind Iraq's Dust Storms*. Retrieved 11 14, 2010, from Army.mil: http://www.army.mil/-news/2008/07/27/11255-the-dirt-behind-iraqs-dust-storms/

Cui, H., Stein, A., & Myers, D. (1995). Extension of Spatial Information, Bayesian Kriging and Updating of Prior Variogram Parameters. *Environmetrics* , 373-384.

Daniels, M., Dominici, F., Samet, J. M., & Zeger, S. L. (2000). Estimating Particulate Matter-Mortality Dose-Response Curves and Threshold Levels: An Analysis of Daily Time-Series for the 20 Largest US Cities. *American Journal of Epidemiology , 152* (5), 397-406.

de Zarate, O., Ezcurra, A., Lacaux, J., & Dinh, P. V. (2000). Emission Factor Estimates of Cereal Waste Burning in Spain. *Atmospheric Environment* (19), 3183-3193.

DeMarini, D. M., Lemieux, P. M., Ryan, J. V., Brooks, L. R., & Williams, R. W. (1994). Mutagenicity and chemical analysis of emissions from the open burning of scrap rubber tires. *Environmental Science & Technology , 28* (1), pp. 136-141.
Department of Defense. (2010, March 30). Directive-type Memorandum (DTM) 09-032 – Use of Open-air Burn Pits in Contingency Operations. Washington, DC: Department of Defense.

Department of the Air Force. (2009). Career Field Education and Training Plan, Bioenvironmental Engineering Specialty. Washington: HQ USAF.

Dominici, F., Zonabetti, A., Zeger, S., Schwartz, J., & Samet, J. (2005). *The National Morbidity, Mortality, and Air Pollution Study, Part IV: Hierarchical Bivariate Time-Series Models—A Combined Analysis of PM10 Effects on Hospitalization and Mortality.* Health Effects Institute, Boston, MA.

Draxler, R. R., Gillette, D. A., S., K. J., & Heller, J. (2001). Estimating PM10 air concentrations from dust storms in Iraq, Kuwait and Saudi Arabia. *Atmospheric Environment , 35: 4315–4330.*

Engelbrecht, J. P., McDonald, E. V., Gillies, J. A., & Gertler, A. W. (2008). *Department of Defense Enhanced Particulate Matter Surveillance Program (EPMSP).* Reno, NV: Desert Research Institute.

Engelbrecht, J. P., McDonald, E. V., Gillies, J. A., Jayanty, R., Casuccio, G., & Gertler, A. W. (2009). Characterizing mineral dusts and other aerosols from the Middle East--Part 1: ambient sampling. *Inhalation Toxicology , 21* (4: 297-326).

Environmental Protection Agency. (2008). *Background Information Document for Updating AP42 Section 2.4 for Estimating Emissions from Municipal Solid Waste Landfills.* Washington, D.C.: U.S. Environmental Protection Agency.

Environmental Protection Agency. (2004). *Developing Spatially Interpolated Surfaces and Estimating Uncertainty.* Research Triangle Park, NC: Environmental Protection Agency Office of Air Quality Planning and Standards.

Environmental Protection Agency. (2011, January 11). *Emissions Factors & AP 42, Compilation of Air Pollutant Emission Factors.* Retrieved January 14, 2011, from U.S. Environmental Protection Agency: http://www.epa.gov/ttn/chief/ap42/index.html

Environmental Protection Agency. (2011). *SI 409 - Lesson 6: Plume Dispersion and Air Quality Modeling.* Retrieved February 11, 2011, from EPA Air Pollution Training Institute Basic Air Pollution Meteorlogy: http://yosemite.epa.gov/oaqps/EOGtrain.nsf/DisplayView/SI_409_6?OpenDocument

Environmental Protection Agency. (2010, December 6). *Technology Transfer Network Support Center for Regulatory Atmospheric Modeling*. Retrieved February 6, 2011, from United States Environmental Protection Agency: http://www.epa.gov/scram001/
Environmental Protection Agency; National Oceanic and Atmospheric Association. (2007). *ALOHA User's Manual.* Washington, D.C.: U.S. Environmental Protection Agency.

EPA. (2010). *Integration of Regional and Local Scale Air Quality Modeling Research with EPA/ORD's Human Exposure and Health Research Program.* Environmental Protection Agency Atmospheric Exposure Integration Branch of the Atmospheric Modeling and Analysis Division. Research Triangle Park, NC: U.S. Environmental Protection Agency.

Esri, Inc. (2010). ArcGIS 10 Help: Natural Neighbor Interpolation.

Estrellan, C. R., & Iino, F. (2009). Toxic Emissions From Open Burning. *Chemosphere* , 193-207.

Gillies, J., Etyemezian, V., Kuhns, H., Nikolic, D., & Gillette, D. (2005). Effect of Vehicle Characteristics on Unpaved Road Dust Emissions. *Atmospheric Environment* , *39* (13), 2341-2347.

Government Accountability Office. (2010). *DoD Should Improve Adherence to Its Guidance on Open Pit Burning and Solid Waste Management.* Washington, DC: Government Accountability Office.

Gullett, B. K., & Linak, W. P. (2007). Characterization of Air Emissions and Residual Ash from Open Burning of Electronic Wastes During Simulated Rudimentary Recycling Operations. *Journal of Material Cycles and Waste Management , 9* (1), pp. 69-79.

Gullett, B. K., & Raghunathan, K. (1997). Observations on the Effects of Process Parameters on Dioxin/Furan Yield in Municipal Waste and Coal Systems. *Chemosphere* , 34: 1027-1032.

Gullett, B. K., Lemieux, P. M., Lutes, C. C., Winterrowd, C. K., & Winters, D. L. (2001). Emissions of PCDD/F from uncontrolled, domestic waste burning. *Chemosphere* , 43: 721-725.

Gullett, B. K., Wyrzykowska, B., Grandesso, E., Touati, A., Tabor, D. G., & Ochoa, G. S. (2010). PCDD/F, PBDD/F, and PBDE Emissions from Open Burning of a Residential Waste Dump. *Environmental Science and Technology , 44* (1).

Hargrove, W., Levine, D., Miller, M., Coleman, P., Pack, D., & Durfee, R. (1996). *GIS and Risk Assessment: A Fruitful Combination.* Retrieved February 6, 2011, from Esri: http://proceedings.esri.com/library/userconf/proc96/TO50/PAP028/P28.HTM

Hoek, G., Beelen, R., de Hoogh, K., Vienneau, D., Gulliver, J., Fischer, P., et al. (2008). A Review of Land-use Regression Models to Assess Spatial Variation of Outdoor Air Pollution. *Atmospheric Environment , 42*.
Huber, A. G.-W. (2004). Modeling Air Pollution from the Collapse of the World Trade Center and Assessing the Potential Impacts on Human Exposures. *EM* , 35-40.

Jarup, L. (2004). Health and Environmental Information Systems for Exposure and Disease Mapping, and Risk Assessment. *Environmental Health Perspectives , 112* (9).

Jerrett, M., Arain, A., Kanaroglou, P., Beckerman, B., Potoglou, D., Sahsuvaroglu, T., et al. (2005). A review and evaluation of intraurban air pollution exposure models. *Journal of Exposure Analysis and Environmental Epidemiology* , 185-204.

Kumagai, S., Kurumatani, N., Tsuda, T., Yorifuji, T., & Suzuki, E. (2010). Increased Risk of Lung Cancer Mortality Among Residents Near and Asbestos Product Manufacturing Plant. *International Journal of Occupational and Environmental Health* , 268-278.

Kutiel, H., & Furman, H. (2003). Dust Storms in the Middle East: Sources of Origin and their Temporal Characteristics. *Indoor and Built Environment* , 419-426.

Lee, H., Wang, L., & Shih, J.-F. (1995). Mutagenicity of Particulates From the Laboratory Combustion of Plastics. *Mutation Research , 136*, 135-144.

Lemieux, P. M. (1998). *Evaluation of Emissions from the Open Burning of Household Waste in Barrels.* National Risk Management Research Laboratory. Cincinnati: United States Environmental Protection Agency.

Lemieux, P., Lutes, C., & Santoianni, D. (2004). Emissions of Organic Air Toxics From Open Burning: A Comprehensive Review. *Progress in Energy and Combustion Science* , 1-32.

Lemieux, P., Lutes, C., Abbott, J., & Aldous, K. (2000). Emissions of Polychlorinated Dibenzo-p-dioxins and Polychlorinated Dibenzofurans From the Open Burning of Household Waste in Barrels. *Environmental Science and Technology , 34*, 377–84.

Longley, P., Goodchild, M., Maguire, D., & Rhind, D. (2011). *Geographic Information Systems & Science, 3 ed.* Hoboken, NJ: Wiley.

Maantay, J. A., Tu, J., & Maroko, A. R. (2009). Loose-Coupling an Air Dispersion Model and a Geographic Information System (GIS) for Studying Air Pollution and Asthma in the Bronx, New York City. *International Journal of Environmental Health Research , 19* (1), 59-79.

Mohammed, M. (2009, July 5). *Sandstorm blankets Iraq, sends hundreds to hospital*. Retrieved December 6, 2010, from Reuters: http://www.reuters.com/article/idUSTRE56419520090705
Mosher, D. L. (2008). *Green warriors : Army environmental considerations for contingency operations from planning through post-conflict.* Santa Monica, CA: RAND Corporation.

Nakao, T., Aozasa, O., Ohta, S., & Miyata, H. (2006). Formation of Toxic Chemicals Including Dioxin-Related Compounds by Combustion From a Small Home Waste Incinerator. *Chemosphere , 62*, 459–468.

National Oceanic and Atmospheric Association. (2010, August 30). *Global Data Assimilation System (GDAS1) Archive Information*. Retrieved February 6, 2011, from Air Resources Laboratory: http://ready.arl.noaa.gov/gdas1.php

National Research Council. (2010). *Review of the Department of Defense Enhanced Particulate Matter Surveillance Program Report.* Washington, D.C.: The National Academies Press.

NCMI (National Center for Medical Intelligence). (2006, December 5). *Environmental Health Risk Assessment: Iraq*. Retrieved November 10, 2010, from National Center for Medical Intelligence: https://www.intelink.gov/ncmi/afmicdocument.php?id=35746#(U)

Nuckols, J. R., Ward, M. H., & Jarup, L. (2004). Using Geographic Information Systems for Exposure Assessment in Environmental Epidemiology Studies. *Environmental Health Perspectives , 112* (9).

Ott, D. K., Kumar, N., & Peters, T. (2008). Passive Sampling to Capture Spatial Variability in PM10-2.5. *Atmospheric Environment* , 746-756.

Riebau, A., Fox, D., Sestak, M., Dailey, B., & Archer, S. (1988). Simple Approach Smoke Estimation Model. *Atmospheric Environment , 22* (4).

Ryan, P. H., & LeMasters, G. K. (2007). A Review of Land-use Regression Models for Characterizing Intraurban Air Pollution Exposure. *Inhalation Toxicology , 19 (Suppl 1)*, 127–133.

Ryan, P., LeMasters, G., Biagini, J., Bernstein, D., Grinshpun, S., Shukla, R., et al. (2005). Is it Traffic Type, Volume, or Distance? Wheezing in Infants Living Near Truck and Bus Traffic. *Journal of Allergy & Clinical Immunology , 116* (2), 279-84.

Ryu, S., Kwon, B., Kim, Y., Kim, H., & Chun, K. (2007). Characteristics of Biomass Burning Aerosol and its Impact on Regional Air Quality in the Summer of 2003 at Gwangju, Korea. *Atmospheric Research , 84* (4), pp. 362–373.

Sage Management. (2010). *SCIPUFF Dispersion Model*. Retrieved October 20, 2010, from Sage Management Web Site: http://www.sage-mgt.net/services/modeling-and-simulation/scipuff-dispersion-model

Schaum, J., Cohen, M., Perry, S., Artz, R., Draxler, R., Frithsen, J., et al. (2010). Screening Level Assessment of Risks Due to Dioxin Emissions from Burning Oil from the BP Deepwater Horizon Gulf of Mexico Spill. *Environmental Science & Technology , 44* (24), 9383–9389.

Sidhu, S., Gullett, B., Striebich, R., Klosterman, J., Contreras, J., & DeVito, M. (2005). Endocrine Disrupting Chemical Emissions From Combustion Sources: Diesel Particulate Emissions and Domestic Waste Open Burn Emissions. *Atmospheric Environment , 39*, 801–811.

Simoneit, B. R., Medeiros, P. M., & Didyk, B. M. (2005). Combustion Products of Plastics as Indicators for Refuse Burning in the Atmosphere. *Environmental Science & Technology , 39* (18), pp. 6961-70.

Smith, B., Wong, C., Smith, T., Boyko, E., Gackstetter, G., & Ryan, M. (2009). Newly Reported Respiratory Symptoms and Conditions Among Military Personnel Deployed to Iraq and Afghanistan: A Prospective Population-based Study. *American Journal of Epidemiology* , 170:1433–1442.

Stark, N. M., White, R. H., & Clemons, C. M. (1997). Heat Release Rate of Wood-Plastic Composites. *SAMPLE Journal , 33* (5).

Stein, A., Isakov, V., Godowitch, J., & Draxler, R. (2007). A Hybrid Modeling Approach to Resolve Pollutant Concentrations in an Urban Area. *Atmospheric Environment , 41*, 9410-9426.

Susott, R., Ward, D., Reardon, J., & Griffith, D. W. (1997). Emissions From Smoldering Combustion of Biomass Measured by Open-Path Fourier Transform Infrared Spectroscopy. *Journal of Geophysical Research , 102* (D15), 18865-18877.

Sykes, R., Parker, S., Henn, D., Cerasoli, D., & Santos, L. (1998). *PC-SCIPUFF Version 1.2 Technical Documentation.* Princeton, NJ: Titan Corporation.

Szema, A. M., Peters, M. C., Weissinger, K. M., Gagliano, C. A., & Chen, J. J. (2010). New-onset asthma among soldiers serving in Iraq and Afghanistan. *Allergy and Asthma Proceedings* , 67-71.

The National Academies. (2010). *Project: Long-Term Health and Consequences of Exposure to Burn Pits In Iraq and Afghanistan*. Retrieved April 10, 2010, from The National Academies Current Projects System: http://www8.nationalacademies.org/cp/projectview.aspx?key=IOM-BSP-09-03

Touma, J. S., Isakov, V., & Ching, J. (2006). Air Quality Modeling of Hazardous Pollutants: Current Status and Future Directions. *Journal of the Air & Waste Management Association , 56*, 547–558.
Tran, H. C., & White, R. R. (1992). Burning Rate of Solid Wood Measured in a Heat Release Rate Calorimeter. *Fire and Materials , 16*, pp. 197-206.

U.S. Air Force. (2010). *A7ZG - ACC IGI&S GeoBase*. Retrieved 10 15, 2010, from Air Force Portal: https://www.my.af.mil/gcss-af/USAF/ep/globalTab.do?channelPageId=s6925EC1340060FB5E044080020E329A9

University of Tennessee. (2007). *Spatial Analysis and Decision Assistance*. Retrieved October 12, 2010, from University of Tennessee Knoxville Web Site: http://www.tiem.utk.edu/~sada/index.shtml

US Army Public Health Command (Provisional). (2010). *Screening Health Risk Assessments, Joint Base Balad, Iraq 11 May-19 June 2009.* Aberdeen Proving Ground, MD: US Army Public Health Command (Provisional).

USACHPPM. (2003). *Technical Guide 230: Chemical Exposure Guidelines for Deployed Military Personnel.* Technical Guide, Aberdeen Proving Ground, MD.

USAPHC (U.S. Army Public Health Command). (2010). Joint Base Balad PM10 Sampling Results for POEMS. Aberdeen Proving Ground, MD.

Valavanidis, A., Iliopoulos, N., Gotsis, G., & Fiotakis, K. (2008). Persistent Free Radicals, Heavy Metals and PAHs Generated in Particulate Soot Emissions and Residue Ash From Controlled Combustion of Common Types of Plastic. *Journal of Hazardous Materials , 156*, 277–284.

Vietas, J. A., Taylor, G., Rush, V., & Deck, A. (2008). *Screening Health Risk Assessment Burn Pit Exposures, Balad Air Base, Iraq and Addendum Report.* Air Force Institute for Operational Health, Brooks City-Base, TX; U.S. Army Center for Health Promotion and Preventive Medicine, Aberdeen Proving Ground, MD.

Wasson, S. J., Linak, W. P., Gullett, B. K., King, C. J., Touati, A., Huggins, F. E., et al. (2005). Emissions of Chromium, Copper, Arsenic, and PCDDs/Fs from Open Burning of CCA-Treated Wood. *Environmental Science & Technology , 39* (22), pp. 8865-8876.

Wevers, M., De Fre, R., & Desmedt, M. (2004). Effect of Backyard Burning on Dioxin Deposition and Air Concentrations. *Chemosphere , 54*.

White, N., teWaterNaude, J., van der Walt, A., Ravenscroft, G., Roberts, W., & Ehrlich, R. (2009). Meteorologically Estimated Exposure but not Distance Predicts Asthma Symptoms in Schoolchildren in the Environs of a Petrochemical Refinery: a Cross-sectional Study. *Environmental Health , 8* (45).

Wilcox, J., Entezam, B., Molenaar, B., & Shreeve, T. (1996). *Characterization of Emissions Produced by the Open Burning/Open Detonation of Complex Munitions.* Strategic Environmental Research and Development Program.
Wilkerson, W. D. (1991). *Dust and Sand Forecasting in Iraq and Adjoining Countries.* Scott AFB, Illinois: Air Weather Service.

Williams, F., & Ogston, S. (2002). Identifying Populations at Risk from Environmental Contamination from Point Sources. *Occupational and Environmental Medicine , 59*, 2-8.

Wilson, J. G., & Zawar-Reza, P. (2006). Intraurban-scale Dispersion Modelling of Particulate Matter Concentrations: Applications for Exposure Estimates in Cohort Studies. *Atmospheric Environment , 40*, 1053-1063.

Wong, D., Yuan, L., & Perlin, S. (2004). Comparison of Spatial Interpolation Methods for the Estimation of Air Quality Data. *Journal of Exposure Analysis and Environmental Epidemiology , 14*, 404-415.

World Health Organization. (2005). *Principles of Characterizing and Applying Human Exposure Models.* Geneva: World Health Organization.

Zhou, Y., & Levy, J. (2007). Factors Influencing the Spatial Extent of Mobile Source Air Pollution Impacts: a Meta-analysis. *BMC Public Health , 7*, 89.

Zhu, D., Nussbaum, N. J., Kuhns, H. D., Oliver Chang, M.-C., Sodeman, D., Uppapalli, S., et al. (2009). In-Plume Emission Test Stand 2: Emission Factors for 10- to 100-kW U.S. Military Generators. *Journal of Air and Waste Management , 59*, 1446–1457.

Zou, B., Wilson, J. G., Zhan, F. B., & Zeng, Y. (2009). Air pollution exposure assessment methods utilized in epidemiological studies. *Journal of Environmental Monitoring* , 475-490.

REPORT DOCUMENTATION PAGE

Form Approved
OMB No. 074-0188

1. REPORT DATE *(DD-MM-YYYY)*	**2. REPORT TYPE**	**3. DATES COVERED** *(From – To)*
24-03-2011	Master's Thesis	Jun 2010 – Mar 2011

4. TITLE AND SUBTITLE

Retrospective Geospatial Modeling of PM10 Exposures from Open Burning at Joint Base Balad, Iraq

5a. CONTRACT NUMBER

5b. GRANT NUMBER

5c. PROGRAM ELEMENT NUMBER

6. AUTHOR(S)

Rinker, John P., MSgt, USAF

5d. PROJECT NUMBER
N/A

5e. TASK NUMBER

5f. WORK UNIT NUMBER

7. PERFORMING ORGANIZATION NAMES(S) AND ADDRESS(S)
Air Force Institute of Technology
Graduate School of Engineering and Management (AFIT/ENV)
2950 Hobson Way
WPAFB OH 45433-7765

8. PERFORMING ORGANIZATION REPORT NUMBER

AFIT/GIH/ENV/11-M03

9. SPONSORING/MONITORING AGENCY NAME(S) AND ADDRESS(ES)
USAF School of Aerospace Medicine, Risk Analysis Branch
1050 Forrer Blvd
Kettering OH 45420
(937) 656-8555 DSN (986-8555) attn: Lt Col Darrin Ott (Darrin.Ott@wpafb.af.mil)

10. SPONSOR/MONITOR'S ACRONYM(S)
USAFSAM/OEHR

11. SPONSOR/MONITOR'S REPORT NUMBER(S)

12. DISTRIBUTION/AVAILABILITY STATEMENT
APPROVED FOR PUBLIC RELEASE; UNLIMITED DISTRIBUTION.

13. SUPPLEMENTARY NOTES
This material is declared the work of the U.S. Government and is not subject to copyright protection in the United States.

14. ABSTRACT

Predicting, determining, and linking theater-related source-specific exposures to health effects has proven difficult. The purpose of this research is to delineate retrospective exposure zones using spatially interpolated particulate air sampling point data from Joint Base Balad, create burn pit exposure isopleths from dispersion model outputs, and merge into a combined exposure model in GIS. Interpolated monitoring results and dispersion modeled results were combined to compare modeled exposures across base. Burn pit contribution to total PM10 was also modeled. The combined dispersion and interpolation map showed elevated concentrations within a 1 kilometer buffer of the burn pit. Buildings within this area were identified by geoprocessing. The east side of the base receives greater burn pit-specific PM10, compared to the west side. The west side showed high ambient PM10 from monitoring results, but it is unclear whether this was due to spatial or temporal effects. High temporal variability highlights the need for temporally representative sampling across the geographical area throughout the year. It was shown that source-specific individual exposure can be estimated with dispersion model isopleth maps and individual time-activity patterns. All modeling performed can all be refined with improved estimates of emission rates.

15. SUBJECT TERMS
Retrospective Exposure Modeling; Dispersion Modeling; Geographical Information Systems

16. SECURITY CLASSIFICATION OF:			**17. LIMITATION OF ABSTRACT**	**18. NUMBER OF PAGES**	**19a. NAME OF RESPONSIBLE PERSON**
REPORT	**ABSTRACT**	**c. THIS PAGE**			DIRK P. YAMAMOTO, Lt Col, USAF, AFIT/ENV
U	**U**	**U**	**UU**	199	**19b. TELEPHONE NUMBER** *(Include area code)* (937) 255-3636, ext 4511; email: Dirk.Yamamoto@afit.edu

Standard Form 298 (Rev. 8-98) Prescribed by ANSI Std. Z39-18